Assessing Effects of Object Detection Performance on Simulated Crash Outcomes for an Automated Driving System

Andrew J. Galloway

Thesis submitted to the faculty of the Virginia Polytechnic Institute and State University in partial fulfillment of the requirements for the degree of

Master of Science

In

Biomedical Engineering

Zachary R. Doerzaph, Chair

Luke E. Riexinger

Miguel A. Perez

Loren J. Stowe

May 3rd, 2023

Blacksburg, Virginia

Keywords: automated vehicles, perception systems, operational safety, collision avoidance

Assessing Effects of Object Detection Performance on Simulated Crash Outcomes for an Automated Driving System

Andrew J. Galloway

ABSTRACT (ACADEMIC)

Highly Automated Vehicles (AVs) have the capability to revolutionize the transportation system. These systems have the possibility to make roads safer as AVs do not have limitations that human drivers do, many of which are common causes of vehicle crashes (e.g., distraction or fatigue) often defined generically as human error. The deployment of AVs is likely to be very gradual however, and there will exist situations in which the AV will be driving in close proximity with human drivers across the foreseeable future. Given the persistent crash problem in which the majority of crashes are attributed to driver error, humans will continue to create potential collision scenarios that an AV will be expected to try and avoid or mitigate if developed appropriately.

The absence of unreasonable risk in an AVs ability to comprehend and react in these situations is referred to as operational safety. Unlike advanced driver assistance systems (ADAS), highly automated vehicles are required to perform the entirety of the dynamic driving task (DDT) and have a greater responsibility to achieve a high level of operational safety. To address this concern, scenario-based testing has increasingly become a popular option for evaluating AV performance. On a functional level, an AV typically consists of three basic systems: the perception system, the decision and path planning system, and vehicle motion control system. A minimum level of performance is needed in each of these functional blocks to achieve an adequate level of operational safety.

The goal of this study was to investigate the effects that perception system performance (i.e., target object state errors) has on vehicle operational safety in collision scenarios similar to that created by human drivers. In the first part of this study, recent annual crash data was used to define a relevant crash population of possible scenarios involving intersections that an AV operating as an urban taxi may encounter. Common crash maneuvers and characteristics were combined to create a set of testing scenarios that represent a high

percentage of the overall crash population. In the second part of this study, each test scenario was executed using an AV test platform during closed road testing to determine possible real-world perception system performance. This provided a measure of the error in object detection measurements compared to the ideal (i.e., where a vehicle was detected to be compared to where it actually was). In the third part of this study, a set of vehicle simulations were performed to assess the effect of perception system performance on crash outcomes. This analysis simulated hypothetical crashes between an AV and one other collision partner. First an initial worst-case impact configuration was defined and was based on injury outcomes seen in crash data. The AV was then simulated to perform a variety of evasive maneuvers based on an adaptation of a non-impaired driver model. The impact location and orientation of the collision partner was simulated as two states: one based on the object detection of an ideal perception system and the other based on the object detection of the perception system from the AV platform used during the road testing. For simulations in which the two vehicles contacted each other, a planar momentum-impulse model was used for impact modeling and injury outcomes were predicted using an omni-directional injury model taken from recent literature.

Results from this study indicate that errors in perception system measurements can change the perceived occupant injury risk within a crash. Sensitivity was found to be dependent on the specific crash type as well as what evasive maneuver is taken. Sensitivities occurred mainly due to changes in the principal direction of force for the crash and the interaction within the injury risk prediction curves. In order to achieve full operational safety, it will likely be important to understand the influence that each functional system (perception, decision, and control) may have on AV performance in these crash scenarios.

Assessing Effects of Object Detection Performance on Simulated Crash Outcomes for an Automated Driving System

Andrew J. Galloway

GENERAL AUDIENCE ABSTRACT

Highly Automated Vehicles (AVs) have the capability to revolutionize the transportation system. These systems have the possibility to make roads safer as AVs do not have many of the limitations that human drivers do, many of which are common causes of vehicle crashes (e.g., distraction or fatigue). AVs will be expected to drive alongside human drivers, and so these drivers are likely to continue to be at fault in causing crashes. As part of ensuring safety, AVs will reasonably be expected to try and avoid or help reduce the severity of these crashes. AVs operate using three main systems: the perception system which consists of sensors that see the objects around the AV, the decision and path planning system, which makes decision on what the AV will do, and the vehicle motion control system. Due to the nature of the real-world, these systems may not work exactly as intended which may affect the ability of the AV to react to possible crash scenarios. Because of this, the goal of this study was to investigate the effects that perception system performance (i.e., target object state errors) has on the ability of an AV to react to crash scenarios similar to those created by human drivers. This study first defined crash scenarios using real-world crash data. A real-world perception system was then tested in these scenarios to determine object detection performance. Based on this performance, effects on safety were assessed through vehicle crash simulations. Results from this analysis showed that safety can vary based on both perception system performance and crash scenario. This highlights that it will be important to address system performance in order to achieve high levels of driving safety.

ACKNOWLEDGEMENTS

My first acknowledgement is to Dr. Clay Gabler. I'm grateful to have been welcomed into your lab and although I unfortunately only knew you for a short time, your influence left a lasting impact on me and ignited my passion for the automotive and safety industry. I'd like to acknowledge my advisor, Dr. Zac Doerzaph, for welcoming me to the Virginia Tech Transportation Institute and for your guidance throughout my time there. My time and experiences at VTTI is something I will lean on for the rest of my career. I'd also like to acknowledge Dr. Luke Riexinger. From working with you as an intern to completion of this thesis, you've always been a large influence for me both as a mentor and as a friend. I'd like to acknowledge the rest of my graduate committee, Loren Stowe, and Dr. Miguel Perez, for their guidance during my time at VTTI. Loren, your inputs were invaluable in completing this thesis and the time I spent working on research projects with you was invaluable for me. Lastly, I'd like to acknowledge my family as well as the friends I've made while at Virginia Tech for your support.

TABLE OF CONTENTS

ABSTRACT (ACADEMIC) ii
GENERAL AUDIENCE ABSTRACT iv
ACKNOWLEDGEMENTS v
TABLE OF CONTENTS vi
LIST OF FIGURES viii
LIST OF TABLES x
LIST OF ABBREVIATIONS xi
1. Introduction and Objectives 1
1.1 Automated Vehicles: Overview 1
1.2 AV Operational Safety 3
1.3 Automated Driving Systems: Functional System Overview 6
1.4 Related Work 7
1.5 Research Objectives 9
2. Characterizing AV Relevant Crash Scenarios using Real-World Crash Data 11
2.1 Introduction and Research Objectives 11
2.2 Data Sources 11
2.2.1 Crash Report Sampling System 11
2.2.2 KABCO Injury Coding and Conversion to AIS Scale 12
2.2.3 Target Population Case Selection 14
2.3 Target Population Characterization and Probability of Crash Scenario Exposure 17
2.3.1 Crash Scenario Template 17
2.3.2 Selected Data Elements and Scenario Element Characterization 18
2.3.3 Assigning Vehicle Roles 19
2.3.4 Calculating Probability of Crash Scenario Exposure 19
2.4 Results 22
2.4.1 Maneuver Level Factors 22
2.4.2 Target Vehicle Level Factors 27
2.4.3 Environmental Level Factors 29
2.5 Summary of Crash Scenarios 36
2.6 Discussion and Limitations 41
2.7 Conclusions 44
3. Characterizing Perception System Performance in Relevant Crash Scenarios 45

3.1 Introduction and Research Objectives 45
3.2 ADS Perception System Overview 45
3.3 Study Testing Facilities 47
3.4 Data Collection Overview 48
3.5 Data Processing Overview 49
3.6 Results of Performance Characterization 52
3.7 Discussion and Limitations 57
3.8 Conclusions 59
4. Evaluating Simulated Crash Outcomes based on Perception System Performance 60
4.1 Introduction and Research Objectives 60
4.2 Crash Simulation Modeling 60
4.2.1 Defining Worst-Case Impact Orientation for Selected Crash Scenarios 61
4.2.2 Effects of Perception System Performance on Crash Orientation 65
4.2.3 Modeling AV Evasive Maneuvers 67
4.2.4 Modeling Impact Dynamics 70
4.2.5 Modeling Injury Risk in both Vehicles 71
4.3 Results 72
4.4 Discussion and Limitations 79
4.5 Conclusions 83
5. Conclusions 84
Appendix A: List of CRSS Data Elements and Definitions 86
References 88

LIST OF FIGURES

Figure 1. Overview of SAE Levels of Automation defined in SAE J3016 2
Figure 2. Breakdown of Operational Safety components 4
Figure 3. Overview of main functional subsystems for an ADS 6
Figure 4. Comparison of selected crashes to all 1st harmful event vehicle crashes with selected years of CRSS 16
Figure 5. Breakdown of MAIS from each crash, shown for each year in CRSS 17
Figure 6. Scenario generation template 18
Figure 7. Generalized crash maneuvers for all selected crashes and all selected MAIS2+F crashes 22
Figure 8. Specific crash modes within “Same Direction, Rear End” crash type 23
Figure 9. Specific crashes modes within “Turn Into Path” crash type 24
Figure 10. Specific crashes modes within “Turn Across Path” crash type 25
Figure 11. Specific crashes modes within “Straight Paths” crash type 26
Figure 12. Cumulative distribution of vehicle travel speed in all selected crashes and all injury crashes 27
Figure 13. Turning vehicle body type classification 28
Figure 14. Breakdown of lighting condition (top), weather condition (middle), and type of intersection (bottom) for all crashes and all injury crashes 30
Figure 15. Breakdown of number of traffic lanes, roadway alignment, roadway grade, sightline obstructions, trafficway description, and traffic control present for the traveling through vehicle and the turning vehicle 32
Figure 16. Distribution of vehicle travel speed from all Rear-End, LTAP/OD, LTAP/LD, and SCP crashes in the US from 2004 to 2019 43
Figure 17. ADS retrofitted Lincoln MKZ (Left) and trunk mounted perception system (right) 46
Figure 18. ADS sensor suite consisting of camera and lidar sensors in the forward, rear, and cross-traffic FOVs 46
Figure 19. Top view of the Virginia Smart Roads Surface Street Expansion (SSE). Features include a large intersection, roundabout, and different lane configurations 47
Figure 20. Euclidian based position filter 50
Figure 21. Overview of primary performance measures of interest 51
Figure 22. DGPS and filtered perception system detections for each trial during the Rear-End scenario 52
Figure 23. DGPS and filtered perception system detections for each trial during the LTAP/OD scenario 52
Figure 24. DGPS and filtered perception system detections for each trial during the LTAP/LD scenario 53
Figure 25. DGPS and filtered perception system detections for each trial during the SCP scenarios 53
Figure 26. Cumulative distribution of X/Y position error for each crash scenario 54
Figure 27. Cumulative distribution of TV heading error for each crash scenario 55
Figure 28. Cumulative distribution of TV velocity error for each crash scenario 56
Figure 29. Distribution of y position error for each sensor FOV, broken out by successful sensor fusion 58
Figure 30. SCP scenario detections shown with sensor fusion information 58
Figure 31. Overview of crash simulation model 61
Figure 32. Impact clock-point diagram 62
Figure 33. Breakdown of impact clock point on both the traveling through vehicle and the turning vehicle 63
Figure 34. Final assumed initial worst-case impact orientations 65
Figure 35. Example LTAP/LD crash scenario in which the predicted position and the actual position of the other vehicle result in different impact orientations 66

Figure 36. Three categories of AV evasive paths: primarily braking, braking while steering left, and braking while steering right 69
Figure 37. Example injury curves from (McMurry 2021) for varying delta-v and PDOF 71
Figure 38. Percent of simulated evasive paths with a collision for each scenario, activation point, and perception system performance 73
Figure 39. AV impact speed for each evasive maneuver category, broken out by crash scenario, activation point, and perception system performance 74
Figure 40. AV delta-v for each evasive maneuver category, broken out by crash scenario, activation point, and perception system performance 75
Figure 41. Turning vehicle delta-v for each evasive maneuver category, broken out by crash scenario, activation point, and perception system performance 75
Figure 42. AV PDOF for each evasive maneuver category, broken out by crash scenario, activation point, and perception system performance 76
Figure 43. Turning vehicle PDOF for each evasive maneuver category, broken out by crash scenario, activation point, and perception system performance 77
Figure 44. AV probability of MAIS3+F injury for each evasive maneuver category, broken out by crash scenario, activation point, and perception system performance 78
Figure 45. Turning vehicle probability of MAIS3+F injury for each evasive maneuver category, broken out by crash scenario, activation point, and perception system performance 78
Figure 46. Summary of difference in injury risk prediction for the ideal system and the measured system 79
Figure 47. Example simulation outputs showing the change in impact orientation between the ideal perception system (right) and the measured perception system (left) for the LTAP/OD crash scenario and 70% activation point under primarily braking. 80
Figure 48. Highlight of injury risk sensitivities. The difference in injury outcomes between an ideal and a measured system differ greatly depending on where on the curve they fall. 81

LIST OF TABLES

Table 1. KABCO Injury Coding Scheme 13
Table 2. KABCO to AIS Scale Conversion Table 14
Table 3. Full breakdown of target population crashes from CRSS 15
Table 4. List of CRSS data elements used for scenario characterization 19
Table 5. Categorization of scenario factors based on possible influence on perception system performance 21
Table 6. Breakdown of Generalized Crash Maneuver 23
Table 7. Breakdown of "Same Direction, Rear End" Crash Type 24
Table 8. Breakdown of "Turn Into Path" Crash Type 24
Table 9. Breakdown of "Turn Across Path" Crash Type 25
Table 10. Breakdown of "Straight Paths" Crash Type 26
Table 11. Binned travel speed for the traveling through and turning vehicles 28
Table 12. Turning vehicle body-type 29
Table 13. Breakdown of lighting condition, weather condition, and type of intersection 31
Table 14. Breakdown of number of traffic lanes, roadway alignment, roadway grade, sightline obstructions, trafficway description, and traffic control present for the traveling through vehicle 33
Table 15. Breakdown of number of traffic lanes, roadway alignment, roadway grade, sightline obstructions, trafficway description, and traffic control present for the turning vehicle 34
Table 16. Summary of probability of exposure for each selected crash scenario 44
Table 17. List of perception systems measures needed for characterization 48
Table 18. List of ground truth variables used to characterize performance 49
Table 19. Summary of X/Y position error statistics 54
Table 20. Summary of TV heading error statistics 55
Table 21. Summary of TV velocity error statistics 56
Table 22. Summary of median X/Y position error, heading error, and speed error 59
Table 23. Breakdown of impact clock point on both the traveling through vehicle and the turning vehicle 63
Table 24. Summary of AV initial speed used during crash simulations 69

LIST OF ABBREVIATIONS

ACC – Adaptive Cruise Control

ADS – Automated Driving System

AIS – Abbreviated Injury Scale

AUR – Absence of Unreasonable Risk

AV – Automated Vehicle

CDS – Crashworthiness Data System

CRSS – Crash Report Sampling System

DAS – Driving Automation System

DDT – Dynamic Driving Task

DGPS – Differential Global Positioning System

FARS – Fatality Analysis Reporting System

GES – General Estimates System

LTAP/LD – Left Turn Across Path / Lateral Direction

LTAP/OD – Left Turn Across Path / Opposite Direction

NASS – National Automotive Sampling System

NHTSA – National Highway Traffic Safety Administration

NMVCCS – National Motor Vehicle Crash Causation Survey

ODD – Operational Design Domain

PDOF – Principal Direction of Force

SCP – Straight Crossing Path

SOTIF – Safety of the Intended Functionality

SSE – Surface Street Expansion

SUT – System Under Test

VDOT – Virginia Department of Transportation

VTTI – Virginia Tech Transportation Institute

1. Introduction and Objectives

The safety of automated vehicles must be evaluated and proven before large scale adoption into the transportation system can happen. Vehicles must be safe across a larger variety of aspects than vehicles on the roads today. Due to the promising benefits of recent active safety systems, it is reasonable to expect that the same capabilities (i.e., safety benefits) will exist for automated vehicles. Particularly, the ability for an automated vehicle to avoid collisions with other road users has the possibility to greatly decrease the crash problem. In order to achieve this, automated vehicle systems must operate smoothly and without fault. However, no system will ever be perfect and so there exists a need to understand when and where system level performance causes concerns related to achieving safety.

The goal of this study was to develop and apply a method that assesses the effects of perception system level performance on the ability for an automated vehicle to perform collision avoidance in relevant crash scenarios. A hybrid method is presented that allows for this the assessment of a real-world automated vehicle and identifies areas of possible safety concerns. This study first characterized a relevant crash population and identified a set of common crash scenarios. Within each scenario, the performance of a real-world perception system was then characterized. The method then describes a series of vehicle crash simulations that were performed in order to identify where and when safety concerns may arise for a particular automated vehicle.

1.1 Automated Vehicles: Overview

An Automated Vehicle (AV) is a term that refers to an automotive vehicle that is equipped with an Automated Driving System (ADS). An ADS is characterized as a system meeting the requirements for either level 3, 4, or 5 of automation defined by the SAE J3016 standard (SAE International, 2018). This standard defines 6 levels of automation (Figure 1) ranging from no automation (level 0) to complete automation (level 5). Each level of automation is defined based on how much of the Dynamic Driving Task (DDT) is supported by the automation system. The DDT refers to the actions that a driver is required to

perform in order to operate a vehicle in on-road traffic and includes but isn't limited to steering, acceleration/deceleration through the throttle and brakes, monitoring of the surrounding environment, and maneuver planning that includes evasive actions (SAE International, 2018).

Automation levels 0 to 2, typically referred to as Driving Automation Systems (DAS), involve the DDT being shared by the driver and the system with the primary driving responsibility being placed on the driver. ADS equipped vehicles (levels 3 to 5) shift the primary responsibility of the DDT completely to the system when active. An increasingly common example of a level 1 DAS is Adaptive Cruise Control (ACC). This system operates by providing acceleration/deceleration control of the vehicle in order to maintain both speed and/or following distance to a leading vehicle. The responsibility to provide steering as well as maintain safety, however, continues to fall on the driver. An example of a level 4 ADS is the Waymo Driver (Favarò et al., 2023) where within set operating conditions, this vehicle operates as an urban taxi and can provide the full required DDT including the ability to monitor and ensure safe operation.

<table>
<tr><th colspan="7">Levels of Automation (Adapted from SAE J3016)</th></tr>
<tr><td></td><td colspan="3">Driver Support Features</td><td colspan="3">Automated Driving Features</td></tr>
<tr><td></td><td>0</td><td>1</td><td>2</td><td>3</td><td>4</td><td>5</td></tr>
<tr><td>Overview</td><td colspan="3">You <u>are</u> driving whenever these driver support features are engaged, even if your feet are off the pedals and you are not steering</td><td colspan="3">You <u>are not</u> driving whenever these driver support features are engaged, even if you are sitting in “the driver’s seat”</td></tr>
<tr><td>Driving Responsibility</td><td colspan="3">You must constantly supervise these support features; you must steer, brake, or accelerate as needed to maintain safety</td><td>When the feature requests, you must drive</td><td colspan="2">These automated driving features will not require you to take over driving</td></tr>
<tr><td>Features</td><td>Limited to providing warnings and momentary assistance</td><td>Provide steering or brake or acceleration support</td><td>Provide steering and brake or acceleration support</td><td colspan="2">Features can drive the vehicle under limited conditions and will not operate unless all requirements are met</td><td>Same as L4, but features can drive anywhere in all conditions</td></tr>
</table>

Figure 1. Overview of SAE Levels of Automation defined in SAE J3016

1.2 AV Operational Safety

Because an ADS must perform the entirety of the DDT, future AVs will require a high degree of emphasis to be placed on ensuring safe operation past that which is already required for vehicles with no automation (e.g., occupant protection). The United States Code for Motor Vehicle Safety (Title 49, Chapter 301) defines motor vehicle safety as "the performance of a motor vehicle or motor vehicle equipment in a way that protects the public against unreasonable risk of accidents occurring because of the design, construction, or performance of a motor vehicle, and against unreasonable risk of death or injury in an accident…" where accident is referring to a crash (NHTSA, 2008). The term "unreasonable risk" is derived from the notion that all activities invite some risk of bodily harm and so, there is a level of risk that the public consensus deems as acceptable (i.e., reasonable risk).

The term "risk" can further be expressed as the joint probability of the likelihood of a hazardous event happening, and the possible severity of that hazardous event. The likelihood term can further be defined as the probability of exposure to a certain event and the probability that hazardous outcomes cannot be prevented (for example by the driver). Combined, these three probability terms compute a measure of safety risk (Equation 1). As is often the case in automotive risk assessment, risk can be the probability of a certain degree of occupant injury resulting from a collision with another road user or roadside object/feature.

$$Safety\ Risk = Severity\ of\ Event\ x\ (Exposure\ of\ Event\ x\ Controllability) \quad (1)$$

The absence of unreasonable risk (AUR) when achieved by an AV in an operational domain can be referred to as operational safety. The term "Operational Safety" commonly refers to the prevention of hazards attributed with three main categories: functional safety, safety of the intended functionality, and behavioral safety (Figure 2).

Figure 2. Breakdown of Operational Safety components

Functional safety (defined by the ISO-26262 standard) is defined as the absence of unreasonable risk due to hazards caused by malfunctioning behavior of electrical/electronic systems (ISO, 2021). This standard addresses a framework for the reduction of risk to an acceptable level by devising safety control functions. In contrast to intrinsic safety, in which safety is assured by completely removing the causes of danger, functional safety implements controls or actions that lower the probability of hazardous events from occurring to an acceptable level. To achieve this, functional safety considers both systemic failures, which arise from failures created during design (ex. software bugs), and random failures that occur after deployment (e.g., hardware failures due to degradation).

Safety of the intended functionality (called SOTIF and defined by the ISO-21448 standard) is a complementary standard that addresses operational safety concerns outside of the ISO-26262 standard. Functional safety is typically referred to as 'inward looking' whereas SOTIF focuses on a 'look outwards' safety approach (Ploeg et al., 2021) and relates to hazardous behavior not caused by system malfunctions. This standard defines safety as "the absence of unreasonable risk of the intended functions" (ISO, 2019). A more detailed definition as it relates to AVs is "the ability of an automation system to correctly comprehend the environmental situation and behave safely, by ensuring that the systems and components are operating within their design boundaries and, if not, by activating appropriate countermeasures" (Ploeg et al., 2021). Examples of this are usually related to environmental perception such as performance limitations that may arise in camera-based systems exposed to direct sunlight (e.g., sunrise or sunset).

Building off the ideas developed as a part of SOTIF is the notion of behavioral safety. This has been described as "An aspect of system safety that focuses on how a system should behave normally in its environment to avoid hazards and reduce the risk of mishaps: for instance, detect objects and respond in a safe way (slow down, stop, turn, change lane, etc.)" (Webb et al., 2020) where the term "mishap" refers to a crash. Behavioral safety focuses on the programmed behavior of the AV, while assuming that all system level components are operating as intended. Three possible components within behavioral safety are roadway regulatory compliance, conflict avoidance, and collision avoidance (Favarò et al., 2023). Regulatory compliance refers to the ability of the AV to obey all relevant traffic laws (e.g., yield to other vehicles when required). Conflict avoidance refers to the ability of the AV to act in a safe manner around other road users so as to not create collision events. An example of this is ensuring a safe following distance to other vehicles. Lastly, collision avoidance refers to the ability of the AV to prevent or mitigate collision scenarios. Broadly, these can be collision scenarios that are unintentionally initiated by the AV or by other road users.

All three behavioral safety components are important to address during an AV safety assessment. Conflict scenarios initiated by other drivers, however, are likely to continue to be sources of crash risk even as safety risk from the other operational/behavioral safety components diminish due to improved AV development and best practices. This is because AV adoption is likely to be gradual and so AVs will be expected to interact with human driven vehicles across its entire operational domain. The National Motor Vehicle Crash Causation Survey (NMVCCS), a detailed crash study conducted by the National Highway Traffic Administration (NHTSA) between 2005 and 2007, found that the majority of the recorded crashes could be attributed to some form of driver error (NMVCCS, 2008). Due to different driver limitations, such as drowsiness and the ability to be distracted, behaviors like failing to stop for a red traffic signal or failing to yield to other vehicles were common driver errors that caused collisions. Human drivers will continue to make these driving errors and are likely to create conflicts with future AVs. Thus, the need for the AV to detect and evade or mitigate these scenarios is crucial to achieving operational safety.

1.3 Automated Driving Systems: Functional System Overview

The ability for an AV to perceive and react to crash scenarios initiated by other road users may be influenced, however, by ADS sub-system level performance limitations and errors. Functionally, an automated driving system relies on three main systems to provide the full DDT: perception, motion planning, and maneuver control (Behere and Torngren, 2015). An overview of these three systems is shown in Figure 3.

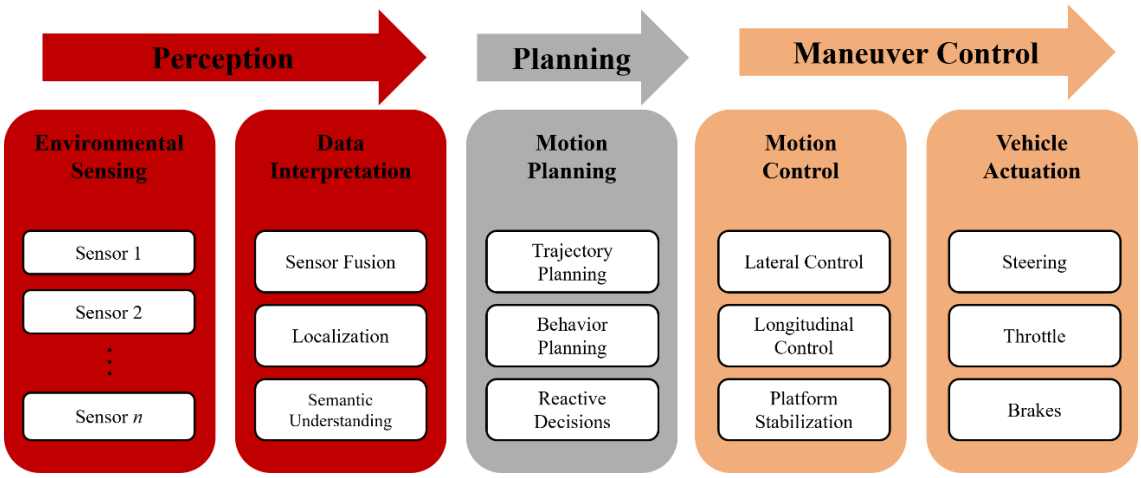

Figure 3. Overview of main functional subsystems for an ADS

Within the perception system, information about the vehicles environment, such as roadway geometry and other road users, is collected using a suite of onboard sensors. Modern AVs most commonly use cameras, radar, and lidar to perceive this environment (Marti et al., 2019). The information collected by each sensor is also fused (i.e., sensor information from multiple sensors is combined into one measurement) to provide a more accurate representation of the vehicle's surroundings. The benefit of this is that the inherent limitations of each sensor are negated. For example, camera and lidar sensors can exhibit degraded performance in foggy conditions, whereas radar functions normally (Kocic et al., 2018). Under these kinds of conditions, fusing sensing systems ensure that object detection is still achieved (at least partially). Using data supplied from additional sensors such as GPS, the AV can localize itself within its surroundings. Combined sensor information is also used to identify and classify these surroundings as different possible object types which is referred to as semantic understanding (e.g., vehicle, pedestrian, traffic cone, etc.).

Outputs from the perception system are then used by the motion planning system. Motion planning is responsible for interpreting the readings from the perception system in order to determine how the vehicle will interact with other road users. This involves creating a trajectory path to navigate from point A to point B (Behere and Torngren, 2015) while also ensuring that all relevant traffic laws are obeyed, and that the operation of the AV maintains a safe and predictable path with respect to other road users (behavioral planning). Included within this system is the responsibility to detect and decide how to react to possible threats that may cause a collision (reactive decisions).

Once a motion path is determined, the control of the vehicle is accomplished by the maneuver control system. The system achieves the planned trajectory waypoints by manipulating the vehicle throttle, brakes, and steering to provide the longitudinal and lateral motion that is required (Behere and Torngren, 2015). This system also works with the stability systems within the vehicle (ABS, ESC, etc.) to keep the vehicle in a stable condition. Active safety systems may also be integrated within this system to alter vehicle motion based on a reactive decision.

During critical driving activities, such as in moments of collision avoidance, all three functional systems must work together to achieve a desired task and each system may have upstream or downstream effects on the overall driving result. For example, in this system of systems, motion planning relies on accurate perception outputs to make safe driving decisions, such as plotting a course of action during an emerging collision event. Because of this, there is a benefit in understanding the contributions of subsystem level performance in addition to understanding system performance as a whole.

1.4 Related Work

The inspiration for this study largely comes from a series of white papers and journal publications produced by the Waymo safety team. In March of 2023, Waymo published a white paper of their company approach for how to determine that an AV is free from unreasonable risk. This has been released with the intent of fostering a dialog within the AV community so that other AV manufactures may consider these

practices and approaches in their own safety validation. The white paper addresses the same topic area as this thesis with a strong emphasis on behavioral safety (Favarò et al., 2023).

Behavioral safety, specifically crash events caused by other drivers, has generally been a well published topic from Waymo in the past few years. Scanlon et al. (2021) presented a method for the analysis and reconstruction of crash events aimed towards AV safety assessment. This study presented results of hypothetical crash simulations in which one of the human drivers was replaced with the Waymo ADS and assessed the possible crash and injury benefits of their system in these crashes. A similar study by Scanlon et al. (2022) simulated the collision avoidance effectiveness of the Waymo ADS compared to a human driver model. In addition to this study, the white paper by Kusano et al. (2022) presented an overview of the Waymo evaluation approach for these simulations. Generally, these papers have detailed Waymo's process for simulating and evaluating how well the Waymo ADS system performs within reconstructed crashes. However, these studies detail the assessment of the entire Waymo ADS platform and do not specifically detail the effects of any of the functional subsystems (e.g., the perception system).

Related specifically to perception systems, multiple studies have sought to address the perception system's specific contribution to achieving operational safety. In a study by Berk et al. (2020), a method for assessing the reliability of ADS perception system was presented. The method in this study detailed safety evaluation in all aspects and did not focus on collision avoidance. A paper by Wishart et al. (2022) looked at the sensitivity of various operational safety metrics on the perception level errors. This study builds off of previous work from the same authors and details an approach that evaluates metrics associated with AV conflict avoidance. Previous studies such as by Johansson and Nilsson (2016) have also provided methods for perception systems to meet the functional safety requirements of ISO-26262.

1.5 Research Objectives

The primary objective of this study was to develop and apply a hybrid method that assesses the influence of perception system performance (i.e., object detection state errors) on crash and injury risk for a hypothetical AV that is reacting to a collision scenario. The goal of the method was to determine where and when weaknesses may exist for a specific perception system and AV operating under a specific use case and allows for areas of safety concern to be identified. The hybrid method presented accomplishes this by simulating driving performance within common crash scenarios using perception system performance measured from a real-world ADS platform. Within the notion of safety risk, this method assesses the influence of perception system performance on hazardous event severity for a reference AV.

As a secondary study objective, the probability of exposure for an AV to a set of crash scenarios was determined. This objective characterized a target population of real-world crashes that may be relevant for future AVs operating as urban taxis. From this crash population, a set of high-level crash scenarios were then defined. This objective was included within the method for two main reasons. The first reason is that perception system performance is likely to be situationally dependent and vary between different crash scenarios and other factors such as environmental conditions. Therefore, it is important that the method also be exercised within the context of specific crash scenarios that are likely to be highly relevant for the intended use case of the AV. The second reason is that this objective begins to assess the possible exposure to different crash scenarios, which when combined with crash severity computes risk.

The specific project objectives were as follows:

1. Capture data for enabling simulation of AV perception system performance.
    a. Use nationally representative crash data to estimate exposure to a set of common crash scenarios for a hypothetical AV operating as an urban taxi.
    b. Measure and characterize the (perception system) performance of a prototype ADS platform in each of the defined common crash scenarios.
2. Simulate possible crash outcomes within the identified common crash scenarios, accounting for the effects of both an ideal perception system and the measured perception system, as well as certain AV evasive action assumptions.
3. Compute occupant injury risk as a function of crash scenario, evasive action, and perception system performance.

2. Characterizing AV Relevant Crash Scenarios using Real-World Crash Data

2.1 Introduction and Research Objectives

The objective of this chapter was to characterize a target population of real-world crashes based around the use case of an AV operating as an urban taxi. From this crash population, characteristics from each crash (e.g., maneuver type, environmental conditions, and roadway type) were combined to create a set of high-level crash scenarios. For each scenario, the probability of exposure within the crash population was calculated. The crash population was assumed to also represent a future crash population and that future AVs will be exposed to similar crash scenarios at a similar frequency to human drivers today. The urban taxi use case, such as the Waymo Driver mentioned previously, is a relevant example for which these scenarios can be defined and is the use case used during this study.

One challenge to defining these scenarios is that future AVs may theoretically be exposed to a large amount of driving and/or collision scenarios (Knauss et al., 2017). However, exposure to the majority of possible scenarios is likely to be very small and therefore represents an overall small safety risk. This chapter focuses on characterizing the crash scenarios with a high possible exposure for an AV as these represent the highest overall impact on achieving robust collision avoidance operational safety.

The summary of this chapter is as follows: This chapter used nationally representative police-reported crash data to characterize a relevant crash population of intersection vehicle crashes whose situations and conditions may be similar to that which a hypothetical urban taxi AV may be exposed too. Crash maneuvers and characteristics from these crashes were then combined to create a set of crash scenarios and the probability of exposure to each scenario as it relates to a possible future crash population was computed.

2.2 Data Sources

2.2.1 Crash Report Sampling System

The chapter used crashes recorded within the Crash Report Sampling System (CRSS) database. CRSS is a nationally representative probability sample of the estimated 5 to 6 million police-reported crashes involving vehicles, pedestrians, and cyclists that happen annually in the United States (NHTSA,

2022). To be eligible to be included in CRSS, a crash report must have been completed by the police and involved at least one motor vehicle and resulted in property damage, injury, or death. Although CRSS does not report on all crashes in the US, the focus on just the police-reported crashes allows for the analysis of the crashes of greatest concern. CRSS builds upon the NASS/GES database and began in 2016. At the time of writing this thesis, crash data from the years 2016, 2017, 2018, 2019, and 2020 are available. Data from the years 2016 to 2019 was specifically used during the analysis. The year 2020 was excluded due to the possible impacts of the COVID-19 pandemic on crash frequency, severity, and other primary crash factors.

Because the inclusion of all nationwide police reported crashes is not feasible, CRSS employs sampling designs to produce a nationally representative probability sample of all crashes. For every case recorded in CRSS, a nationally represented weight is also calculated. This represents the estimated total number of annual crashes similar to the selected crash case. Unless reported otherwise, these weighted estimates were used during the calculation of results. The survey package in R (Lumley, 2019) was used in order to account for the sampling variance inherent in the CRSS database (Zhang et al., 2019). Due to the unavailability of information present in many of the crashes, many variables in CRSS use imputed data to account for these unknowns and these variables were used when available.

2.2.2 KABCO Injury Coding and Conversion to AIS Scale

As part of the CRSS database, injury information for all occupants involved in the crash is reported using the KABCO injury coding scheme which allows non-medical personnel the ability to record injury information when creating the crash report. Table 1 shows a breakdown of the KABCO injury scale (NHTSA, 2022).

Table 1. KABCO Injury Coding Scheme

KABCO Code	Severity	Description
0 (O)	No Apparent Injury	No physical evidence of injury, and the person reports normal function.
1 (C)	Possible Injury	Possible injuries are those reported by the person/indicated by behavior, but no wounds are readily evident. Examples include possible concussion and complaints of pain.
2 (B)	Suspected Minor Injury	Any injury that is evident at the scene of the crash, other than fatal/serious injuries. Examples include abrasions/bruises, and minor lacerations.
3 (A)	Suspected Serious Injury	Non-fatal injuries that result in sever lacerations, broken extremities, crash injuries, significant burns, unconsciousness at crash scene, and paralysis.
4 (K)	Fatal Injury	Any injury that results in death within 30 days of the crash.
5 (-)	Injured, Severity Unknown	It is known that the person was injured, but severity was unknown.
6 (-)	Died Prior to Crash	Refers to non-motor vehicle related fatalities (ex. Heart attack victims).
9 (U)	Unknown/Not Reported	Injury information was not reported by police and/or no coding block exits for the state in which the crash occurred.

One limitation of the KABCO coding scheme is that injury assessments are often imprecise and inconsistently coded between US states (Beau, 2014). This limitation was addressed by converting KABCO injury estimates to the Abbreviated Injury Scale (AIS) (AAAM, 2015). Conversion was accomplished using a translator (Table 2) from Najm et al. (2013) which was derived using crashes from the years 1982 to 1986 of the old National Automotive Sampling System (NASS) and the years 2000 to 2007 of the NASS Crashworthiness Data System (CDS). This translator, adapted from a similar approach by Willke et al. (1999), compared the KABCO injury levels from the police-reports to the MAIS injury level determined by the NASS CDS investigator for the same crashes. This allowed for a more accurate representation of the severity of the injuries present in these crashes. For this study, it was assumed that the discrepancies between KABCO and MAIS remained consistent year to year in order to apply the conversion to the more recent crash data.

Table 2. KABCO to AIS Scale Conversion Table

	Police-Reported Injury Severity System						
MAIS	O	C	B	A	K	U	
	No Injury	Possible Injury	Non Incapacitating	Incapacitating	Fatality	Injured, Severity Unknown	Unknown
0	0.92458	0.23203	0.06995	0.03341	0	0.22274	0.42883
1	0.07329	0.69145	0.78039	0.55819	0	0.61725	0.41108
2	0.00201	0.06413	0.11026	0.20748	0	0.10289	0.08667
3	0.00009	0.01061	0.0308	0.1407	0	0.04072	0.04748
4	0	0.00148	0.0063	0.03859	0	0.00418	0.00609
5	0.00003	0.00012	0.0009	0.01702	0	0.01174	0.00277
Killed	0	0.00018	0.0014	0.00461	1	0.00048	0.01708
Total	1	1	1	1	1	1	1

Source: 1982-1986 Old NASS and 2000-2007 CDS

For crashes involving fatalities, NHTSA recommends that these crashes be analyzed using the Fatality Reporting System (FARS) database since it contains reports for every fatal traffic crash and provides a better estimate compared to CRSS. However, because this analysis focused on all crashes (any injury outcome) and the relatively small frequency of fatal crashes, fatalities were taken from CRSS.

2.2.3 Target Population Case Selection

A target population of crashes within CRSS were selected as those that were consistent with a high-level description of the Operational Design Domain (ODD) of an urban taxi. Additional criteria were included to be consistent with the real-world testing completed as part of Chapter 3. Crashes were selected based on the following criteria and filters.

- Crashes that happened within an urban environment. CRSS defines "urban" as crashes happening in an area with a population of 250,000 or greater.
- Only crashes that were recorded to occur within or near an intersection were considered. This focused the target population on a large proportion of the annual crashes within an urban environment (NHTSA, 2021).
- Crashes were limited to only those involving two total motor vehicles.
- Crashes that only involved vehicles and those crashes in which the first harmful event that caused injury and/or property damage was a collision with another vehicle. This excluded other

crash types such as pedestrian/cyclist crashes which are fundamentally different and not included in this study.

- Only crashes in which both vehicles were some type of passenger vehicle or light truck/van were included.
- Crashes were excluded if they occurred within a work zone as this was assumed to be outside the scope of "normal" operating conditions.

Table 3 shows the breakdown of number of cases and estimated number of annual crashes for each year in CRSS after filters are applied. This study considered a target population of 49,346 cases from CRSS, which represents an estimated 6,884,406 crashes.

Table 3. Full breakdown of target population crashes from CRSS

	2016		2017		2018		2019	
	Cases	Weight	Cases	Weight	Cases	Weight	Cases	Weight
All Crashes	46,511	6,821,129	54,969	6,452,285	48,443	6,734,416	54,409	6,755,841
Urban Zone	34,957	5,107,030	42,579	4,940,479	37,874	5,180,975	42,256	5,155,753
Crashes that happened in and around an intersection	16,159	2,305,467	19,272	2,117,791	17,299	2,267,319	19,823	2,312,128
Crashes involving 2 vehicles	11,891	1,870,733	14,055	1,745,784	12,816	1,876,380	14,644	1,918,401
1st Harmful Event is Vehicle Collision	11,824	1,864,018	13,988	1,741,431	12,763	1,872,407	14,579	1,913,658
Crashes involving passenger and/or light trucks/vans	11,371	1,776,031	13,119	1,642,802	11,876	1,757,212	13,550	1,790,896
Crashes not in a Work Zone	11,181	1,748,257	13,022	1,630,521	11,731	1,734,597	13,412	1,771,031

Figure 4 highlights the target population compared to the entire population of crashes in which the 1st harmful event was a vehicle crash within the selected years of CRSS. On average, the target population represented approximately 36% of all vehicle collisions in CRSS for each given year. The remaining

crashes not included in the target population included but was not limited to crashes with pedestrians/cyclists, single vehicle and multi-vehicle crashes, and crashes on rural roadways.

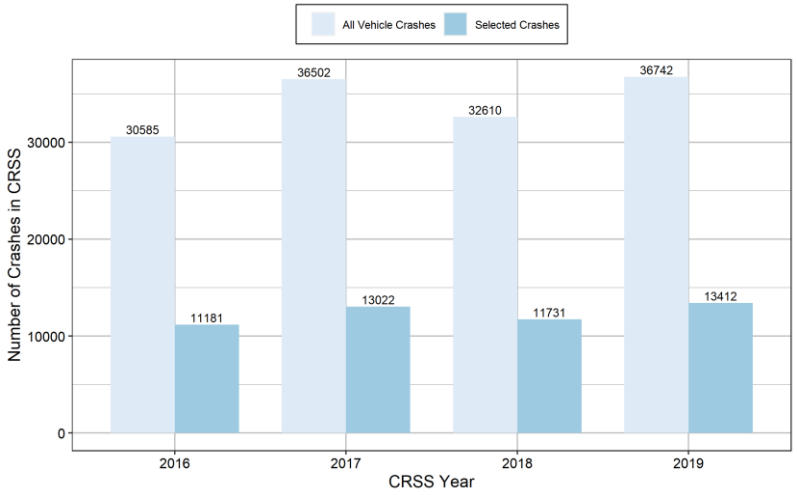

Figure 4. Comparison of selected crashes to all 1st harmful event vehicle crashes with selected years of CRSS

Figure 5 shows the breakdown of injury severity for each selected year in CRSS. After applying the conversion matrix described in Table 2 to the maximum reported KABCO injury for each case, the majority of crashes were predicted to involve no injury or a maximum injury with an AIS score of 1 (minor injury). Injuries with a maximum AIS score of 2 (moderate) or higher including fatalities (MAIS2+F) were predicted to represent 4.37% of the selected crashes which totaled to an estimated 20,539 crashes with an MAIS2+F injury. This represents a relatively small proportion of the entire target population. This may be because compared to all crashes recorded within CRSS, this study excluded many of the crashes that typically involved high injury severity (e.g., single-vehicle crashes, pedestrian/cyclist crashes, crashes involving heavy vehicles, and crashes happening in rural areas).

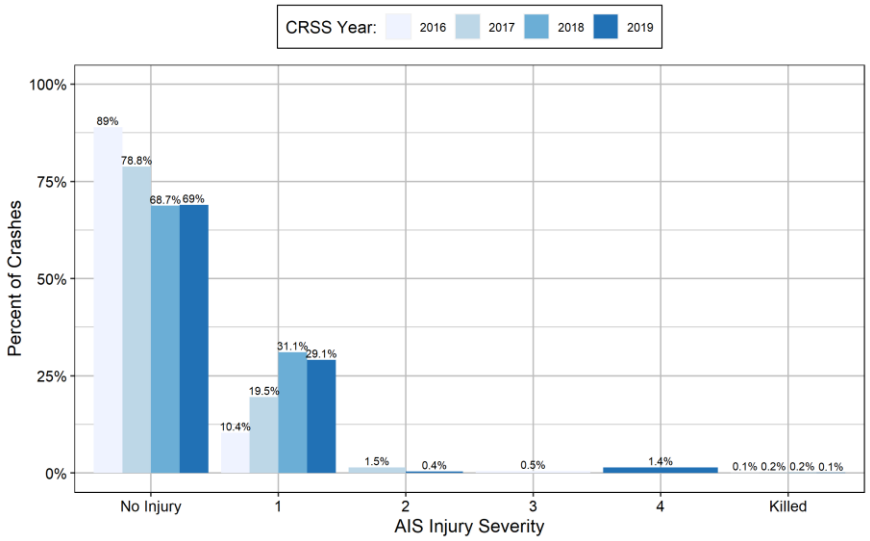

Figure 5. Breakdown of MAIS from each crash, shown for each year in CRSS

2.3 Target Population Characterization and Probability of Crash Scenario Exposure

2.3.1 Crash Scenario Template

Crash scenarios defined in this chapter followed a crash scenario template that was adapted from the ISO-21448 standard (ISO, 2019) and is referenced in Figure 6. Using common scenario typology, the crash scenarios defined in this chapter represent functional scenarios. A functional scenario refers to a high-level overview of a scenario in which entities within a domain and the relations of those entities are described using linguistic scenario notation (Menzel et al., 2018). A scene was defined as the unique environmental, target vehicle (i.e., the non-AV vehicle), and vehicle maneuver factors present at a specific point in time. A crash scenario was defined as the time progression of these different scenes. For this study, the basis of each crash scenario consisted of three primary scenes: pre-maneuver scene, critical maneuver scene, and post-maneuver scene. Due to testing constraints discussed further in Chapter 3, this study defined crash scenarios that are functionally similar to actual crashes, but with no actual crash event. As such, the post-maneuver scene was included as if no crash event occurred, and the vehicles continued past each other. Environmental and target vehicle factors were assumed to remain unchanged for each maneuver scene but were specific for each crash scenario.

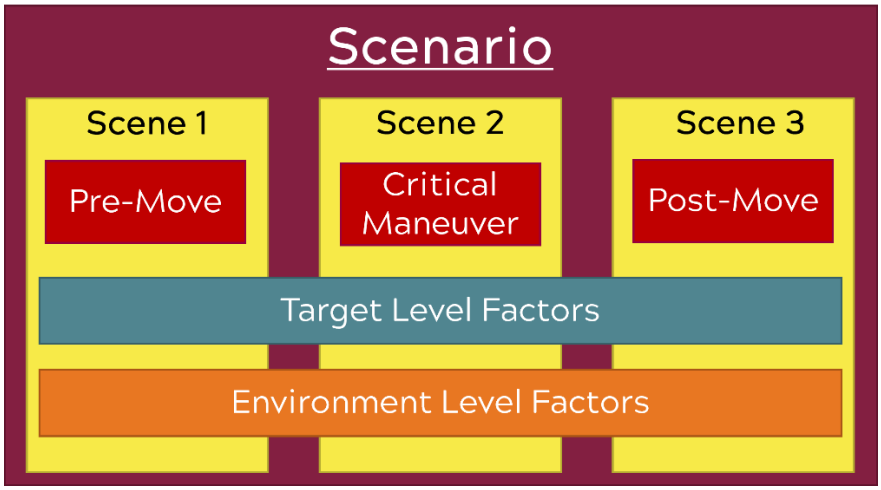

Figure 6. Scenario generation template

2.3.2 Selected Data Elements and Scenario Element Characterization

Within CRSS, there exists a large number of coded data elements used to describe various aspects of the environment, actors/vehicles involved in each crash, and vehicle occupants. Many of these can be used during crash scenario creation and this study considered data elements that were determined to be most relevant to high level scenario description, and/or data elements that are known to have influence on ADS perception system performance (e.g., weather effects). A list of all CRSS data elements used to characterize the target population, along with relevance to the scenario generation template, is shown in Table 4. A list of all data elements used in this thesis (including filtering) along with detailed data element definitions is also referenced in Appendix A.

Characterization was done by calculating the weighted proportion of crashes for each level coded within a selected data element. The goal was to determine the relative frequency of each element level within the crash population in order to choose the element levels that represent a high proportion of the selected crashes.. The weighted proportion of each element level was calculated for two datasets: one which included all the selected target population crashes, and another which only included the MAIS2+F crashes. This was done to represent the probability of exposure in any possible crash separately from the probability of exposure in a minor to fatal injury causing crash as non-injury causing crashes are over-represented within the selected target population.

Table 4. List of CRSS data elements used for scenario characterization

Maneuver Factors		Target Factors		Environmental Factors	
CRSS Element	SAS Variable	CRSS Element	SAS Variable	CRSS Element	SAS Variable
Generalized Crash Type	ACC_TYPE	Travel Speed	TRAV_SP	Lighting Condition	LGT_COND
		NCSA Body Type	BODY_TYPE	Weather Condition	WEATHER
				Type of Intersection	TYP_INT
				Number of Travel Lanes	VNUM_LAN
				Roadway Alignment	VALIGN
				Roadway Grade	VPROFILE
				Driver's Vision Obscured By…	MVISOBSC
				Trafficway Description	VTRAFWAY
				Traffic Control Device	VTRAFCON

2.3.3 Assigning Vehicle Roles

Within each crash, each vehicle was assigned the role of either the traveling through vehicle or the turning vehicle. The traveling through vehicle was the vehicle driving straight through the intersection and was assumed to have the right-of-way in the scenario. The turning vehicle was defined as the other vehicle in the scenario. In most cases, this vehicle was performing some type of turning maneuver in front of the traveling through vehicle and failed to yield causing the crash. In certain crash modes (e.g., rear end collisions) this vehicle may not turning however this label still applied. Vehicle roles were assigned using the generalized crash type variable that is coded as part of CRSS. This study assumed that the traveling through vehicle was the hypothetical AV, and the turning vehicle was a human driver. This also assumed that the AV is operating without fault in these scenarios, and that the human driver (turning vehicle) makes some type of error and encroaches into the path of the AV (traveling through vehicle).

2.3.4 Calculating Probability of Crash Scenario Exposure

The probability of exposure to a specific crash scenario within a future population of crashes was computed as the probability of the crash scenario appearing within the selected target population. To compute this, this study first assumed that all maneuver, target vehicle, and environmental scenario factors are independent of each other (i.e., no elements influenced the probability of other elements occurring

within a crash scenario). The probability of exposure to a crash scenario was then computed as the joint probability of occurrence for all maneuver, target, and environmental factors (Equations 2-5). Probability of scenario exposure was calculated for two populations: the probability of crash scenario exposure within the entire target population, and the probability of crash scenario exposure within crashes of the same crash maneuver. Within each population, the probability of exposure within any crash and the probability of exposure within an injury causing crash was computed.

Exposure was computed as the probability of exposure to all functionally similar crash scenarios. Two crash scenarios were defined as being functionally similar if they were different by one or more scenario factors, however the effect of these differences on perception system performance was expected to be negligible. For example, certain crash types occurring at a 4-way intersection can be assumed to be functionally similar to the exact same crash happening at a T-intersection. This was done to achieve a conservative measure of scenario exposure as it would include more variations within a scenario. Maneuver, target, and environmental level factors were categorized as having "1 – No Influence", 2 – Possible Influence", and "3 – Large Influence" on overall perception system performance (Table 5). Factors with no assumed influence were allowed to vary when defining each scenario and probability of scenario exposure was calculated using Equations 2-5.

$$P_{Maneuver} = P_{Crash\ Type} \quad (2)$$

$$P_{Target} = P_{Rel\ Speed} \cdot P_{Body\ Type} \quad (3)$$

$$P_{Environment} = P_{Light} \cdot P_{Weather} \cdot P_{Inter} \cdot P_{Num\ Lane} \cdot P_{Road\ Align} \cdot P_{Road\ Grade} \cdots P_{Sightline} \cdot P_{Traffic\ Desc} \cdot P_{Traffic\ Contr} \quad (4)$$

$$P_{Scenario} = P_{Maneuver} \cdot P_{Target} \cdot P_{Environment} \quad (5)$$

Table 5. Categorization of scenario factors based on possible influence on perception system performance

Scenario Factor	Level of Influence on Perception System Performance	Comments
Type of Intersection	1-No Influence	Functionally, different intersection types can be similar. For example, vehicles that approach each other laterally may perform the same maneuver regardless of intersection type.
Number of Lanes	1-No Influence	As the number of lanes increases the size of the intersection increases and distances between each vehicle may increase although this is likely to have little or no effect due to the operating ranges of sensors.
Trafficway Description	1-No Influence	As long as roadway divisions do not block sightlines between the vehicles, effect on performance is assumed to be small
Traffic Control	1-No Influence	Traffic control, although important for evaluation of the motion planning system, is assumed to have little influence on perception system operation
Relative Travel Speed	2-Possible Influence	Within each scenario, the relative speed between the vehicles dictates multiple aspects such as time that the AV has to perceive the other vehicle as well as motion of the background and other road users.
Turning Vehicle Body Type	2-Possible Influence	Different vehicle body types represent different possible profiles for the perception system.
Roadway Alignment	2-Possible Influence	Influence on performance is dependent on the severity of the alignment. Large curves may block the sightline between the vehicles however slight curves may not.
Roadway Grade	2-Possible Influence	Similar to roadway alignment, the level of roadway grade may affect performance if the sightline between the vehicles is blocked.
Critical Maneuver	3-Large Influence	Crash maneuver dictates many aspects of the scenario such as distance between vehicles, what parts of the AV's FOV is being used, and the profile of the other vehicle within this FOV.
Lighting Condition	3-Large Influence	Due to the expected widespread use of cameras in ADS perception systems, the direction and level of the lighting condition could have large effects on performance.
Weather Condition	3-Large Influence	Similar to lighting condition, inherent limitations of different sensors in various adverse weather conditions could have large effects on performance.
Sightline Obstructions	3-Large Influence	Sightline obstructions, or situations where a sensor(s) cannot physically detect the other vehicle would have large effects on performance due to loss of information.

2.4 Results

Results are presented for each of the main scene components: maneuver level factors, target vehicle level factors, and environmental level factors.

2.4.1 Maneuver Level Factors

The maneuver level factors consisted of the pre-movement, critical movement, and the post-movement of the turning vehicle with respect to the traveling through vehicle. In this study, the pre-movement and post-movement of the turning vehicle was assumed to be traveling straight as this information was not available as part of CRSS in the case of pre-movement not immediately before the crash. The basis for the critical movement was the generalized crash type variable (SAS variable ACC_TYPE) from CRSS. This represented the movement that the turning vehicle makes during the crash scenario. Figure 7 and Table 6 show the breakdown of crash type for the selected target population. Just over 50% of the selected crashes involved some kind of same direction rear-end crash. The majority of the rest of the selected crashes (48%) involved either a turn across path, turn into path, or straight across path crash maneuver. Crashes involving an MAIS2+F injury predominantly involved these latter crash types with the rear-end crashes representing the rest of the injury crashes.

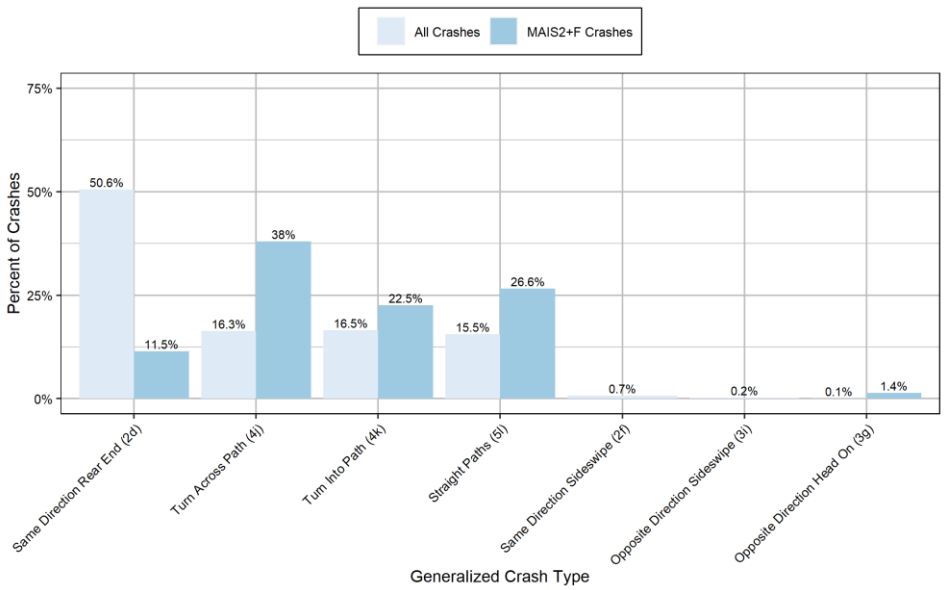

Figure 7. Generalized crash maneuvers for all selected crashes and all selected MAIS2+F crashes

Table 6. Breakdown of Generalized Crash Maneuver

Crash Type	Percent of Selected Crashes	Percent of MAIS2+F
Same Direction Rear End	50.59%	11.47%
Turn Into Path	16.51%	22.54%
Turn Across Path	16.32%	37.96%
Straight Paths	15.55%	26.61%
Same Direction Sideswipe	0.71%	0.00%
Opposite Direction Sideswipe	0.21%	0.00%
Opposite Direction Head On	0.09%	1.42%

Specific crash maneuver was further defined for the four crash maneuvers with the highest proportion of the selected crashes as the remaining crash modes represented only 1% of crashes/injuries and were excluded. Specific crash maneuver was coded based on the PC23 Crash diagram included as part of CRSS (NHTSA 2022).

Figure 8 and Table 7 show the three specific crash modes within the "Same Direction, Rear End" crash type. Crashes in which the lead vehicle (turning vehicle) was stopped in the lane of travel represented the majority of the crashes and injuries (45.17% and 9.47% respectfully).

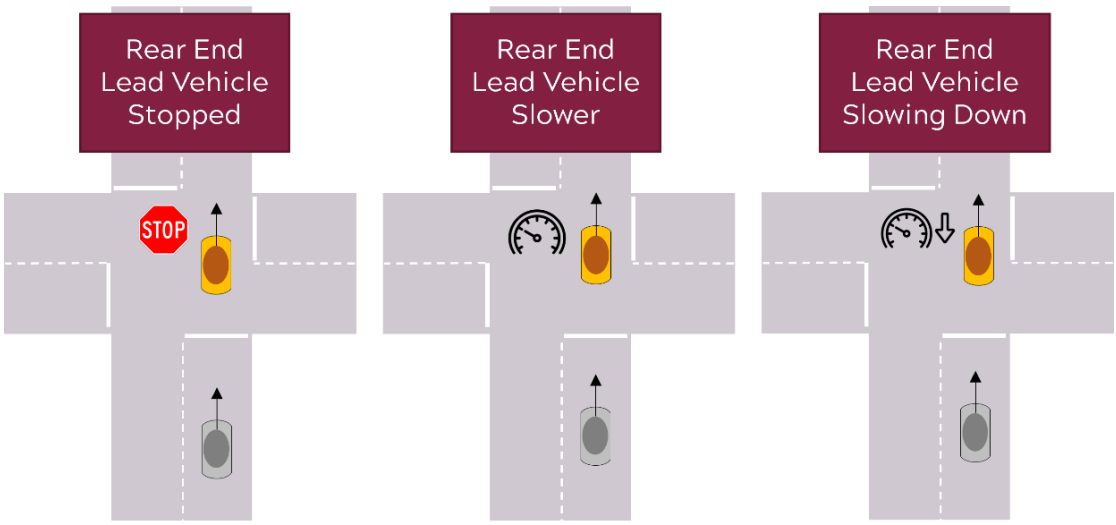

Figure 8. Specific crash modes within "Same Direction, Rear End" crash type

Table 7. Breakdown of "Same Direction, Rear End" Crash Type

Crash Type	Percent of Selected Crashes	Percent of MAIS2+F
Lead Vehicle Stopped	45.17%	9.47%
Lead Vehicle Slower	2.58%	2.0%
Lead Vehicle Slowing Down	2.83%	0%

Figure 9 and Table 8 show the four specific crash modes within the "Turn Into Path" crash type. Crashes in which the turning vehicle turned into the traveling vehicles opposite direction from the right side represented the majority of the crashes and injuries (8.39% and 20.11%).

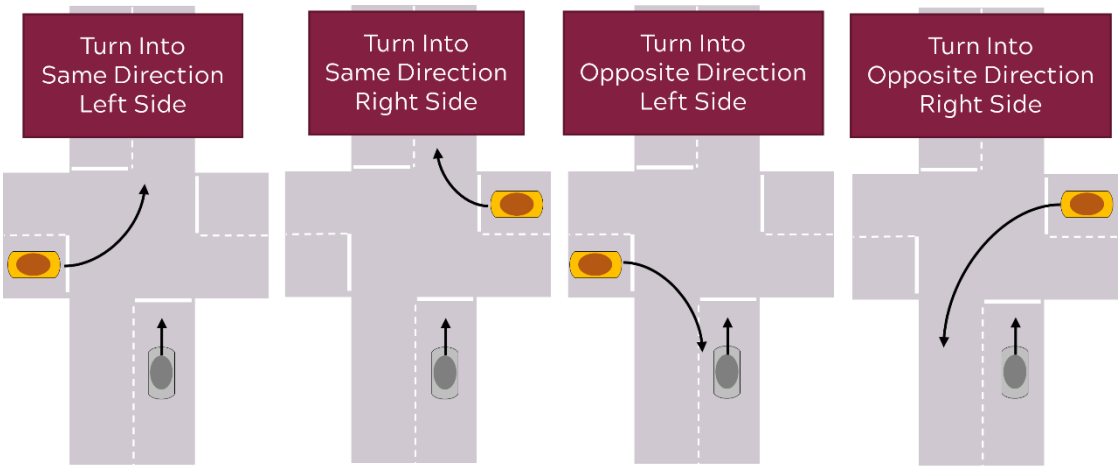

Figure 9. Specific crashes modes within "Turn Into Path" crash type

Table 8. Breakdown of "Turn Into Path" Crash Type

Crash Type	Percent of Selected Crashes	Percent of MAIS2+F
Turn Into Same Direction Left Side	3.0%	0.0%
Turn Into Same Direction Right Side	3.83%	1.36%
Turn Into Opposite Direction Left Side	1.29%	1.08%
Turn Into Opposite Direction Right Side	8.39%	20.11%

Figure 10 and Table 9 show the three specific crash modes within the "Turn Across Path" crash type. Crashes involving a left turn across path from the opposite direction represented the majority of the crashes and injuries (13.89% and 37%).

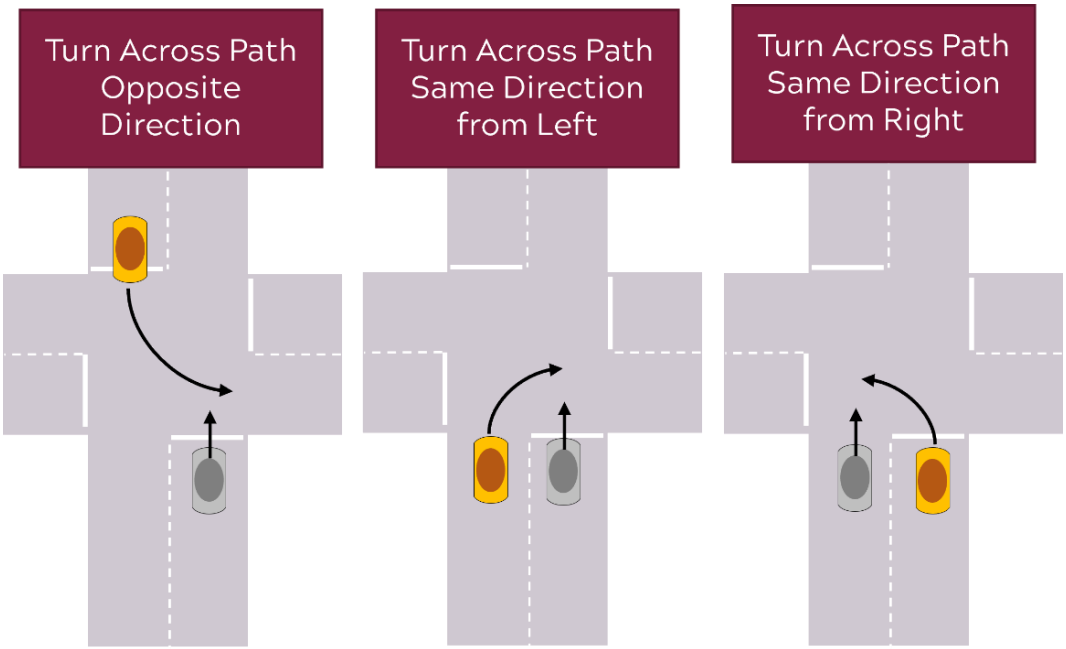

Figure 10. Specific crashes modes within "Turn Across Path" crash type

Table 9. Breakdown of "Turn Across Path" Crash Type

Crash Type	Percent of Selected Crashes	Percent of MAIS2+F
Turn Across Path Opposite Direction	13.89%	37.0%
Turn Across Path Same Direction, Left	1.08%	0.0%
Turn Across Path Same Direction, Right	1.35%	0.95%

Figure 11 and Table 10 shows the two specific crash modes within the "Straight Paths" crash type. An equal proportion of vehicles originating from the right and left was seen for all selected crashes. Crashes in which the turning vehicle approached from the left side represented a much higher proportion of injuries (17.56%) than when the vehicle approached from the right side (9.04%).

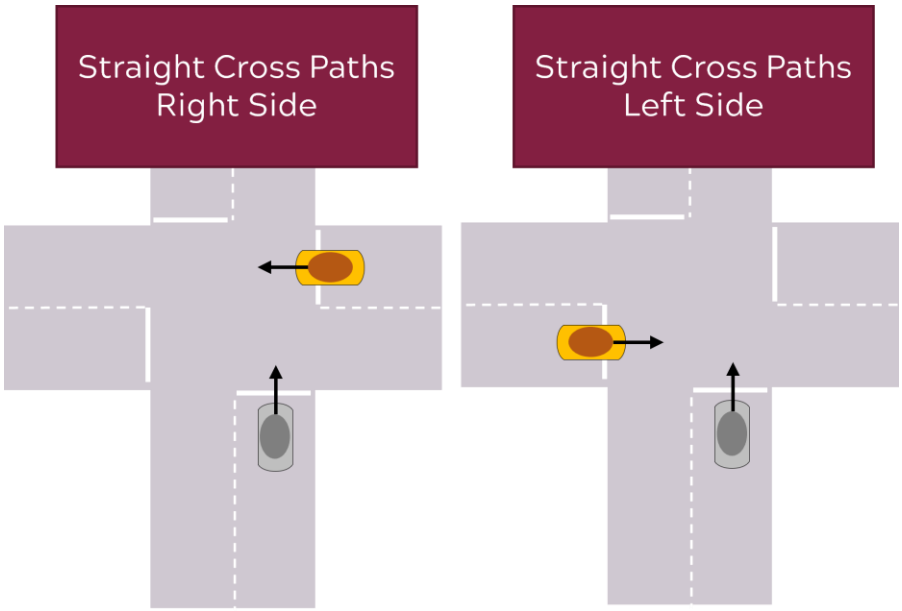

Figure 11. Specific crashes modes within "Straight Paths" crash type

Table 10. Breakdown of "Straight Paths" Crash Type

Crash Type	Percent of Selected Crashes	Percent of MAIS2+F
Straight Crossing Paths Right Side	7.87%	9.04%
Straight Crossing Paths Left Side	7.68%	17.56%

In summary, five main crash maneuvers were identified as being most prevalent: Rear End (lead vehicle stopped), Left Turn Across Path from the Opposite Direction (LTAP/OD), Left Turn Across Path from the Right Side Lateral Direction (LTAP/LD), and Left/Right Straight Crossing Paths (LSCP, RSCP). Crashes that involved one of these crash maneuvers represented 83% of the selected crashes and 93.16% of the selected maximum injured occupants. As such, the probability that a future AV may encounter any one of these scenarios (given a crash scenario happens) is likely to be high. These crash modes were used as the basis for each crash scenario, with the target and environmental factors being characterized within each crash mode (reported within tables) as well as within the entire crash population (reported within figures).

2.4.2 Target Vehicle Level Factors

Target vehicle level factors consisted of a description of the turning vehicle body classification as well as vehicle travel speed for both the traveling through vehicle and the turning vehicle as recorded in CRSS. The combination of the two travel speeds provides a measure of relative speed between the vehicles in each crash.

The distribution of travel speeds for each vehicle, broken out by maneuver type defined in the previous section (SCP left and right grouped together), for all selected crashes and all selected injury crashes are shown in Figure 12. Binned travel speeds are shown in Table 11. Within all crashes, median travel speed was between 10 to 25mph for the turning vehicle and 15 to 35mph for the traveling through vehicle. In all injury crashes, median travel speed was similar in the turning vehicle but was higher in the traveling through vehicle (between 35 and 40 mph).

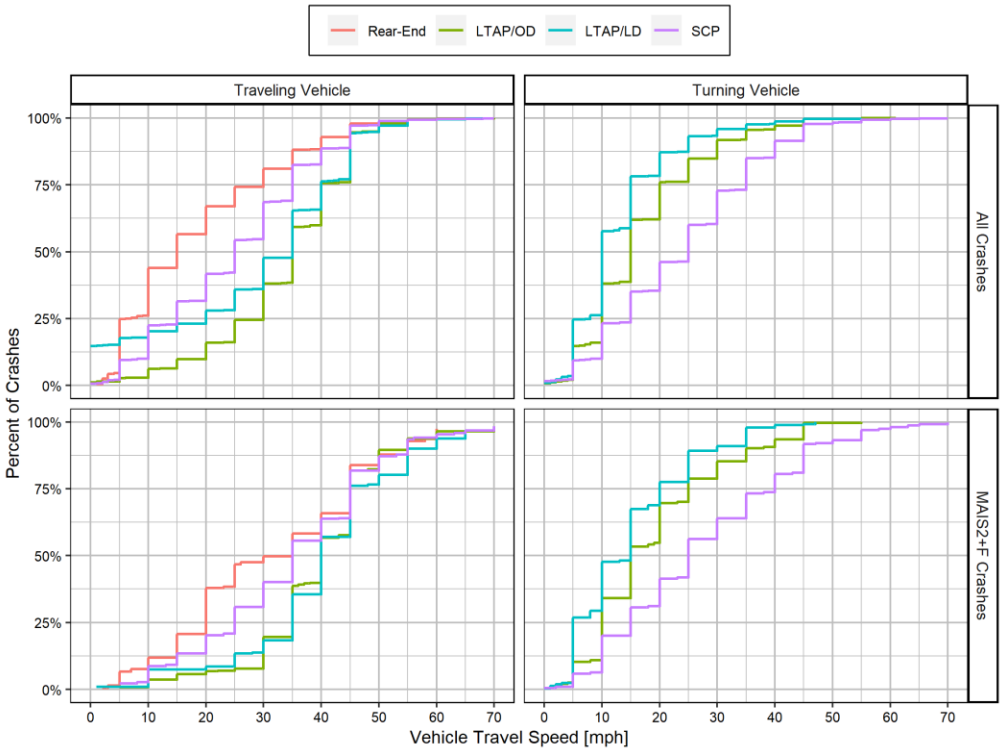

Figure 12. Cumulative distribution of vehicle travel speed in all selected crashes and all injury crashes

Table 11. Binned travel speed for the traveling through and turning vehicles

Traveling Through Vehicle								
	Rear-End		LTAP/OD		LTAP/LD		SCP	
	Crashes	MAIS2+F	Crashes	MAIS2+F	Crashes	MAIS2+F	Crashes	MAIS2+F
0-25 mph	74.21%	46.67%	24.47%	7.77%	35.93%	13.44%	54.37%	30.85%
25-50 mph	24.52%	41.15%	73.6%	81.67%	61.25%	66.78%	44.43%	56.31%
50-75 mph	1.17%	12.18%	1.86%	8.29%	2.74%	17%	1.04%	12.05%
75+ mph	0.1%	0%	0.08%	2.27%	0.08%	2.79%	0.17%	0.79%
Turning Vehicle								
	Rear-End		LTAP/OD		LTAP/LD		SCP	
	Crashes	MAIS2+F	Crashes	MAIS2+F	Crashes	MAIS2+F	Crashes	MAIS2+F
0-25 mph	100%	100%	84.8%	78.82%	93.14%	89.15%	60.02%	56.2%
25-50 mph	0%	0%	14.93%	20.77%	6.59%	10.85%	38.29%	36.87%
50-75 mph	0%	0%	0.27%	0.42%	0.27%	0%	1.55%	6.67%
75+ mph	0%	0%	0%	0%	0%	0%	0.15%	0.27%

The breakdown of turning vehicle body type is shown in Figure 13. Body type was characterized using the vPIC body type classification listed in Appendix C of the CRSS Analytical User's Manual (NHTSA 2022). Within the selected crashes, the turning vehicle was predominantly a sedan passenger vehicle (48.8%). Sport Utility vehicles represented the next highest proportion of selected crashes (23.4%). The proportion of all crashes with a certain body type was also similar to all injury crashes.

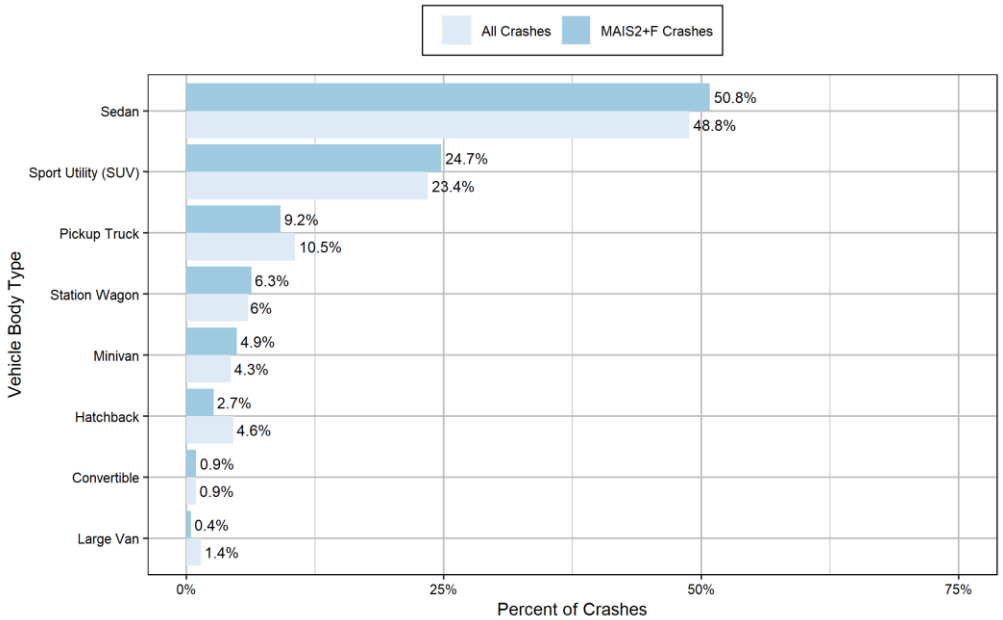

Figure 13. Turning vehicle body type classification

Table 12. Turning vehicle body-type

	Rear-End		LTAP/OD		LTAP/LD		SCP	
	Crashes	MAIS2+F	Crashes	MAIS2+F	Crashes	MAIS2+F	Crashes	MAIS2+F
Sedan	46.6%	40.69%	53.18%	56.13%	49.02%	55.92%	50.92%	50.89%
Sport Utility (SUV)	25.65%	29.54%	19.98%	18.3%	22.19%	23.39%	21.56%	25.25%
Pickup Truck	10.07%	12.16%	10.02%	7.78%	12.1%	9.41%	11.65%	7.66%
Station Wagon	6.25%	7.82%	5.31%	7.61%	6.62%	4.49%	5.13%	6.04%
Minivan	4.68%	8.64%	4.85%	4.5%	3.34%	2.98%	4.05%	4.35%
Hatchback	4.12%	0.5%	4.69%	4.01%	5.49%	1.89%	4.79%	3.98%
Large Van	1.53%	0%	1.16%	0.4%	0.72%	0.78%	0.95%	0.84%
Convertible	1.1%	0%	0.81%	1.26%	0.52%	1.14%	0.95%	1%

2.4.3 Environmental Level Factors

Environmental level scene factors were used to describe the scenario surroundings and environment factors present and consisted of the following: lighting, weather, type of intersection, number of lanes present for each vehicle, roadway alignment for each vehicle, roadway grade for each vehicle, recorded sightline obstructions for each vehicle, trafficway description for each vehicle, and traffic control present for each vehicle. These variables provided a high-level description of the environment that each of the vehicles was operating in.

Table 13 and Figure 14 show the breakdown of the general environmental factors: lighting condition, weather condition, and type of intersection. These factors were the same for both vehicles in each crash. Crashes typically occurred at either a four-way intersection or at a T-intersection. Crashes also predominately occurred during clear/cloudy weather and during daylight conditions. A large proportion of the injury crashes also occurred during dark lighted conditions (22.6%). These trends were also similar, although varied across the four main crash modes. LTAP/OD and SCP crash predominantly occurred in 4-way intersections whereas Rear-End and LTAP/LD occurred at both.

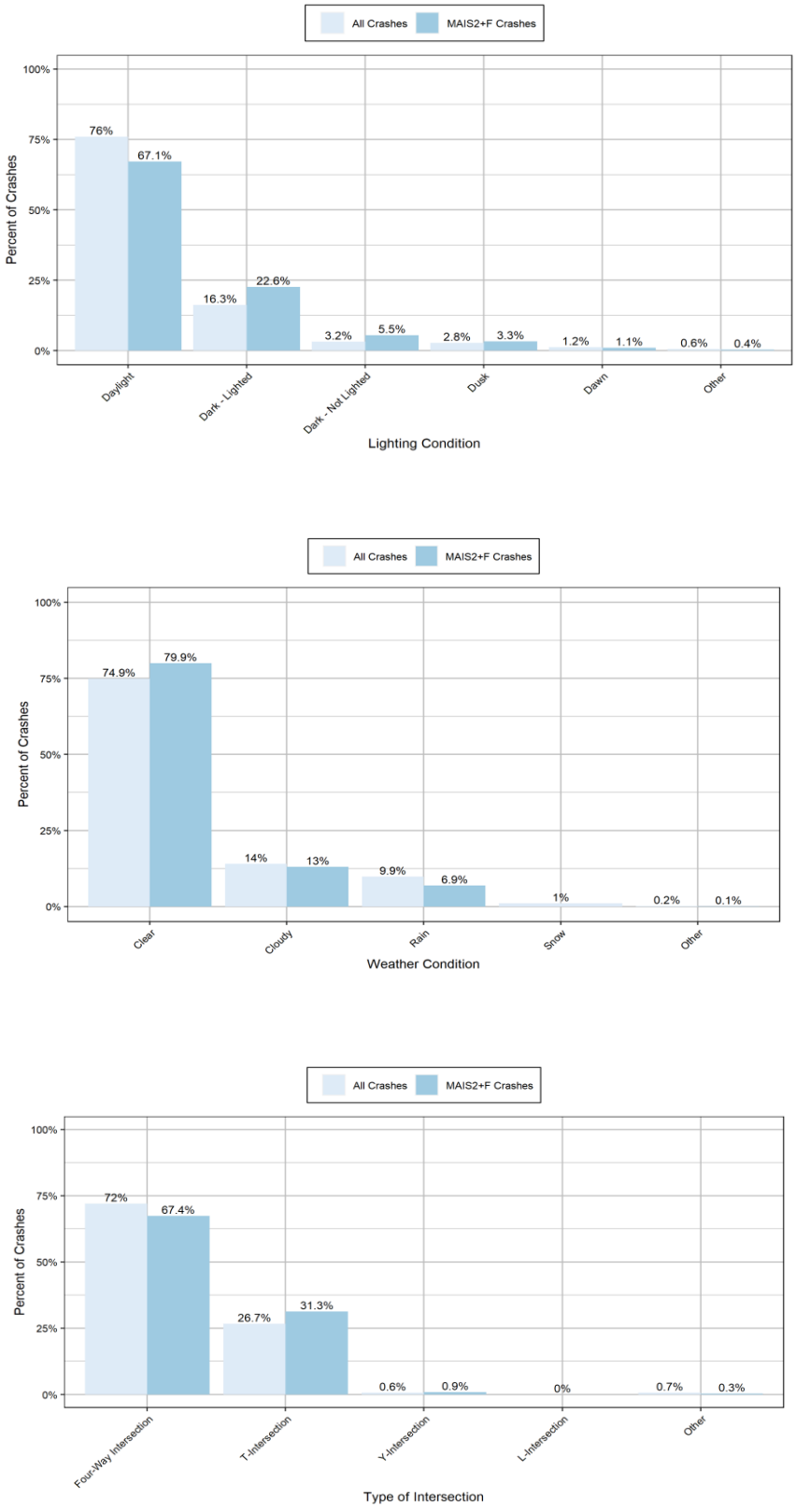

Figure 14. Breakdown of lighting condition (top), weather condition (middle), and type of intersection (bottom) for all crashes and all injury crashes

Table 13. Breakdown of lighting condition, weather condition, and type of intersection

Lighting Condition								
	Rear-End		**LTAP/OD**		**LTAP/LD**		**SCP**	
	Crashes	MAIS2+F	Crashes	MAIS2+F	Crashes	MAIS2+F	Crashes	MAIS2+F
Daylight	78.51%	81.47%	66.35%	59.44%	76.25%	68.07%	77.53%	67.41%
Dark-Lighted	14.3%	11.15%	24.98%	30.61%	14.1%	22.55%	15.6%	22.53%
Dark-Not Lighted	3.51%	3.7%	3.3%	5.88%	4.07%	7.2%	1.98%	5.53%
Dusk	2.29%	2.68%	3.26%	2.77%	3.08%	1.51%	3%	2.71%
Dawn	0.98%	1%	1.63%	0.9%	1.81%	0.67%	1.39%	1.35%
Other	0.41%	0%	0.48%	0.4%	0.69%	0%	0.49%	0.47%
Weather Condition								
	Rear-End		**LTAP/OD**		**LTAP/LD**		**SCP**	
	Crashes	MAIS2+F	Crashes	MAIS2+F	Crashes	MAIS2+F	Crashes	MAIS2+F
Clear	72.58%	86.56%	80.01%	76.35%	76.45%	74.58%	75.47%	80.66%
Cloudy	15.55%	10.07%	11.31%	13.12%	12.64%	20.68%	14.03%	11.58%
Rain	10.48%	3.38%	8.04%	10.53%	9.7%	4.74%	9.28%	7.29%
Snow	1.26%	0%	0.39%	0%	0.83%	0%	1.1%	0%
Other	0.13%	0%	0.26%	0%	0.39%	0%	0.13%	0.47%
Type of Intersection								
	Rear-End		**LTAP/OD**		**LTAP/LD**		**SCP**	
	Crashes	MAIS2+F	Crashes	MAIS2+F	Crashes	MAIS2+F	Crashes	MAIS2+F
4-Way Intersection	72%	52.04%	76.32%	68.68%	48.63%	54.64%	93.57%	95.12%
T-Intersection	26.55%	45.61%	22.83%	30.2%	50.62%	45.04%	5.24%	4.88%
Y-Intersection	0.77%	2.35%	0.41%	0%	0.5%	0.32%	0.28%	0%
L-Intersection	0%	0%	0%	0%	0.1%	0%	0%	0%
Other	0.68%	0%	0.45%	1.12%	0.14%	0%	0.915	0%

Figure 15 shows the breakdown of the vehicle specific environmental factors: number of lanes present, roadway alignment, roadway grade, recorded sightline obstructions, trafficway description, and traffic control that was present. Typically, crashes occurred on straight, level roadways with between two and six lanes and no sightline obstructions for either driver. Roadways were typically two-way with and without division. When present, traffic controls were either a traffic light or a stop sign. Results were generally similar between all crashes and all injury crashes. Results were also similar for each vehicle. Table 14 and Table XX show a breakdown of factors for the traveling through and turning vehicle. Like before, trends were similar although varied across the crash types.

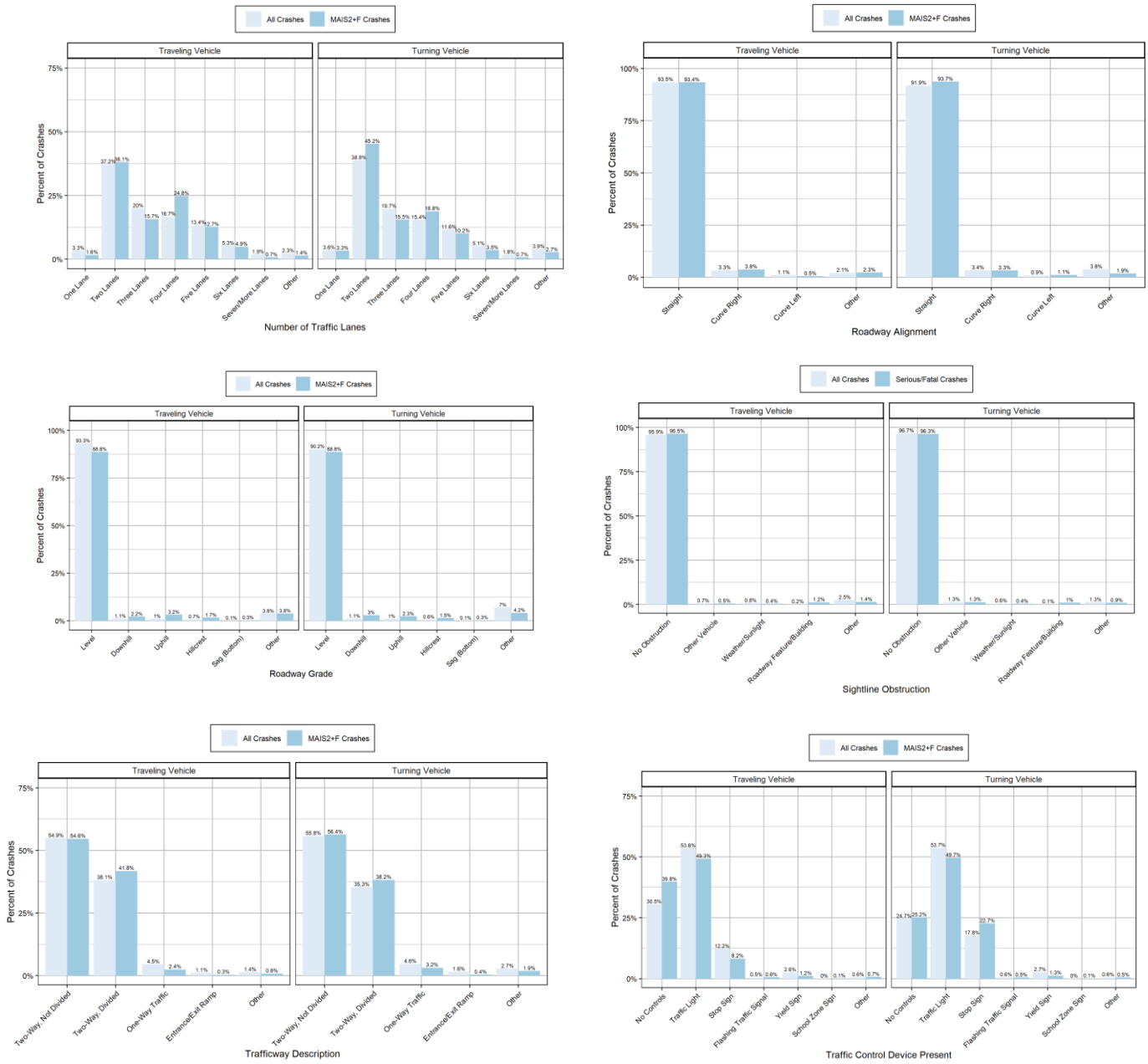

Figure 15. Breakdown of number of traffic lanes, roadway alignment, roadway grade, sightline obstructions, trafficway description, and traffic control present for the traveling through vehicle and the turning vehicle

Table 14. Breakdown of number of traffic lanes, roadway alignment, roadway grade, sightline obstructions, trafficway description, and traffic control present for the traveling through vehicle

Number of Traffic Lanes								
	Rear-End		**LTAP/OD**		**LTAP/LD**		**SCP**	
	Crashes	MAIS2+F	Crashes	MAIS2+F	Crashes	MAIS2+F	Crashes	MAIS2+F
One Lane	5.88%	5.18%	0.4%	0.79%	0.55%	0%	1.43%	0.26%
Two Lanes	31.28%	45.34%	23.28%	18.72%	46.47%	44.2%	57.18%	52.57%
Three Lanes	21.93%	8.75%	21.72%	19.78%	16.12%	22.9%	13.74%	9.79%
Four Lanes	17.44%	25.48%	23.68%	36.03%	15.53%	9.46%	9.49%	19.95%
Five Lanes	15.24%	9.27%	18.74%	16.35%	13.46%	16.6%	7.16%	9.98%
Six Lanes	5.86%	5.49%	7.35%	5.6%	3.66%	4.65%	2.71%	3.65%
Seven+ Lanes	2.14%	0.25%	3.34%	1.62%	1.4%	0%	0.45%	0.75%
Other	0.23%	0.22%	1.49%	1.11%	2.81%	2.19%	7.84%	3.05%
Roadway Alignment								
	Rear-End		**LTAP/OD**		**LTAP/LD**		**SCP**	
	Crashes	MAIS2+F	Crashes	MAIS2+F	Crashes	MAIS2+F	Crashes	MAIS2+F
Straight	92.27%	87.36%	98.64%	97.42%	94.59%	96.76%	89.17%	90.94%
Curve Right	6.45%	12.41%	0.28%	2.06%	2.32%	1.62%	0.54%	0%
Curve Left	1.12%	0%	0.5%	0.52%	2.52%	0.70%	0.48%	0.53%
Other	0.16%	0.22%	0.59%	0%	0.56%	0.92%	9.27%	8.54%
Roadway Grade								
	Rear-End		**LTAP/OD**		**LTAP/LD**		**SCP**	
	Crashes	MAIS2+F	Crashes	MAIS2+F	Crashes	MAIS2+F	Crashes	MAIS2+F
Level	96.04%	84.67%	97.7%	94.53%	90.98%	89.5%	81.8%	84.13%
Downhill	1.4%	5.73%	0.53%	0.95%	1.59%	1.62%	0.61%	0.47%
Uphill	1.35%	6.31%	0.62%	3.51%	1.28%	1.07%	0.56%	1.35%
Hillcrest	0.93%	1.85%	0.4%	1%	0.64%	5.27%	0.45%	0.59%
Sag (Bottom)	0.13%	1.22%	0.02%	0%	0.08%	0%	0.03%	0%
Other	0.16%	0.22%	0.72%	0%	5.43%	2.54%	16.55%	13.46%
Sightline Obstructions								
	Rear-End		**LTAP/OD**		**LTAP/LD**		**SCP**	
	Crashes	MAIS2+F	Crashes	MAIS2+F	Crashes	MAIS2+F	Crashes	MAIS2+F
No Obstruction	94.99%	96.36%	97.85%	97.74%	97.27%	93.63%	94.55%	95.82%
Other Vehicle	0.12%	0%	1.54%	0.75%	1.34%	1.1%	1.41%	0.52%
Weather/Sunlight	0.82%	1%	0.26%	0.4%	0.76%	0%	1.25%	0.23%
Roadway Feature/Building	0.1%	0.32%	0%	0%	0.24%	5.27%	0.49%	1.31%
Other	3.96%	2.23%	0.35%	1.11%	0.39%	0%	2.3%	2.13%
Trafficway Description								
	Rear-End		**LTAP/OD**		**LTAP/LD**		**SCP**	
	Crashes	MAIS2+F	Crashes	MAIS2+F	Crashes	MAIS2+F	Crashes	MAIS2+F
Two-Way, Not Divided	50.77%	54.38%	48.44%	44.18%	66.41%	53.85%	67.55%	67.5%

Two-Way, Divided	41.94%	38.73%	50.81%	55.82%	31.62%	45.37%	19.84%	24.64%
One-Way	5.21%	5.26%	0.08%	0%	0%	0%	6.35%	5.18%
Entrance/Exit Ramp	1.96%	1.41%	0%	0%	0.1%	0%	0.59%	0%
Other	0.12%	0.22%	0.67%	0%	1.87%	0.77%	5.67%	2.67%
Traffic Control Device								
	Rear-End		**LTAP/OD**		**LTAP/LD**		**SCP**	
	Crashes	MAIS2+F	Crashes	MAIS2+F	Crashes	MAIS2+F	Crashes	MAIS2+F
No Controls	21.3%	39.15%	29.35%	28.74%	55.04%	61.62%	27.58%	32.23%
Traffic Light	64.38%	51.03%	67.69%	70.25%	29.83%	29.46%	34.68%	38.99%
Stop Sign	8.58%	4.66%	2.73%	0.53%	12.9%	6.87%	34.04%	24.6%
Flashing Signal	0.34%	0%	0.15%	0%	0.36%	0.7%	1.69%	2.11%
Yield Sign	5.21%	4.94%	0%	0%	0.15%	0%	0.41%	0%
School Zone	0.02%	0%	0.01%	0.48%	0%	0%	0.12%	0%
Other	0.17%	0.22%	0.07%	0%	1.72%	1.35%	1.48%	2.08%

Table 15. Breakdown of number of traffic lanes, roadway alignment, roadway grade, sightline obstructions, trafficway description, and traffic control present for the turning vehicle

Number of Traffic Lanes								
	Rear-End		**LTAP/OD**		**LTAP/LD**		**SCP**	
	Crashes	MAIS2+F	Crashes	MAIS2+F	Crashes	MAIS2+F	Crashes	MAIS2+F
One Lane	6.07%	5.18%	0.51%	0.98%	1.82%	6.95%	1.32%	1.84%
Two Lanes	31.38%	45.34%	20.93%	16.34%	55.81%	72.3%	60.05%	62.8%
Three Lanes	21.91%	8.75%	22.93%	21.35%	15.41%	12.04%	14.36%	15.97%
Four Lanes	17.53%	25.71%	24.09%	33.68%	6.25%	1.19%	8.62%	7.98%
Five Lanes	14.99%	9.27%	18.56%	19.47%	2.22%	0%	5.25%	6.05%
Six Lanes	5.95%	5.49%	7.46%	6.0%	1.83%	0%	2.79%	1.38%
Seven+ Lanes	2.09%	0.25%	3.9%	1.65%	0.25%	0.47%	0.41%	0%
Other	0.09%	0%	1.63%	0.53%	16.41%	7.04%	7.19%	3.99%
Roadway Alignment								
	Rear-End		**LTAP/OD**		**LTAP/LD**		**SCP**	
	Crashes	MAIS2+F	Crashes	MAIS2+F	Crashes	MAIS2+F	Crashes	MAIS2+F
Straight	92.4%	87.59%	98.51%	97.71%	83.34%	94.43%	90.73%	94.98%
Curve Right	6.41%	12.41%	0.4%	0.17%	0.36%	0.7%	0.69%	0%
Curve Left	1.1%	0%	0.59%	2.12%	1.03%	0.35%	0.46%	1.33%
Other	0.09%	0%	0.5%	0%	15.26%	4.52%	8.13%	3.69%
Roadway Grade								
	Rear-End		**LTAP/OD**		**LTAP/LD**		**SCP**	
	Crashes	MAIS2+F	Crashes	MAIS2+F	Crashes	MAIS2+F	Crashes	MAIS2+F
Level	96.12%	84.61%	97.27%	94.53%	70.06%	85.69%	82.98%	88.39%
Downhill	1.38%	6.32%	0.54%	3.69%	0.79%	0.32%	1.07%	1.25%
Uphill	1.36%	6.31%	0.59%	0.78%	1.48%	0.0%	0.31%	1.35%
Hillcrest	0.93%	1.54%	0.47%	1.1%	0.27%	5.27%	0.24%	0%

Sag (Bottom)	0.13%	1.22%	0.02%	0%	0.29%	0%	0.14%	0%
Other	0.09%	0.0%	1.1%	0%	27.11%	8.72%	15.26%	9.01%
Sightline Obstructions								
	Rear-End		**LTAP/OD**		**LTAP/LD**		**SCP**	
	Crashes	MAIS2+F	Crashes	MAIS2+F	Crashes	MAIS2+F	Crashes	MAIS2+F
No Obstruction	99.73%	100%	92.01%	96.78%	92.36%	91.34%	96.38%	97.08%
Other Vehicle	0.01%	0%	4.32%	2.14%	3.55%	2.2%	1.42%	1.03%
Weather/Sunlight	0.24%	0%	1.06%	0.54%	1.5%	0%	0.53%	0%
Roadway Feature/Building	0%	0%	0%	0%	0.18%	5.27%	0.29%	0.84%
Other	0.03%	0%	2.61%	0.54%	2.42%	1.2%	1.38%	1.05%
Trafficway Description								
	Rear-End		**LTAP/OD**		**LTAP/LD**		**SCP**	
	Crashes	MAIS2+F	Crashes	MAIS2+F	Crashes	MAIS2+F	Crashes	MAIS2+F
Two-Way, Not Divided	50.76%	54.88%	50.35%	55.57%	68.52%	60.9%	68.57%	71.43%
Two-Way, Divided	41.89%	38.45%	48.76%	44.43%	15.29%	26.38%	19.61%	22.32%
One-Way	5.31%	5.26%	0.23%	0%	1.55%	7.14%	6.47%	3.04%
Entrance/Exit Ramp	1.95%	1.41%	0.07%	0%	2.91%	0%	0.43%	0.24%
Other	0.09%	0%	0.59%	0%	11.73%	5.57%	4.92%	2.97%
Traffic Control Device								
	Rear-End		**LTAP/OD**		**LTAP/LD**		**SCP**	
	Crashes	MAIS2+F	Crashes	MAIS2+F	Crashes	MAIS2+F	Crashes	MAIS2+F
No Controls	20.87%	40.03%	27.3%	26.03%	17.93%	3.45%	30.75%	20.37%
Traffic Light	64.86%	50.11%	68.27%	71.52%	28.14%	28.76%	34.44%	39.33%
Stop Sign	8.7%	4.66%	3.51%	1.62%	51.2%	67.07%	31.31%	36.74%
Flashing Signal	0.34%	0%	0.42%	0%	0.37%	0.7%	1.75%	1.63%
Yield Sign	5.22%	0%	0.24%	0%	0.11%	0%	0.28%	0.23%
School Zone	0.02%	0%	0.01%	0.48%	0%	0%	0.04%	0%
Other	0%	0%	0.24%	0.36%	2.26%	0%	1.43%	1.7%

2.5 Summary of Crash Scenarios

Based on the characterized crash population, five main crash scenarios were defined. The basis for each scenario was the specific crash type where the five crash modes with the highest proportions were chosen (rear-end, LTAP/OD, LTAP/LD, SCP Left and Right). The basis for target vehicle and environmental level factors were chosen based on the element proportions within each subset of crashes involving these maneuver types. Multiple factors were chosen if there was no assumed influence on perception performance and the factor that represented the highest proportion of crashes was chosen for factors with possible to large assumed influence. The five crash scenarios and the probability of exposure for each are summarized below.

Crash Scenario 1	
Description: Turning vehicle is stopped in travel lane. AV approaches at constant speed and passes on the left and turns back into the initial travel lane.	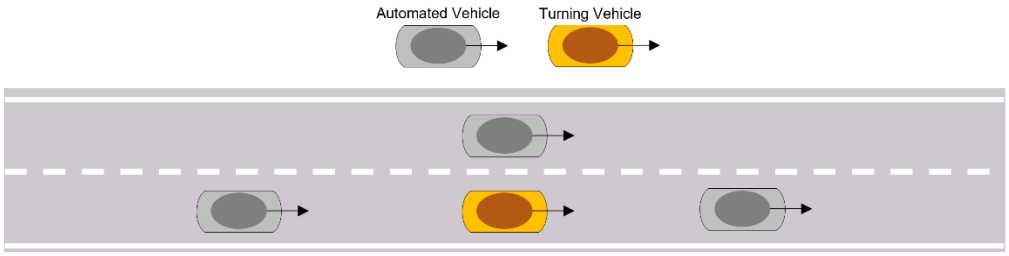

		All Target Population Crashes		All Target Population Rear-End Crashes	
	Factor Level(s)	**Crashes**	**MAIS2+F**	**Crashes**	**MAIS2+F**
Crash Maneuver	Rear-End (Stopped)	45.17%	9.47%	100%	100%
Target	0-25mph	51.5%	21.8%	74.21%	46.67%
	Sedan or SUV	72.2%	75.5%	72.25%	70.23%
Environmental	Daylight	76%	67.1%	78.51%	81.47%
	Clear Weather	74.9%	79.9%	72.58%	86.56%
	4-Way or T Intersection	98.7%	98.7%	98.55%	97.65%
	2,3,4, or 5 Lanes	87.3%	91.3%	85.89%	88.84%
	Straight Roadway	93.5%	93.4%	92.27%	87.36%
	Level Roadway	93.3%	88.8%	96.04%	84.67%
	No Visual Obstructions	95.9%	96.5%	94.99%	96.36%
	2-Way (Divided or Un-Divided)	93.0%	96.4%	92.71%	93.11%
	No Traffic Controls, Stop Sign, or Taffic Light	96.3%	97.3%	94.26%	94.84%
Probability of Crash Scenario Exposure		**0.062**	**0.006**	**0.190**	**0.126**

Crash Scenario 2	
Description: Both vehicles approach intersection from opposing lanes, turning vehicle turns left and proceeds into the lateral adjacent lane on the AVs right side.	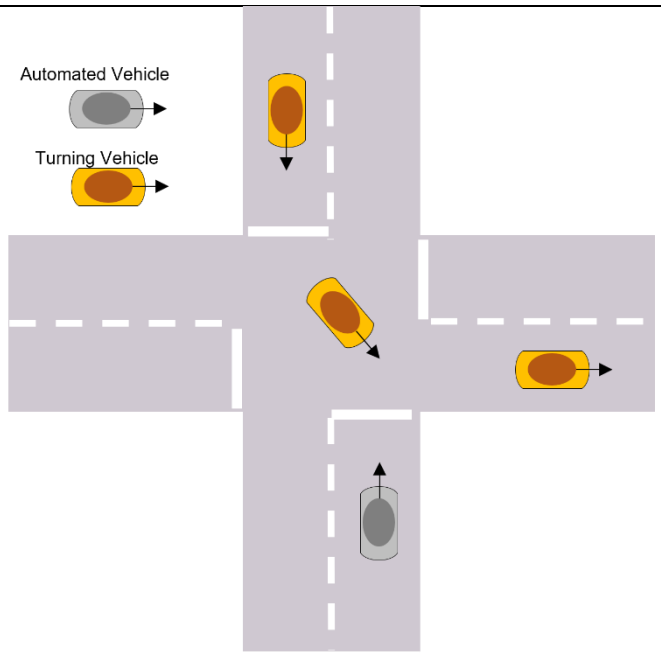

		All Target Poppulation Crashes		All Target Population LTAP/OD Crashes	
	Factor Level(s)	**Crashes**	**MAIS2+F**	**Crashes**	**MAIS2+F**
Crash Maneuver	LTAP/OD	13.89%	37%	100%	100%
Target	0-25mph	51.5%	21.8%	84.8%	78.82%
	Sedan or SUV	72.2%	75.5%	73.16%	74.43%
Environmental	Daylight	76%	67.1%	66.35%	59.44%
	Clear Weather	74.9%	79.9%	80.01%	76.35%
	4-Way or T Intersection	98.7%	98.7%	99.15%	98.88%
	2,3,4, or 5 Lanes	87.3%	91.3%	87.42%	90.88%
	Straight Roadway	93.5%	93.4%	98.64%	97.42%
	Level Roadway	93.3%	88.8%	97.7%	94.53%
	No Visual Obstructions	95.9%	96.5%	97.85%	97.74%
	2-Way (Divided or Un-Divided)	93.0%	96.4%	99.25%	100%
	No Traffic Controls, Stop Sign, or Taffic Light	96.3%	97.3%	99.77%	99.52%
Probability of Crash Scenario Exposure		**0.019**	**0.022**	**0.267**	**0.214**

Crash Scenario 3	
Description: Both vehicles approach intersection from lateral lanes, turning vehicle turns left and proceeds into the adjacent lane to the AVs left side.	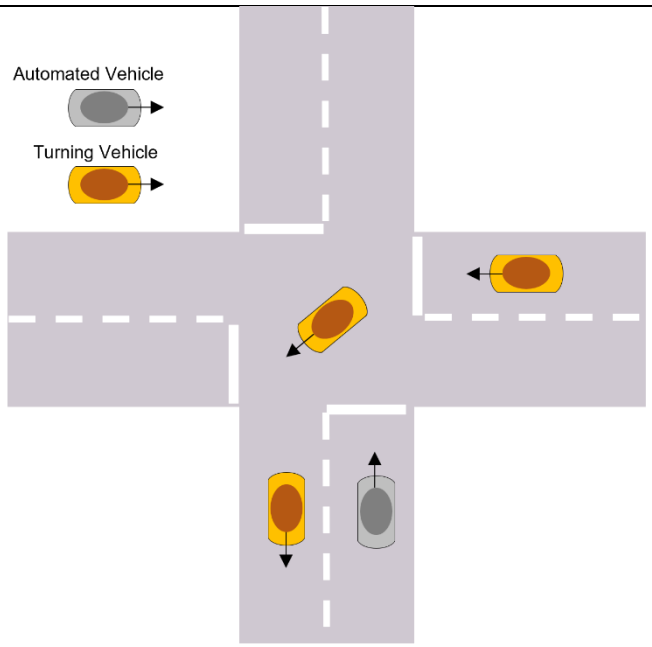

		All Target Poppulation Crashes		All Target Population LTAP/LD Crashes	
	Factor Level(s)	**Crashes**	**MAIS2+F**	**Crashes**	**MAIS2+F**
Crash Maneuver	LTAP/LD	8.39%	20.11%	100%	100%
Target	0-25mph	52%	23%	93.14%	89.15%
	Sedan or SUV	72.2%	75.5%	71.21%	79.31%
Environmental	Daylight	76%	67.1%	76.25%	68.07%
	Clear Weather	74.9%	79.9%	76.45%	74.58%
	4-Way or T Intersection	98.7%	98.7%	99.25%	99.68%
	2,3,4, or 5 Lanes	87.3%	91.3%	91.58%	93.16%
	Straight Roadway	93.5%	93.4%	94.59%	96.76%
	Level Roadway	93.3%	88.8%	90.98%	89.5%
	No Visual Obstructions	95.9%	96.5%	97.27%	93.63%
	2-Way (Divided or Un-Divided)	93.0%	96.4%	98.03%	99.22%
	No Traffic Controls, Stop Sign, or Taffic Light	96.3%	97.3%	97.77%	97.95%
Probability of Crash Scenario Exposure		**0.012**	**0.013**	**0.282**	**0.263**

Crash Scenario 4 & 5	
Description: Both vehicles approach intersection from lateral lanes, turning vehicle proceeds straight through the intersection and passes in front of the AV. Test is repeated with turning vehicle traveling from left/right side.	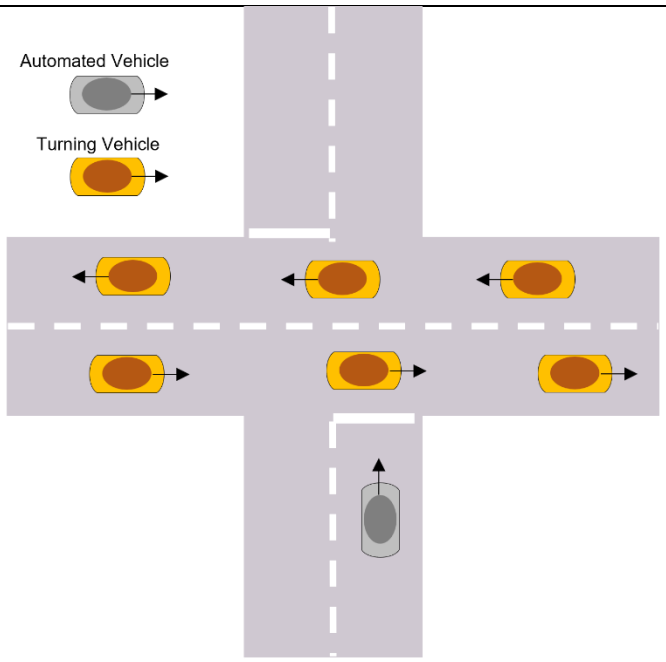

		All Target Poppulation Crashes		All Target Population SCP Crashes	
	Factor Level(s)	**Crashes**	**MAIS2+F**	**Crashes**	**MAIS2+F**
Crash Maneuver	SCP Left or Right	15.55%	26.6%	100%	100%
Target	0-25mph	52%	23%	60.02%	56.2%
	Sedan or SUV	72.2%	75.5%	72.48%	76.14%
Environmental	Daylight	76%	67.1%	77.53%	67.41%
	Clear Weather	74.9%	79.9%	75.47%	80.66%
	4-Way or T Intersection	98.7%	98.7%	98.81%	100%
	2,3,4, or 5 Lanes	87.3%	91.3%	87.57%	92.29%
	Straight Roadway	93.5%	93.4%	89.17%	90.94%
	Level Roadway	93.3%	88.8%	81.8%	84.13%
	No Visual Obstructions	95.9%	96.5%	94.55%	95.82%
	2-Way (Divided or Un-Divided)	93.0%	96.4%	87.39%	92.14%
	No Traffic Controls, Stop Sign, or Taffic Light	96.3%	97.3%	96.3%	95.82%
Probability of Crash Scenario Exposure		**0.021**	**0.017**	**0.128**	**0.139**

2.6 Discussion and Limitations

Within the target crash population, the majority of crashes involved one of five crash modes: Rear-End in which the lead vehicle is stopped, left turn across path from the opposite direction (LTAP/OD), left turn across path from the right lateral direction (LTAP/LD), and straight crossing paths from either the left or right side (SCP). This was the scenario factor that was found to vary the most within the crashes, whereas the environmental and target factors were found to be very similar across all crashes, as well as similar across the crash modes. Within each scenario level, one to two factors were consistently present across all the crash modes, with variations seen for a select few factors. This highlights that most of the environmental conditions, roadway layout, and turning vehicle characteristics were generally the same for a majority of the crashes within the target population.

However, the probability of exposure to one of the defined crash scenarios within the entire crash population was comparatively low. The total probability of exposure to any one of the five scenarios was 0.114 within all target population crashes and 0.058 within all target population injury crashes. This highlights that for the chosen scenario elements, while individual occurrence is high, the probability of all elements occurring within the same crash was low. Within crashes involving a specific maneuver, the probability of exposure to a scenario was comparatively higher. The lowest probability was 0.128 for the SCP scenarios and the highest being 0.282 for the LTAP/LD scenario. This represents a much higher testing coverage within each subset of the target population. While conditions across all crash modes were comparable, this also highlights that the LTAP/OD and LTAP/LD scenarios varied the least within each subset of crashes compared to the Rear-End and SCP crashes.

Within the five selected crash scenarios, the probability of exposure of each scenario within the entire crash population was determined to be less than 5% in all scenarios. The reason for this highlights a unique problem in defining scenario exposure as the joint probability of all scenario elements. By describing each crash scenario with more or less elements, the computed probability of exposure is greatly affected. This study chose scenario elements based on the availability of data elements within the CRSS database and

based on relevance to the scenario creation specific to this study. The addition or remission of one or more scenario elements would alter the final results which highlights the need for future methods to agree on a set typology for describing crash scenarios.

This study was also affected by the inherent limitations of the CRSS database and police-reported crash data in general. KABCO injury data is normally imprecise and can vary in consistency across the entire database, and so conversion to AIS may also be inaccurate. Another limitation with police-reported crash data is the unavailability and/or inaccuracy of what is recorded. A possible example could be the recorded sightline obstructions for each crash. Within the selected CRSS cases, almost all crashes were recorded as having no sightline obstructions present. This, however, is likely to be inaccurate as findings from Sandin (2009) showed that within LTAP/OD, LTAP/LD, and SCP crashes, sightline obstructions are often contributing factors for these crashes. Because crash reports are usually produced after the crash has occurred any sightline obstructions that may have been present may not be captured.

Another limitation is that the probability of scenario exposure was computed assuming that all scenario factors were independent of each other. However, in actuality this may not be the case and some factors may be related to each other. For example, the size and layout of the intersection may be a factor into the frequency and severity of any sightline obstructions that are created.

This study additionally assumed that crashes which occurred during the years 2016 to 2019 will be similar to the future crashes that AVs will be exposed to. If the fundamental characteristics of these crashes were to change from year to year, then the probability of exposure to these crash scenarios may be different in the future. However, if the fundamental aspects of each crash do not change (or can be shown to change predictably), then it is hypothesized that crashes in the near future may also be functionally similar. One possible defining metric is the travel speeds of both vehicles. To address this assumption, crash data from the General Estimates System (NASS GES) was used (NHTSA, 2019). GES is the predecessor of CRSS and is also a nationally representative sample of all crashes in the US.

Figure 16 shows the distribution of recorded travel speed (all vehicles) for all rear-end, LTAP/OD, LTAP/LD, and SCP crashes in the years 2004 to 2015 in GES and 2016 to 2019 in CRSS. For each of the four crash modes, the variation in travel speed was very minimal across each year.

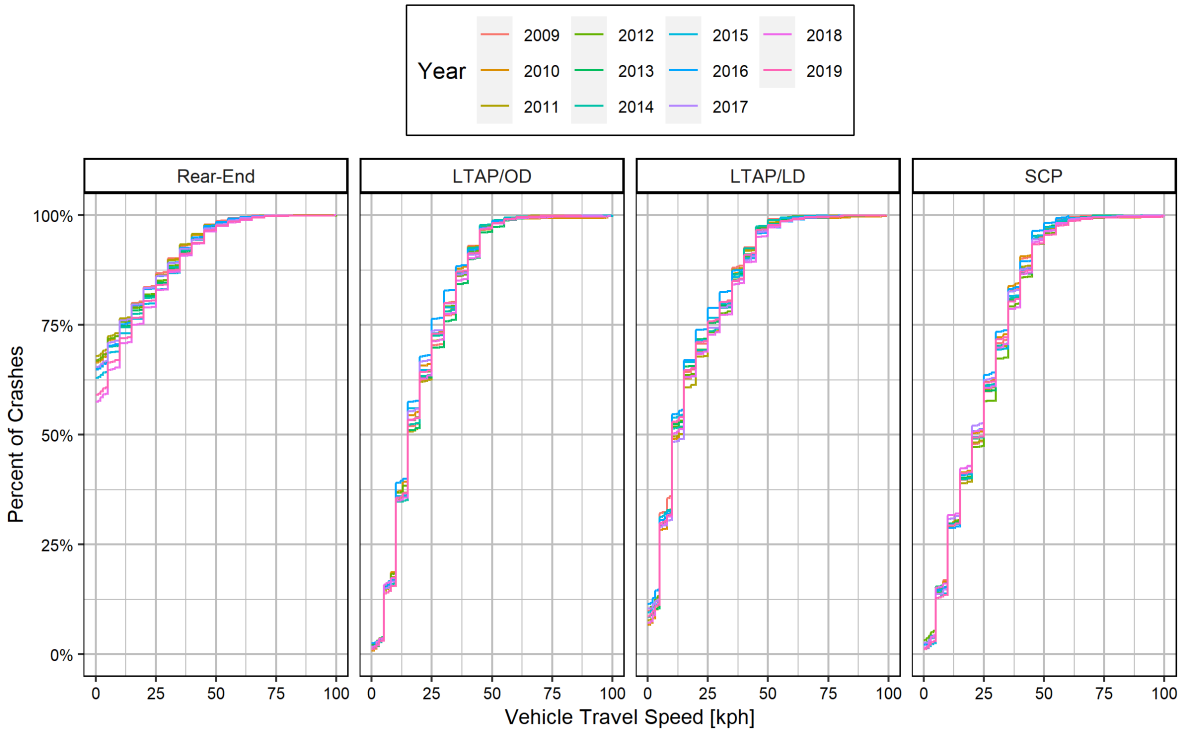

Figure 16. Distribution of vehicle travel speed from all Rear-End, LTAP/OD, LTAP/LD, and SCP crashes in the US from 2004 to 2019

2.7 Conclusions

The objective of this chapter was to use nationally representative crash data to characterize a target population of crashes that is likely to be relevant for future AVs operating as urban taxis. From this crash population, crash scenarios were defined and the probability of exposure to these scenarios was computed. In summary, five unique crash scenarios were defined using crash maneuver as a basis. Within each scenario, target and environmental factors were largely the same between each scenario. The probability of exposure for each scenario, however, varied significantly. Table 16 summarizes the probability of exposure for each scenario. Within the entire selected crash population (approximately 36% of all vehicle collisions in the US annually) the probability of exposure was between 0.012 for scenario 3 (LTAP/LD) and 0.062 for scenario 1 (Rear-End). The probability of exposure within the injury causing crashes was also similar. Within crashes of a specific crash maneuver, probability of exposure for each scenario was much higher with scenario 2 representing almost 30% of all LTAP/OD crashes within the crash population.

Table 16. Summary of probability of exposure for each selected crash scenario

	Probability of Exposure in All Crashes		Probability of Exposure in All Maneuver Specific Crashes	
	Crashes	MAIS2+F	Crashes	MAIS2+F
Crash Scenario 1	0.062	0.006	0.190	0.126
Crash Scenario 2	0.019	0.022	0.267	0.214
Crash Scenario 3	0.012	0.013	0.282	0.263
Crash Scenario 4 & 5	0.021	0.017	0.128	0.139

3. Characterizing Perception System Performance in Relevant Crash Scenarios

3.1 Introduction and Research Objectives

The objective of this chapter was to perform real-world driving tests and characterize the perception system performance of a prototype ADS platform. The benefit of real-world characterization is that it provides a context for actual scenario based risk for future AVs. In the previous chapter, five crash scenarios were defined that represent a high level of exposure within a relevant crash population. The goal of this chapter was to measure perception system performance in each of these scenarios. In an ideal world, performance in each scenario would be similar, however this is not likely so each scenario will be assessed individually. Perception system performance was defined as the magnitude and frequency of errors in perception system state measurements (e.g., relative position, relative speed, relative heading) of other road users and objects. Results from this chapter will then act as a basis for the analysis in Chapter 4.

This chapter first provides an overview of the ADS perception system that was characterized during testing. An overview of the testing facilities and testing process is then described. This chapter outlines the perception system outputs of interest and describes the filtering approaches applied to the measured data. Results are presented as a summary of perception system performance for each crash scenario.

3.2 ADS Perception System Overview

The ADS perception system under test (SUT) used in this study was a Lincoln model MKZ that was retrofitted with a commercial hardware and software perception system. (Figure 17). This was a flagship system that is representative of advanced perception systems for future AVs. This system works by providing full sensor fusion, object identification, and localization from data collected by an on-board suite of sensors, specifically an array of camera and radar sensors. Figure 18 shows an overview of this sensor suite.

Mounted on top of the vehicle were 7 cameras which provide a full 360-deg view around the vehicle. Two front facing cameras (one 60-deg FOV and one 120-deg FOV) provide the forward FOV. A single

rear-facing camera (60-deg FOV) provides the rear FOV. The remaining four cameras (120-deg FOV) provide the front and rear cross-traffic FOVs. Similar to the camera array, the vehicle is equipped with 8 radar units. These units fulfill the same FOV purposes as the camera units with concentration on the front, rear, and cross-traffic FOVs. Within each FOV, the information from each sensor type is fused into the final perception output which was used for this study. This form of testing is known as "grey box" testing as it evaluates the perception system without any knowledge of what the system is doing internally (i.e., without knowing the specific performance of each sensor). During future evaluations of AV performance, especially by third parties, this type of testing will be likely.

Figure 17. ADS retrofitted Lincoln MKZ (Left) and trunk mounted perception system (right)

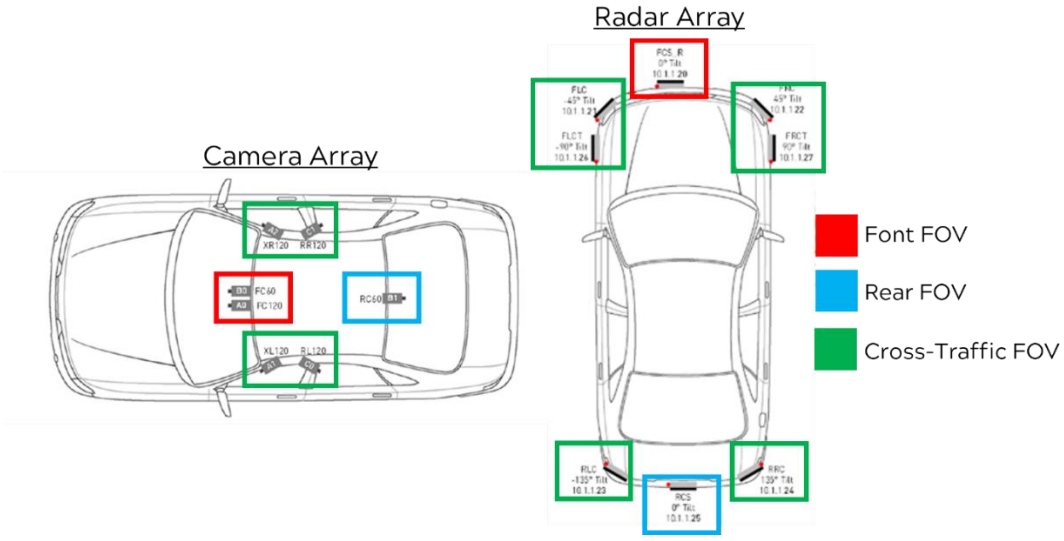

Figure 18. ADS sensor suite consisting of camera and lidar sensors in the forward, rear, and cross-traffic FOVs

3.3 Study Testing Facilities

All data collection was completed using the Virginia Smart Roads Facilities. This is a closed road test track owned by the Virginia Department of Transportation (VDOT) and managed and operated by the Virginia Tech Transportation Institute (VTTI). These testing facilities include private highway, urban, and rural roadway sections which allow for both controlled and safe testing to be conducted under controlled operating conditions. All data collection was conducted on the Smart Roads Surface Street Expansion (SSE) seen in Figure 19. This section has a large central 4-way intersection (or T-intersection depending on the configuration) with crosswalks and was the basis for all test scenarios.

Figure 19. Top view of the Virginia Smart Roads Surface Street Expansion (SSE). Features include a large intersection, roundabout, and different lane configurations.

3.4 Data Collection Overview

The crash scenarios described in Chapter 2 were then executed in order to measure the perception system performance in each scenario. Due to the project constraints, testing only included the interaction of the retrofitted ADS (the traveling through vehicle), and one other vehicle (the turning vehicle). The turning vehicle used in this study was a 2010 red Chevy Impala. As mentioned in Chapter 2, crash scenarios were defined in a way such that no crash occurs, and the turning vehicle passes in front of a stationary traveling through vehicle. This method was selected primarily due to safety considerations for the researchers, and to protect research property (mainly preventing damage of either of the vehicles). With just one vehicle moving during the scenario, the probability of a collision is minimized. Due to the relative low speeds of many of these scenarios, effects of the traveling through vehicle being stationary on perception system performance (ex. effect of background movement, relative speed with other objects or road users) were assumed to be small. Each scenario was repeated three times (3 trials) as this provided an adequate measure of the variability of the system.

During testing, various outputs from the perception system were recorded for further analysis. In order to characterize performance, a basic set of variables were needed and recorded during each trial of each scenario. Table 17 shows a breakdown of the set of variables used in this study. All measures were recorded by the perception system within a relative X/Y space with (0,0) being located at the center of the traveling through vehicles rear axle.

Table 17. List of perception systems measures needed for characterization

Perception System Output	Description
Time	Timestamp of the object detection
Object Classification	Object classification type (car, pedestrian, bicycle, sign, etc.)
Object Location	Object's centroid location in X/Y relative space
Object Velocity	Object's X/Y velocity (magnitude and direction) in space
Object Orientation	Object's alignment/heading in space
Object ID	Object's Identifier from perception system
Object Classification Confidence	Object's confidence as reported by perception system

In order to localize both vehicles in a global X/Y space and provide a ground truth metric, each vehicle was equipped with a Differential Global Position System (DGPS) based ground truth collection system. Ground truth of both vehicles was important during this analysis as it provided an independent reference for calculating errors in the detections. The DGPS was used to dynamically measure the positions of each vehicle with respect to a common time signal from the satellites. Both DGPS systems collected positioning data at 10 Hz and provided accuracy of 10 cm RMS. The precision of the DGPS was less than the width of a lane line and was assumed to be adequate for most driving scenarios. Table 18 provides the ground truth variables that were needed for subsequent data analysis. From the DGPS positions, vehicle position was measured and speed and heading values for each vehicle were determined based on the derivative of the position information.

Table 18. List of ground truth variables used to characterize performance

DGPS Output	Description
Turning Vehicle Position	True location of target in space
Traveling Through Vehicle Position	True location of ADS in space
Turning Vehicle Velocity	True speed of target relative to ADS
Turning Vehicle Heading	True orientation of target
Traveling Through Vehicle Heading	True orientation of ADS

3.5 Data Processing Overview

Data was collected for three trials for all five crash scenarios (15 total test trials). Post processing was completed within MATLAB using the "ROS" toolbox and was split into three categories: (1) data from each trial first needed to be filtered to remove background detections, (2) all filtered detections and ground truth measurements were transformed into a global coordinate system, and (3) the difference between the detections and ground truth were measured and defined as perception system error.

Data filtering was needed as during testing, the perception system was able to detect other vehicles and objects around the general area of the smart roads facilities. These represented objects and vehicles that were not under consideration and so must be filtered out before the data was processed to ensure that perception system performance was being characterized solely by detections of the turning vehicle. To

summarize the approach, two simple filters were applied to remove background and non-relevant objects. First, detections were filtered to those only labeled as a vehicle within the perception system object identification (with at least 50% confidence). This focused the characterization on only the detections that the perception system identified as a vehicle. Next, a simple position filter was applied (Figure 20) and assumed some level of performance for the perception system. Based on a Euclidian range around a ground truth position, any detections within this region were considered valid. Due to the simplicity of this filter, there was some probability that a background detection could be labeled as a target detection, however, due to the nature of the tests and baseline knowledge of the performance of the system, this probability was assumed to be small. For this filter, a pass region of 5m was chosen as this represents the approximate length of the turning vehicle.

Figure 20. Euclidian based position filter

After detection filtering, all remaining detection measurements and all ground truth measures from both vehicles were transformed into a global X/Y coordinate system. At the Smart Roads Facilities, a very accurate measure of the latitude and longitude of the traffic circle on the SSE is known. Using this as the global X/Y system (0,0) and using the DGPS lat/long coordinates of both vehicles, the local coordinates of each vehicle were calculated using the "latlon2local" function in MATLAB. Perception system detections

were processed in a very similar manner except with two coordinate transformations, one to go from ADS local coordinates to global latitude and longitude, and then another to go from global lat/long to the global local coordinates.

After coordinate transforms, the local location of both vehicles was known as well as the local location of each perception system detection. During coordinate transforms, the detections were also interpolated into global GPS epoch time signal and lined up with the ground truth measurements. This created a dataset in which every DGPS reading had a corresponding perception system detection (which consisted of multiple measures like X/Y position and velocity) for every time step. At each point in time, the error for the units of measure (defined as the distance between detected and ground truth values) was computed. The primary measures of interest for this study (shown in Figure 21) were the error in X/Y location, error in turning vehicle heading, and error in the resultant turning vehicle velocity. Total position error was defined as the resultant of Euclidean range error and tangential error.

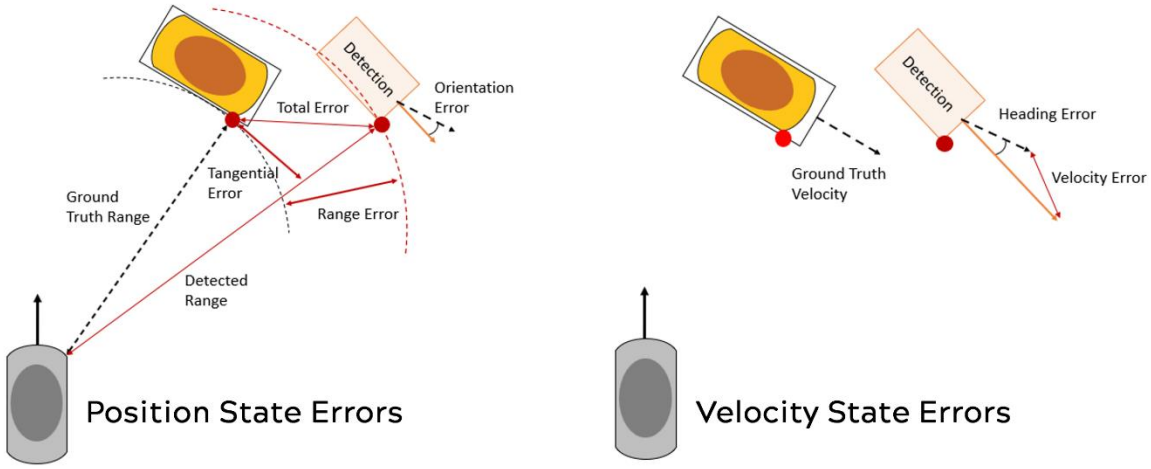

Figure 21. Overview of primary performance measures of interest

3.6 Results of Performance Characterization

Figure 22 through Figure 25 show the DGPS path of the turning vehicle and the perception system detections of the turning vehicle centroid for each crash scenario. In each plot, the black line represents the DGPS path at the vehicle centroid, and the red line represents the perception system detection of this vehicles centroid. The rectangle in each plot represents the position of the traveling through vehicle in each scenario with the coordinate origin located at the rear axle. For each scenario, data from three trials was selected for analysis. Data collection for all trials was completed on the same day of testing during the same conditions. This was done to minimize potential bias created from slightly different weather and lighting conditions that is possible if testing was completed on separate days.

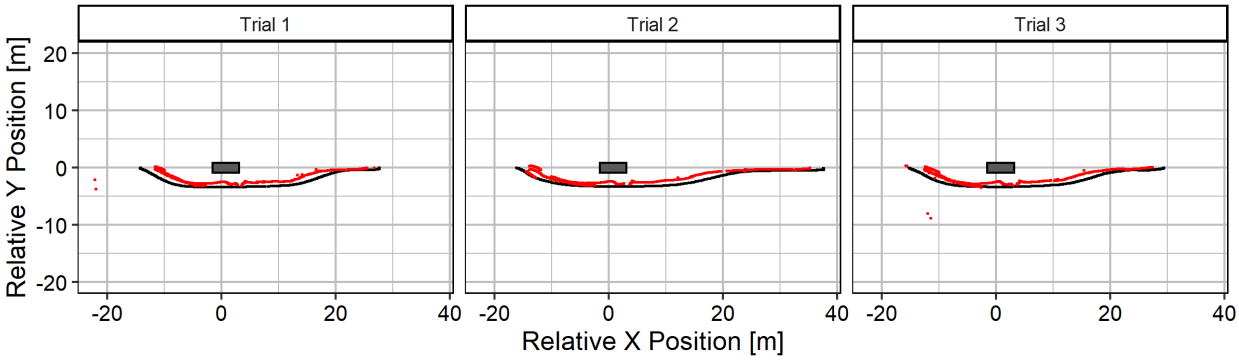

Figure 22. DGPS and filtered perception system detections for each trial during the Rear-End scenario

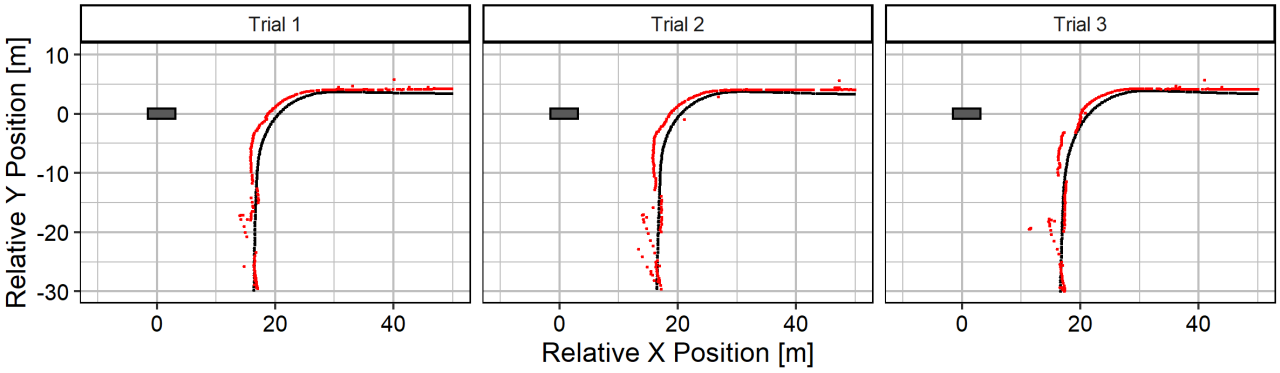

Figure 23. DGPS and filtered perception system detections for each trial during the LTAP/OD scenario

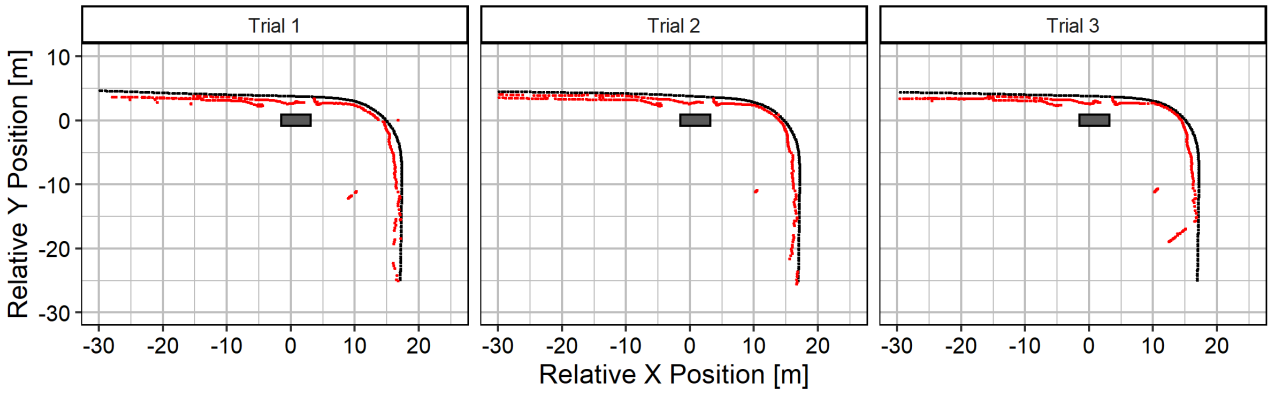

Figure 24. DGPS and filtered perception system detections for each trial during the LTAP/LD scenario

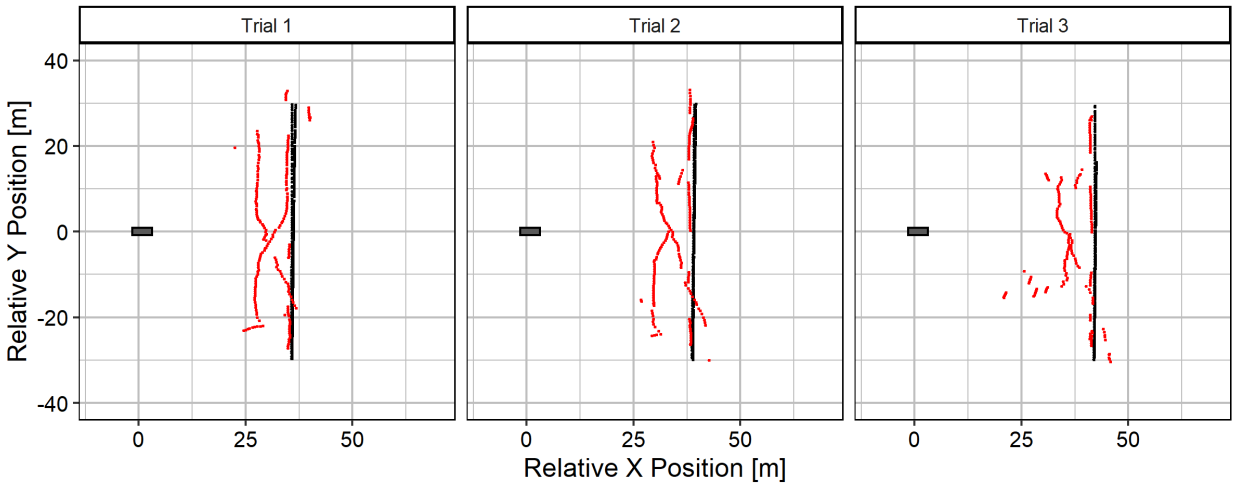

Figure 25. DGPS and filtered perception system detections for each trial during the SCP scenarios

Figure 26 shows the distributions of X and Y centroid position error in meters for each crash scenario. The Rear-End and LTAP/OD crash scenarios showed the best performance whereas the LTAP/LD and SCP scenarios showed higher X position error. All scenarios were very similar with regards to Y position error. Table 19 summarizes the mean, median, standard deviation, and 10th/90th percentiles for X/Y position error.

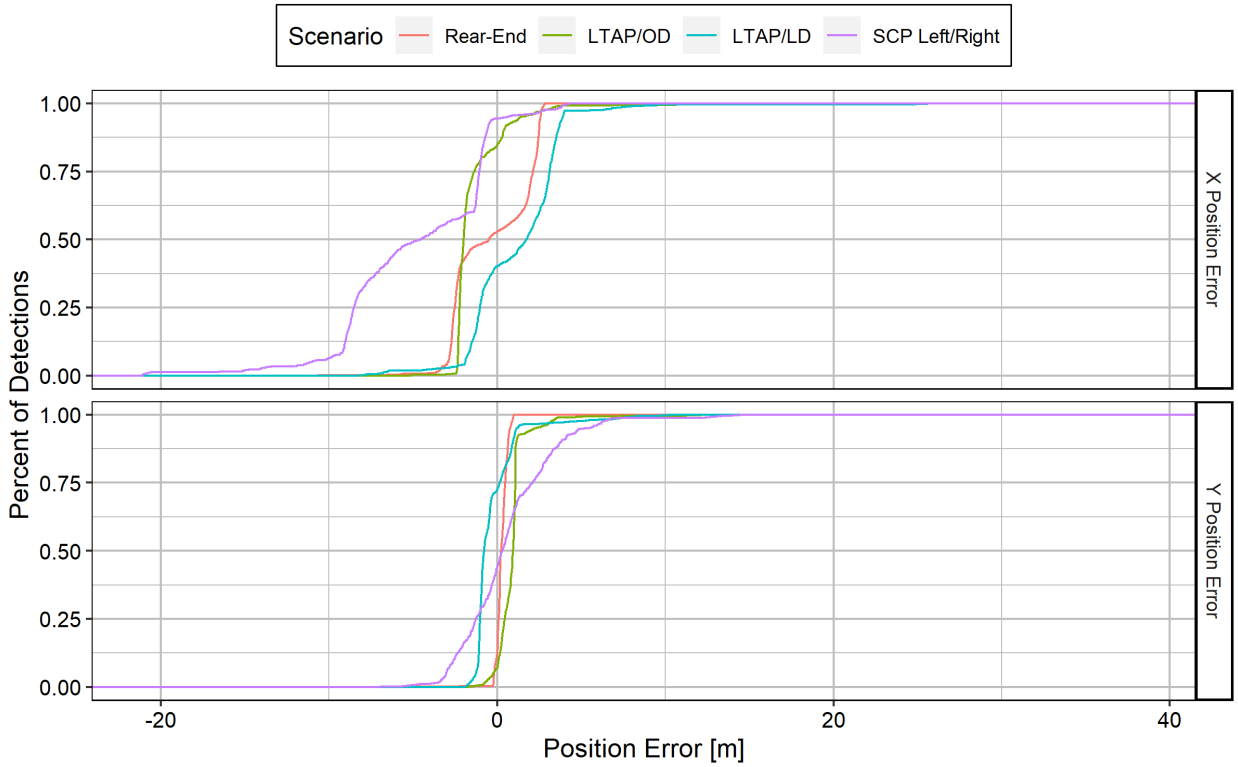

Figure 26. Cumulative distribution of X/Y position error for each crash scenario

Table 19. Summary of X/Y position error statistics

	Crash Scenario	Mean Error [m]	Median Error [m]	Sd Error [m]	10th Percentile Error [m]	90th Percentile Error [m]
X Error	Rear-End	-0.31	-0.52	2.33	-2.77	2.49
	LTAP/OD	-1.38	-1.99	2.05	-2.32	0.38
	LTAP/LD	1.21	1.72	3.04	-1.60	3.60
	SCP Left/Right	-4.85	-4.60	4.45	-9.12	-0.62
Y Error	Rear-End	0.27	0.23	0.37	0.65	-0.07
	LTAP/OD	0.89	0.94	1.05	0.08	1.14
	LTAP/LD	-0.26	-0.78	1.50	-1.11	0.93
	SCP Left/Right	0.58	0.29	2.74	3.76	-2.58

Figure 27 shows the distributions of heading error in degrees for each crash scenario. The Rear-End crash scenario showed the best performance whereas all other scenarios showed both higher error and larger variability. Table 20 summarizes the mean, median, standard deviation, and 10th/90th percentiles for heading error.

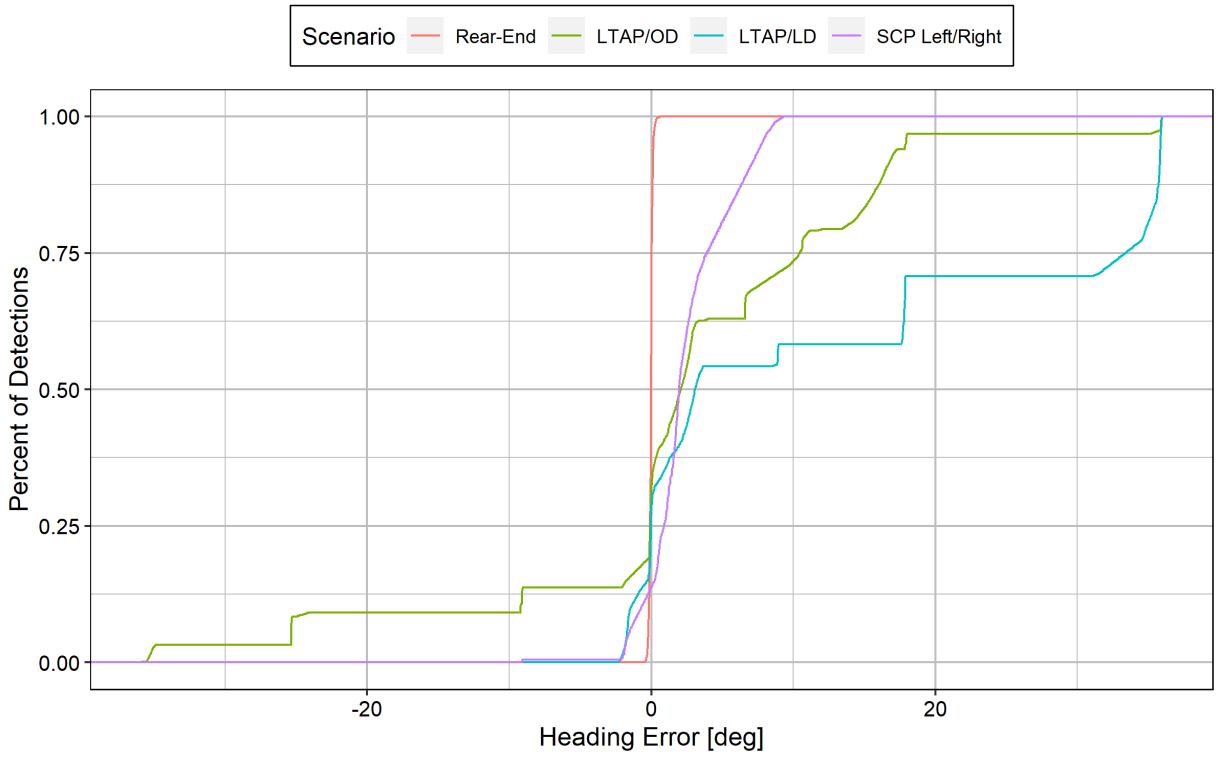

Figure 27. Cumulative distribution of TV heading error for each crash scenario

Table 20. Summary of TV heading error statistics

Crash Scenario	Mean Error [deg]	Median Error [deg]	Sd Error [deg]	10th Percentile Error [deg]	90th Percentile Error [deg]
Rear-End	-0.03	-0.01	0.12	-0.17	0.11
LTAP/OD	2.76	2.06	13.20	16.45	-9.20
LTAP/LD	13.06	3.07	15.22	-1.47	35.78
SCP Left/Right	2.49	1.96	2.75	-0.71	6.82

Figure 28 shows the distributions of resultant velocity error in meters per second for each crash scenario. Similar performance was seen in both the Rear-End and LTAP/OD scenarios with velocity errors between plus/minus 5 m/s with the majority of errors being close to zero. The LTAP/LD and SCP scenarios showed slightly higher and a more variable spread in the error but were comparable to each other. Table 21 summarizes the mean, median, standard deviation, and 10th/90th percentiles for velocity error.

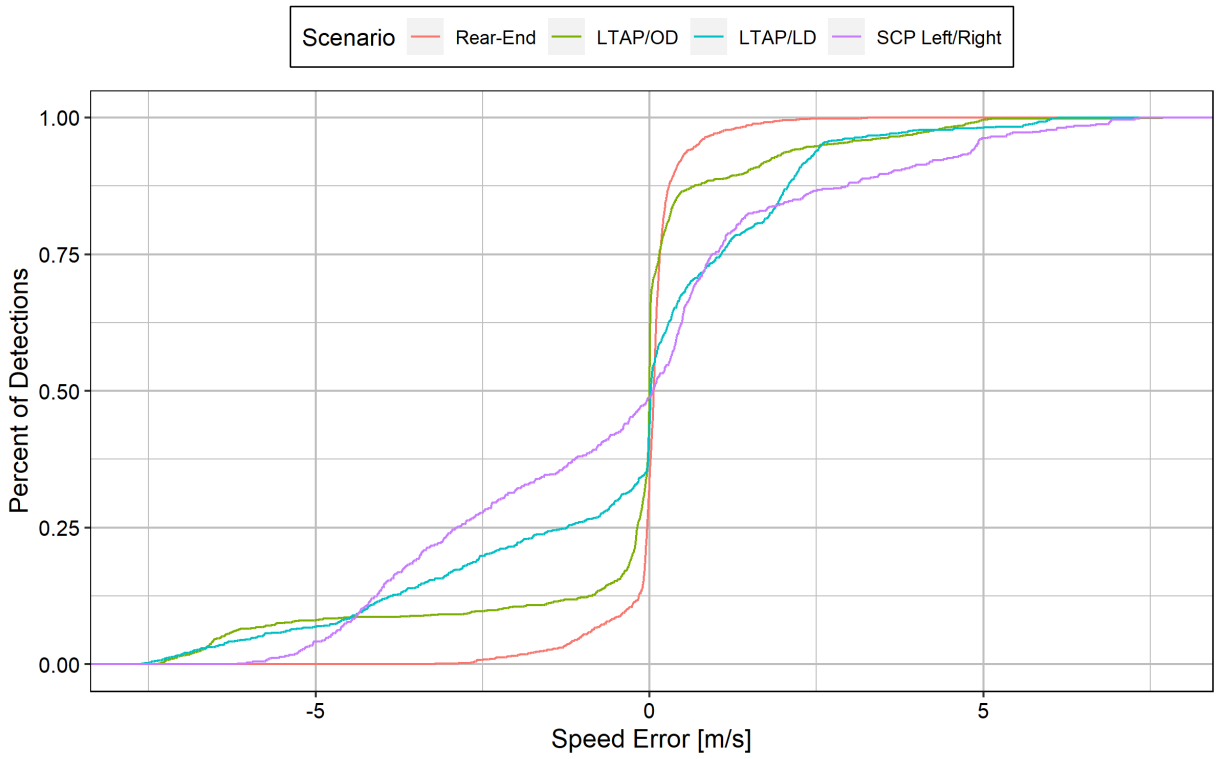

Figure 28. Cumulative distribution of TV velocity error for each crash scenario

Table 21. Summary of TV velocity error statistics

Crash Scenario	Mean Error [m/s]	Median Error [m/s]	Sd Error [m/s]	10th Percentile Error [m/s]	90th Percentile Error [m/s]
Rear-End	0.02	0.06	0.56	0.37	-0.35
LTAP/OD	-0.31	0.00	2.19	-2.27	1.44
LTAP/LD	-0.39	0.02	2.56	-4.26	2.21
SCP Left/Right	-0.43	0.05	2.88	-4.32	3.62

3.7 Discussion and Limitations

Across all five crash scenarios, perception system performance varied but was relatively consistent across all trials. Performance was generally found to be the best in the Rear-End and LTAP/OD scenarios showing similar levels of performance in both positional errors and velocity errors. Performance errors were found to generally be higher in all areas for both the LTAP/LD and SCP scenarios. One possible reason for the difference between these two groups is the percent of time spent by the turning vehicle in each FOV of the perception system. In the Rear-End and LTAP/OD scenarios, the turning vehicle is primarily in the front FOV for most of the maneuver. In the LTAP/LD and SCP scenarios, the turning vehicle is predominantly in the cross-traffic FOVs. This highlights a possible weakness for this perception system in which the cross-traffic FOVs may have trouble accurately measuring the state of objects. Related to operational safety, the AV may then have difficulty measuring objects in these regions, only acquiring a more accurate measure of the other vehicles' state when it is in front of the AV. As such, decision made based on any state measurements may lead to conflicts or hinder the AVs performance.

Another aspect that was found to influence the amount of error seen what the ability for the perception system to fuse its sensor data into one measurement. The system used in this study primarily relied on its cameras to accomplish object detection as well as measure the position of the other vehicle. This information is then supplemented with the radar measurements to create the final perception system output. During the testing, however, this specific system did not always accomplish sensor fusion. Figure 29 shows the distribution of Y position error (i.e., error along the axis of the vehicle) for each FOV on the vehicle and comparing detections with and without sensor fusion. Evident within each FOV, the spread of positional error is much larger when the radar data isn't fused which contributes to some of the larger errors seen in the testing data.

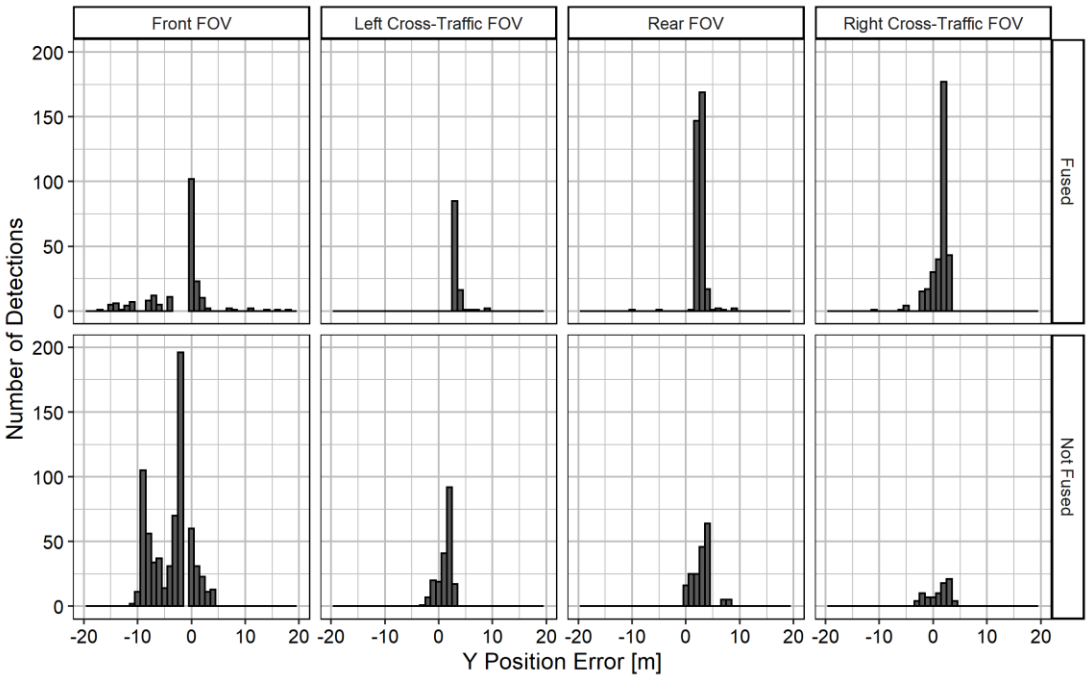

Figure 29. Distribution of y position error for each sensor FOV, broken out by successful sensor fusion

The effect of this is particularly evident within the SCP Left/Right tests, in which large amounts of Y positional error was shown. Figure 30 shows the same test data for each trial, highlighting where the system was able to accomplish sensor fusion. In this particular scenario, the majority of detections with large error are seen when the radar is not being fused.

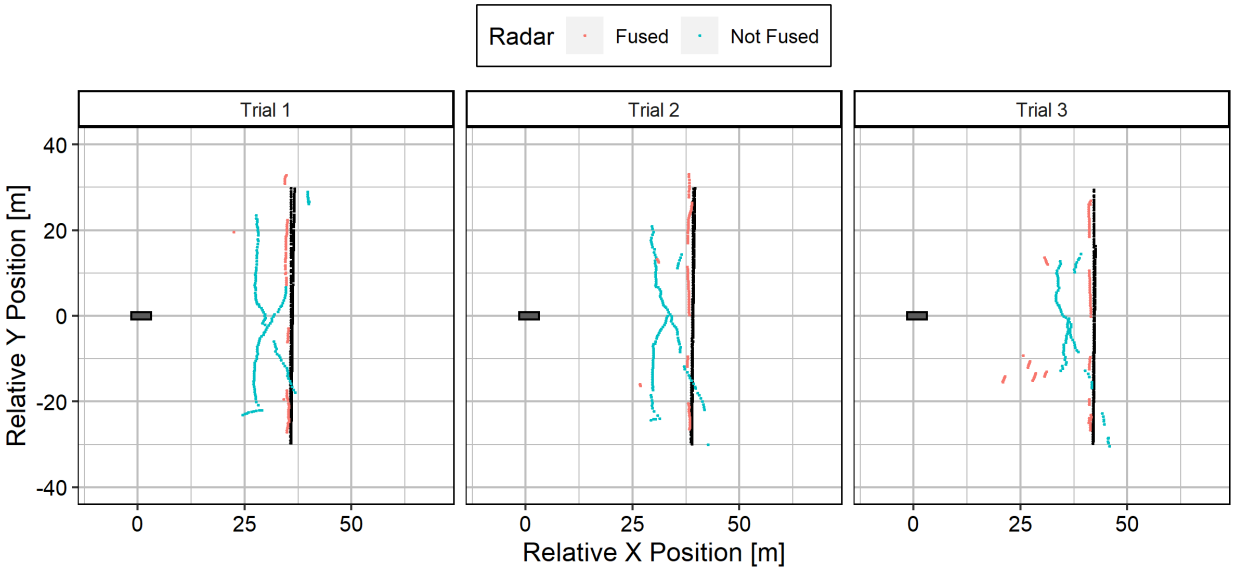

Figure 30. SCP scenario detections shown with sensor fusion information

One limitation of this study was the testing constraint of keeping the traveling through vehicle stationary during all maneuvers. From the crash data, the traveling through vehicle was always moving and mostly traveling faster than the other vehicle. The relative motion between the two vehicles may change the performance of the system and its ability to localize itself. In addition, a moving background may also affect performance. An additional limitation was the filtering done on object detections. Like all filtering methods, there may be an element of bias introduced, for example only keeping the best detections if valid detections exist outside of the inclusion region. This filter may also bias towards larger error if background detections are captured.

3.8 Conclusions

The objective of this chapter was to characterize the performance of a real-world ADS perception system in the crash scenarios defined in Chapter 2. This part of the study conducted closed road testing with a retrofitted ADS vehicle in order to measure scenario specific object detection errors with a focus on errors in X/Y relative position, error in turning vehicle heading, and error in turning vehicle velocity. Perception systems error was computed as the difference between perception system detections and a reference DGPS based ground truth. Table 22 summarizes the median X/Y position, heading, and speed errors for each specific crash scenario. The error measured as part of this chapter was important to characterize in order to assess the safety implications of perception system performance. The results from this chapter provide a measure for where the reference AV perceives the other vehicle to be during each crash scenario. This then forms the basis for the analysis in the next chapter.

Table 22. Summary of median X/Y position error, heading error, and speed error

Crash Scenario	X Position Error [m]	Y Position Error [m]	Heading Error [deg]	Speed Error [m/s]
Rear-End	-0.52	0.23	-0.01	0.06
LTAP/OD	-1.99	0.94	2.06	0.00
LTAP/LD	1.72	-0.78	3.07	0.02
SCP Left/Right	-4.60	0.29	1.96	0.05

4. Evaluating Simulated Crash Outcomes based on Perception System Performance

4.1 Introduction and Research Objectives

The objective of this chapter was to describe a hybrid method that can be used to explore where and when injury risk during collision avoidance is affected by perception system performance for a reference AV. Within each crash scenario defined in Chapter 2, it was assumed that the turning vehicle initiated the crash scenario, and the AV recognizes this and must perform some type of evasive maneuver in order to attempt to prevent or mitigate the crash. This chapter focuses on simulating a range of possible AV evasive paths and modeling the points of impact (or no impact) between the vehicles. For simulations with an impact, injury outcomes in both vehicles are predicted as a measure of risk (severity). This analysis also simulated these crash scenarios both for an ideal perception system (i.e., no object detection state errors) and using the perception system performance characterized in Chapter 3. In this way, the system level effect of perception system performance on crash and injury risk in each scenario and for different conditions can be assessed for a reference AV.

This chapter first provides an overview of the simulation model that was developed. Crash simulation was accomplished through four steps: (1) a worst case impact orientation was defined for each crash scenario, (2) effects of measured perception system performance were incorporated, (3) a range of AV evasive maneuvers were defined based on a driver model, and (4) for simulations that resulted in a collision, collision dynamics and injury prediction are determined to assess collision severity.

4.2 Crash Simulation Modeling

Figure 31 shows an overview of the simulation model that was developed. First, an initial worst-case impact orientation was defined for each crash scenario based on the target population identified in Chapter 2. Next, two initial conditions were defined based on an ideal and the reference perception system performance. The AV was then simulated to perform a range of evasive maneuvers based on parameters

from a driver model taken from recent literature. For simulations that resulted in a collision between the vehicles, impact kinematics were modeled and probability of injury in each vehicle was estimated.

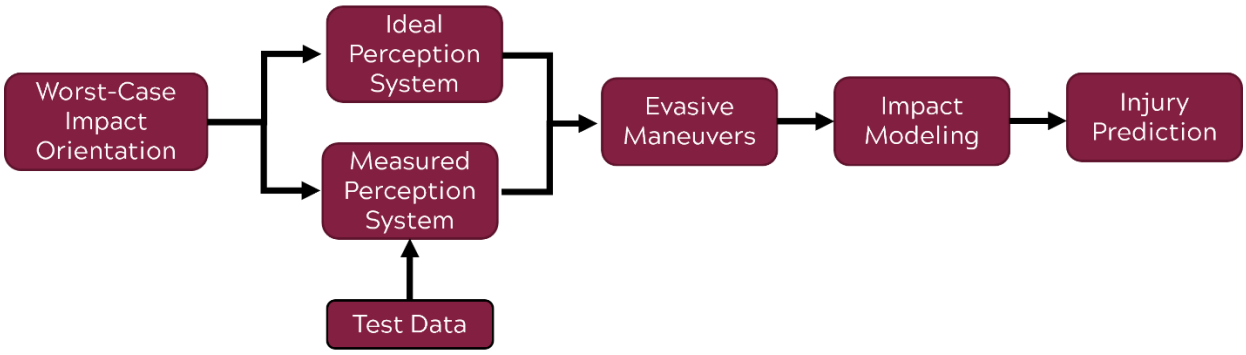

Figure 31. Overview of crash simulation model

4.2.1 Defining Worst-Case Impact Orientation for Selected Crash Scenarios

For each crash scenario, a worst-case impact orientation was assumed as the initial starting orientation for both vehicles during the crash simulations. This point assumed the crash orientation in the case that both vehicles collide and that neither vehicle takes any evasive actions. Worst-case impact orientation was defined as the crash orientation of the two vehicles that historically represents the highest probability of MAIS2+F injury in either vehicle and was defined in a similar way to that of Kusano and Victor (2022). Due to very slight variations in the movement between vehicles, the crash orientation can vary significantly, for example a head-on impact vs a side impact during an LTAP/OD crash scenario. Each configuration can lead to varying levels of injury risk and so this study focused on assessing the situations of highest injury risk.

Crashes from the target population identified in Chapter 2 were used as the basis for determining worst-case impact orientation. Vehicle impact orientation was defined based on the impact of one location on each vehicle. This location was determined using a clock-point scale referenced in Figure 32 which forms the basis for one of the data elements within CRSS and FARS (NHTSA, 2022).

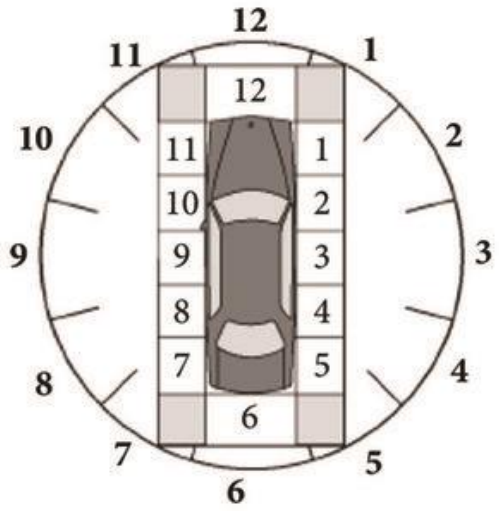

Figure 32. Impact clock-point diagram

Figure 33 and Table 23 show the clock-point impact frequency for both the traveling through vehicle and the turning vehicle broken out by crash type. Within all crash types, the traveling through vehicle was predominantly the striking vehicle with the majority of crashes resulting in an impact at the 12 O'clock position. Impact locations on the turning vehicle varied and were dependent on crash type. In Rear-End crashes, the turning vehicle was always struck at the 6 O'clock location. In LTAP/OD crashes, impacts to the 1, 3, and 5 O'clock positions were common. In the LTAP/LD crashes, impacts to the 7, 9, 11, and 12 O'clock positions were common. This shows the variability for either a frontal or side impact in these crashes. In the SCP crashes, impacts to the front (1 or 11 O'clock) or the side (3 or 9 O'clock) and the rear (5 or 7 O'clock) were common and showed the highest variability. Impacts to the front of each vehicle or to the driver side of the vehicle (clock points 11, 10, 9) also represented a high proportion of the MAIS2+F injury crashes.

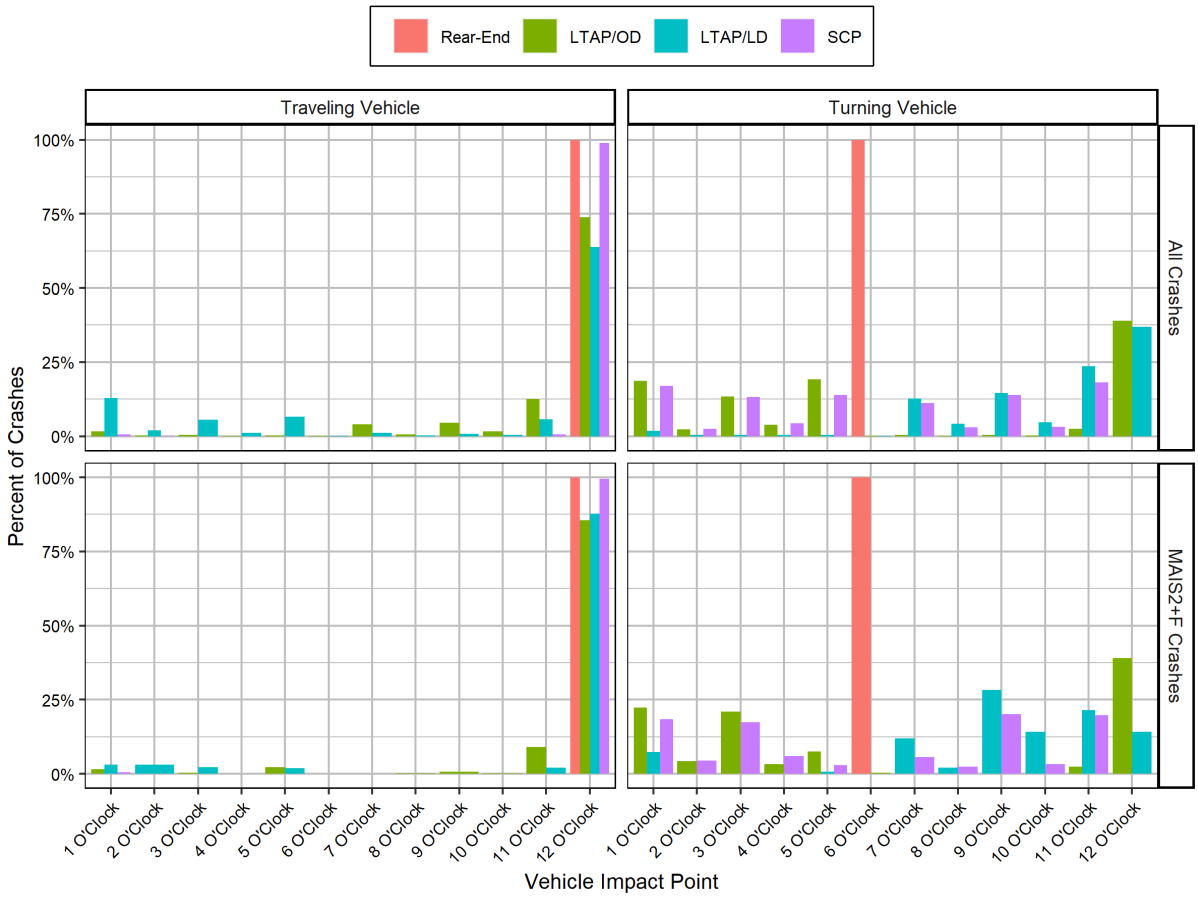

Figure 33. Breakdown of impact clock point on both the traveling through vehicle and the turning vehicle

Table 23. Breakdown of impact clock point on both the traveling through vehicle and the turning vehicle

Traveling Through Vehicle								
	Rear-End		LTAP/OD		LTAP/LD		SCP	
	Crashes	MAIS2+F	Crashes	MAIS2+F	Crashes	MAIS2+F	Crashes	MAIS2+F
1 O'clock	0%	0%	1.62%	1.62%	12.8%	2.99%	0.56%	0.54%
2 O'clock	0%	0%	0.19%	0%	1.89%	3.15%	0.08%	0%
3 O'clock	0%	0%	0.5%	0.42%	5.53%	2.24%	0%	0%
4 O'clock	0%	0%	0.06%	0%	1.18%	0%	0%	0%
5 O'clock	0%	0%	0.21%	2.27%	6.54%	1.81%	0%	0%
6 O'clock	0%	0%	0.17%	0%	0.14%	0%	0%	0%
7 O'clock	0%	0%	4.07%	0%	1.09%	0%	0%	0%
8 O'clock	0%	0%	0.67%	0.17%%	0.19%	0%	0%	0%
9 O'clock	0%	0%	4.56%	0.63%	0.81%	0%	0%	0%
10 O'clock	0%	0%	1.62%	0.2%	0.35%	0%	0%	0%
11 O'clock	0%	0%	12.54%	9.09%	5.72%	2.12%	0.52%	0%
12 O'clock	100%	100%	73.79%	85.59%	63.76%	87.7%	98.85%	99.46%

Turning Vehicle								
	Rear-End		LTAP/OD		LTAP/LD		SCP	
	Crashes	MAIS2+F	Crashes	MAIS2+F	Crashes	MAIS2+F	Crashes	MAIS2+F
1 O'clock	0%	0%	18.72%	22.25%	1.83%	7.37%	16.93%	18.38%
2 O'clock	0%	0%	2.35%	4.24%	0.35%	0%	2.43%	4.42%
3 O'clock	0%	0%	13.3%	20.9%	0.35%	0%	13.18%	17.34%
4 O'clock	0%	0%	3.88%	3.28%	0.34%	0%	4.29%	6.01%
5 O'clock	0%	0%	19.14%	7.55%	0.44%	0.69%	13.86%	2.92%
6 O'clock	100%	100%	0.03%	0.4%	0.17%	0%	0%	0%
7 O'clock	0%	0%	0.38%	0%	12.7%	11.9%	11.08%	5.54%
8 O'clock	0%	0%	0.09%	0%	4.15%	2.01%	2.96%	2.46%
9 O'clock	0%	0%	0.41%	0%	14.58%	28.2%	13.95%	20.07%
10 O'clock	0%	0%	0.23%	0%	4.7%	14.18%	3.23%	3.15%
11 O'clock	0%	0%	2.46%	2.36%	23.57%	21.47%	18.09%	19.72%
12 O'clock	0%	0%	39.01%	39.02%	36.82%	14.19%	0%	0%

Worst-case impact location was chosen based on both the frequency of impact location, as well as the proportion of injury crashes with a certain impact location. Figure 34 shows the final worst-case initial impact orientations used during simulation. From the five base crash scenarios, a total of seven total crash configurations were identified as being relevant. For the Rear-End scenario, impact orientation was assumed to be a full frontal for the traveling through vehicle (12 O'clock) and a full rear impact for the turning vehicle (6 O'clock). In the LTAP/OD scenario, a 12 on 12 impact was chosen as it presented the highest proportion of both crashes and injuries. A similar 12 on 12 impact orientation was chosen for the LTAP/LD scenario. For the two SCP scenarios (approach from left and right), both a frontal and side impact orientation (12 to 11/1 O'clock and 12 to 3/9 O'clock respectfully) were determined to be relevant for simulation due to each configuration representing similar proportions of crashes and injuries. Generally, the impact orientation(s) with the highest proportion of both crashes and injuries were chosen. An exception was with the LTAP/LD scenario that showed a high proportion of injuries during a 9 O'clock impact on the turning vehicle. This impact configuration is similar however to the SCP side orientation and so the 12 O'clock orientation was chosen as it represents the highest proportion of the total crashes (approx. 40%).

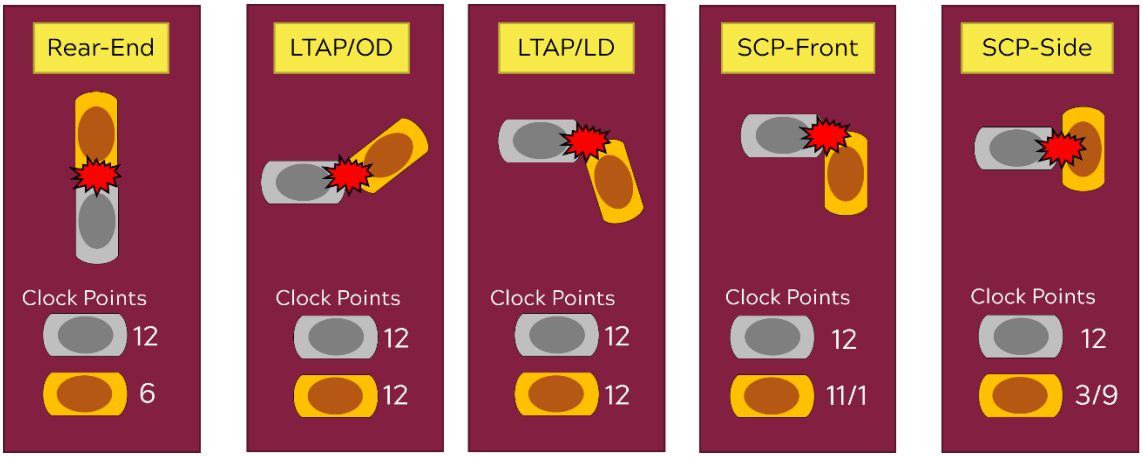

Figure 34. Final assumed initial worst-case impact orientations

4.2.2 Effects of Perception System Performance on Crash Orientation

In the previous chapter, the object detection performance (i.e., measurement accuracy and precision) of an ADS perception system was characterized in five common intersection crash scenarios. During these crash scenarios, the AV will need to perceive the threat and react by making decisions on what kind of evasive maneuver to perform. This reactive decision is likely to be scenario dependent, for example excluding the opposite direction swerve in crossing path crashes as discussed by Scanlon et al. (2022) as a way to incorporate a human driver phenomenon that human drivers will typically swerve into the same direction as the other crossing vehicle (Scanlon, 2017).

Within each scenario, the decision to perform an evasive maneuver may also be dependent on predicted crash outcomes based on the current perceived location of the other vehicle, and the predicted future location of the other vehicle. These perceived crash outcomes, however, are easily influenced by perception system error and depending on the level of error, the location and/or orientation of the other vehicle may differ causing perceived crash outcomes to be different.

To illustrate this, Figure 35 shows a hypothetical LTAP/LD crash scenario in which the AV (grey vehicle) strikes another vehicle (orange vehicle) which entered into the intersection causing a collision. This scenario highlights a possible situation in which the predicted position of the other vehicle (as measured by an incorrect perception system) is different than the actual position of the other vehicle.

Because of this, the perceived crash outcome is different compared to the actual crash outcome where the perceived impact orientation is a forward collision for both vehicles, and the actual orientation is a side impact for the orange vehicle. These two orientations can have very different injury outcomes and so the perceived occupant injury risk in this scenario is different and affected by perception system performance.

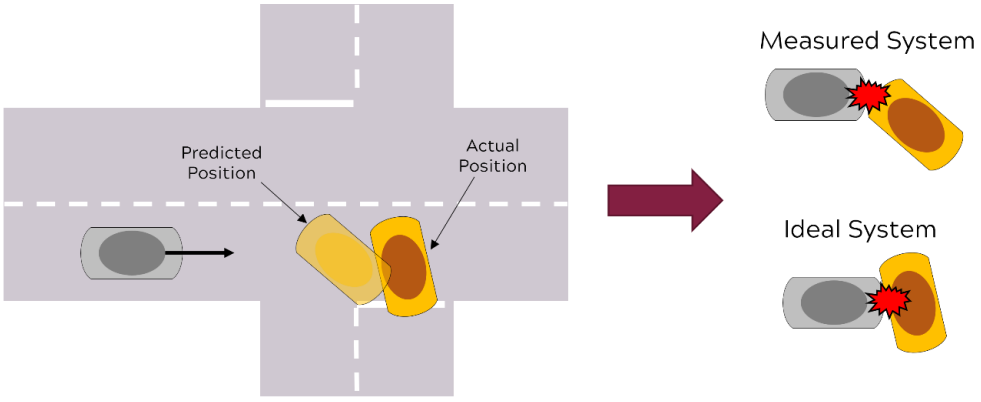

Figure 35. Example LTAP/LD crash scenario in which the predicted position and the actual position of the other vehicle result in different impact orientations

The simulations conducted during this chapter present a hybrid approach in which the simulated position of the turning vehicle (with respect to the AV) is dictated by the results of the real-world ADS perception system characterization from Chapter 3 and the worst-case impact orientation (from crash data) defined previously. For each simulation, one of two initial conditions were used that specified the orientation of the turning vehicle. The first simulated the predicted location from an ideal perception system (i.e., no object detection error) and used a position that meets the worst-case impact orientation. The second simulated the predicted location based on the performance of the perception system from Chapter 3. This location was defined by shifting both the X/Y location and the vehicle heading from the position used for the ideal system. Total X/Y shift reflected a 1s prediction into the future using median X/Y error and median speed error and was computed using Equation 6 and Equation 7. Vehicle heading was shifted using median heading error (Equation 8). For each specific scenario, data from all three trials were combined when computing median. Within possible future crashes, these two conditions represent the actual location of the

turning vehicle during a crash, and where the AV thinks the turning vehicle will be at that same moment during the crash.

$$X = X_{ideal} + X_{error} + \vec{v}_{error} \quad (6)$$

$$Y = Y_{ideal} + Y_{error} + \vec{v}_{error} \quad (7)$$

$$Head = Head_{ideal} + Head_{error} \quad (8)$$

4.2.3 Modeling AV Evasive Maneuvers

Within each crash simulation, the location of the turning vehicle was fixed and the path of the traveling through vehicle was modeled based on some evasive action. This was done to simplify the vehicle simulations and an assumption was made that the path of the turning vehicle was negligible in these scenarios as the traveling through vehicle was predominantly the striking vehicle and was typically traveling faster.

Next a driver model taken from the literature was used to model the AV evasive maneuvers. Many previous approaches that model AV and ADAS collision avoidance based their driving models on the perception, decision, and maneuver characterizes of human drivers. These models typically assumed some level of driver response time and then some level of driver evasive maneuvers. For example, Kusano and Gabler (2012) showed the development of a brake avoidance model that used a probability distribution of response times and a braking response model dictated by a brake application model.

In this study, AV evasive maneuver modeling was accomplished by adapting the reference driver model NIEON (Non-Impaired Eyes always On) developed by Scanlon et al. (2022). This driver response model aims to represent the response of a non-impaired, eyes always on the conflict human driver that is presented with some critical situation that can be avoided or mitigated through either braking and/or steering action. This study adapted this model by primarily applying the response characteristics for evasive braking and steering. The referenced braking evasive model employs a constant jerk magnitude of -30 m/s^3 up to a max braking of 0.8g. The referenced steering evasive model employs a maximum lateral jerk of 16 m/s^3

and a maximum lateral acceleration of 6.4 m/s^2. Combined resultant acceleration was limited to 0.8g where the braking deacceleration was scaled down when in combination with steering. These parameters were used as the limits for a bicycle model which modeled the path taken by the AV during the evasive maneuver using a time step of 0.01s (Equation 9 through Equation 14). The AV was simulated to begin the steering and/or braking maneuver immediately at the start of the simulation.

$$a_{t+1} = a_t + Jerk_t * dt \quad (9)$$
$$v_{t+1} = v_t + a_t * dt \quad (10)$$
$$\dot{\theta}_{t+1} = \dot{\theta}_t + \ddot{\theta}_t * dt \quad (11)$$
$$\theta_{t+1} = \theta_t + \dot{\theta} * dt \quad (12)$$
$$x_{t+1} = x_t + v_t * dt * \cos(\theta_t) \quad (13)$$
$$y_{t+1} = y_t + v_t * dt * sin(\theta_t) \quad (14)$$

Similar to the NIEON model, three different responses were simulated: braking, braking while steering to the right, and braking while steering to the left. The steering responses were defined as any evasive maneuver in which lateral acceleration from steering was above 0.1g. As mentioned previously, the specific maneuver the AV might take and to what degree the maneuver is executed is highly situation dependent and so this study made no assumptions on this aspect. Instead, 50 evasive paths were simulated. The three base paths were braking with max steering to the left, max braking with no steering, and braking with max steering to the right, with the 47 other paths representing a level of braking/steering within these limits. Figure 36 shows the visual proportion of all possible evasive maneuvers within the three categories based on the lateral acceleration threshold.

For each simulation, the two vehicles were first placed within the worst-case impact location and then the AV was moved certain a distance away from the reference impact clock point on the turning vehicle. The distance was defined such that the simulations focused on the most critical situations in which the AV cannot completely avoid the crash with evasive braking alone. Distance varied for each scenario and was primarily based on AV travel speed and an additional scaling factor. The initial distance without any scaling was defined as the distance the AV would travel from an initial speed under the assumed max braking of 0.8g and was calculated using Equation 15. Travel speed was taken as the median travel speed

within all target population crashes for each scenario (see Figure 12). Table 24 provides a summary of median AV initial travel speed for each scenario.

$$x_{brake} = \frac{v_{AV}^2}{2g \cdot \mu_{brake}} \quad 15$$

The simulations assumed that the AV began the evasive maneuver at the start of the simulation and did not alter the braking/steering values after activation (i.e., steering remained constant and did not increase or decrease throughout the maneuver). The distance scaling factor was applied and simulated to have three values which modified the initial distance between the vehicles: 90% of the initial distance, 80% of the initial distance, and 70% of the initial distance. This was an adaptation of the NIEON model and was used to account for a variety of possible effects that determine where and when the AV begins its evasive maneuver. Examples include but are not limited to possible perception or decision system latency and possible sightline obstructions that may prevent a system from realizing a threat until a certain point.

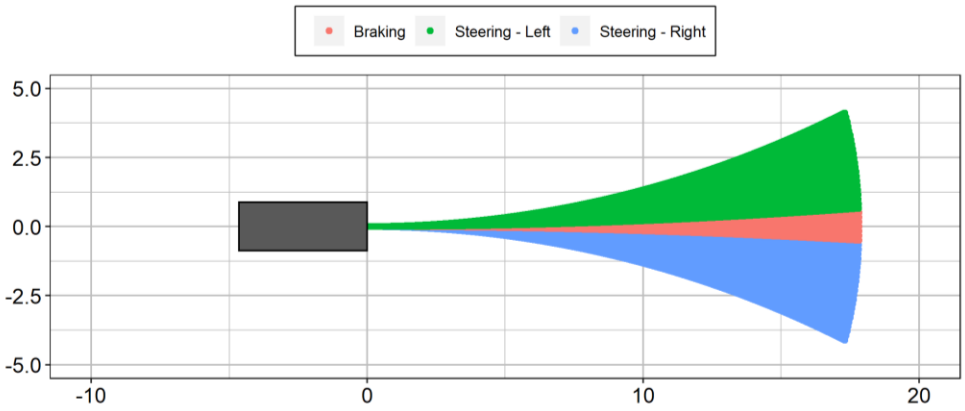

Figure 36. Three categories of AV evasive paths: primarily braking, braking while steering left, and braking while steering right

Table 24. Summary of AV initial speed used during crash simulations

	Rear-End	LTAP/OD	LTAP/LD	SCP-Left	SCP-Right
Travel Speed	15 mph	35 mph	35 mph	25 mph	25 mph

4.2.4 Modeling Impact Dynamics

In each simulation, the AV continued along the defined evasive path until either of two conditions happened: (1) the simulation registered that a collision occurred between the vehicles, or (2) the AV came to a rest as no collision occurred and the AV reached the end of its evasive maneuver. For simulations that did collide, the first point of contact was defined as the first simulation time step in which the Euclidian distance between any clock point on the turning vehicle and any clock point on the AV fell below the threshold of 0.1m. This point represented the approximate impact position for both of the vehicles.

The modeling of collision dynamics was accomplished using the methods described in the vehicle accident textbook by Brach et al. (2022) and used a 2D planar momentum-impulse model to compute primary impact measures. Inputs for the model were primarily vehicle mass/rotational inertia, impact velocity, and impact orientation and the output computed delta-v and principal direction of force (PDOF) for each vehicle. A vehicle mass of 1800kg and rotational inertia of 4300 kgm² was assumed for each vehicle which was the listed upper limit for the mass and the rotational inertia for both the Lincoln MKZ and the Chevy Impala. Each vehicle in the simulation was also assumed to be 4.65m in length and 1.75m wide which were the approximate dimensions of each vehicle as both are four-door sedans of similar mass. The impact velocity of the AV was determined based on the simulations and the impact velocity of the turning vehicle was assumed to be 15 mph.

For each impact orientation, the distance to the center of mass was computed for each vehicle based on which clock points on each vehicle were flagged as the collision point. A momentum and energy balance was then performed by transforming the X/Y momentum components into the tangential and normal components at the point of contact between the vehicles. This model did not take into account the deformation at the point of contact and a coefficient of restitution of 0.3 was chosen which models the transfer of energy along the tangential plane.

4.2.5 Modeling Injury Risk in both Vehicles

From the planar momentum impulse model, the delta-v and PDOF of force from each vehicle was computed in each simulation in which a crash occurs. Occupant injury risk in each vehicle was modeled using continuous omni-directional injury risk curves developed by McMurry et al. (2021). This model was developed from real-world vehicle-to-vehicle collisions and is similar to previously developed injury risk curves that are location specific (e.g., frontal or side) such as those developed by Bareiss (2019). This study focused on the small variations in crash orientation and so the continuous omni-directional model was well suited for this study.

The primary inputs for this model were vehicle delta-v and PDOF (Figure 37). The model was developed across a variety of other injury predictors, however these were assumed to be constant across all simulations and the same for both vehicles. This study assumed that each vehicle only had one occupant which was the driver who was assumed to be a 40 year old belted male. For every impact simulation, this model was used to compute the probability of MAIS3+F for this occupant in each vehicle. This model also incorporates the first and second derivative effects of PDOF in order to model effects of impact orientation.

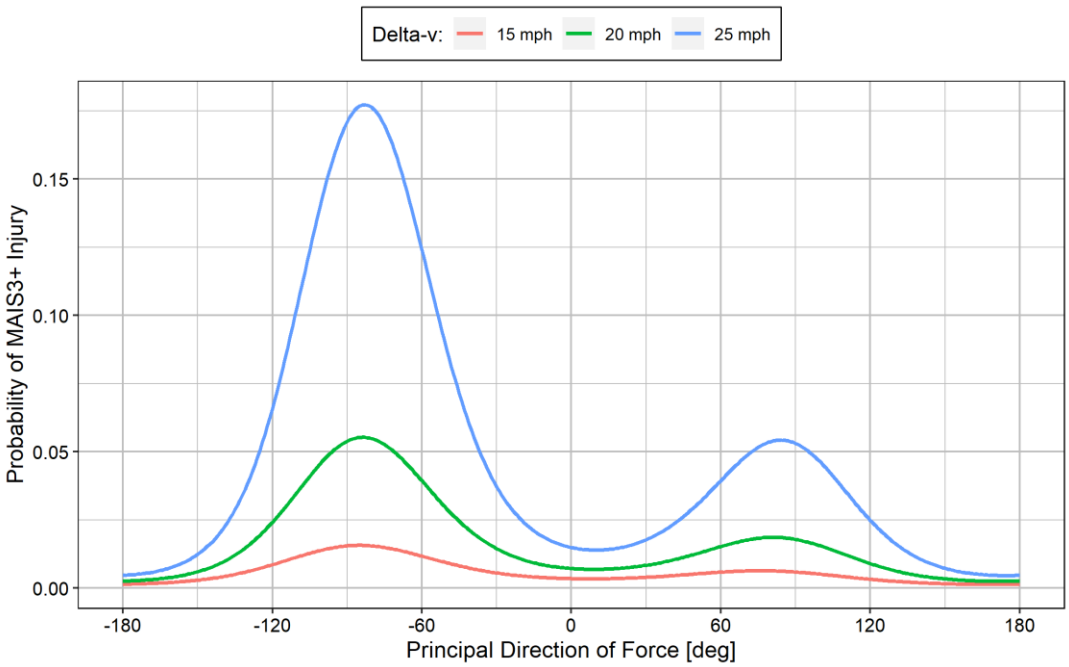

Figure 37. Example injury curves from (McMurry 2021) for varying delta-v and PDOF

4.3 Results

Crash simulations were performed for all seven defined crash scenarios: Rear-End, LTAP/OD, LTAP/LD, SCP-Left with Front Impact (SCP-LF), SCP-Left with Side Impact (SCP-LS), SCP-Right with Front Impact (SCP-RF), and SCP-Right with Side Impact (SCP-RS). For each scenario, evasive actions were also simulated to begin at 90%, 80%, or 70% of the initial braking point. Lastly, simulations were performed in which the location of the turning vehicle was placed based on the object detection of an ideal perception system and based on the object detection performance of the perception system tested in Chapter 3. This created 42 simulation variants that were performed, with each variant having 50 evasive paths which totaled to 2,100 unique simulations.

Figure 38 shows the percentage of simulation trajectories that resulted in a collision, broken out by crash scenario, activation distance, and perception system performance. Because evasive steering was applied, there was some proportion of the 50 evasive paths that avoided the other vehicle, and this was always the evasive paths with high steering values. Generally, there were no large differences due to perception system performance in any of the crash scenarios. The percentage of paths with a collision also generally increased across all the scenarios as the AV began evading closer as there was less time to turn out of the way.

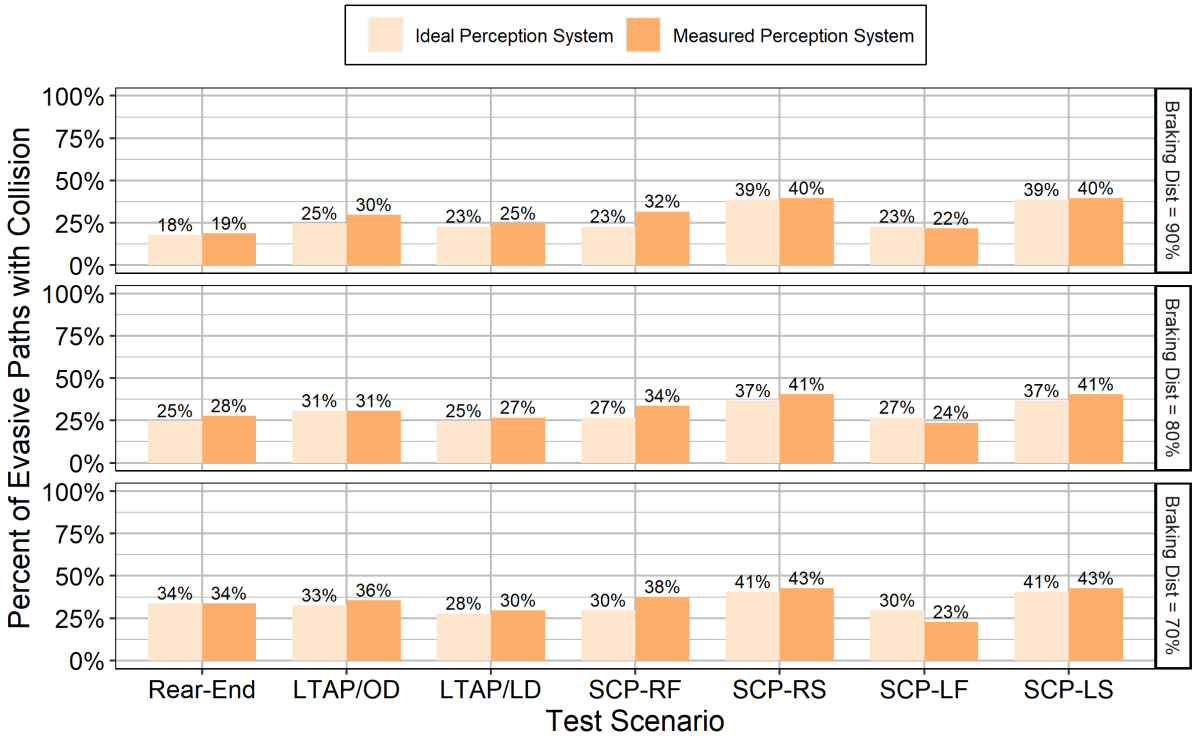

Figure 38. Percent of simulated evasive paths with a collision for each scenario, activation point, and perception system performance

For the paths that were simulated to collide, Figure 39 shows the impact speed for each evasive maneuver and broken out by crash scenario, activation point, and perception system performance. Generally, there were no differences seen due to perception system performance in any of the crash scenarios. This was likely because the X/Y position and speed error from the reference perception system was small enough that the impact point wasn't significantly changed. Impact speed increased as the AV began evading closer and differences between crash scenarios were largely because of the different initial speed conditions. The spread in impact speed across the simulations was also small. Overall, for a given activation point, the AV was simulated to crash at a similar impact speed regardless of evasive maneuver and crash scenario.

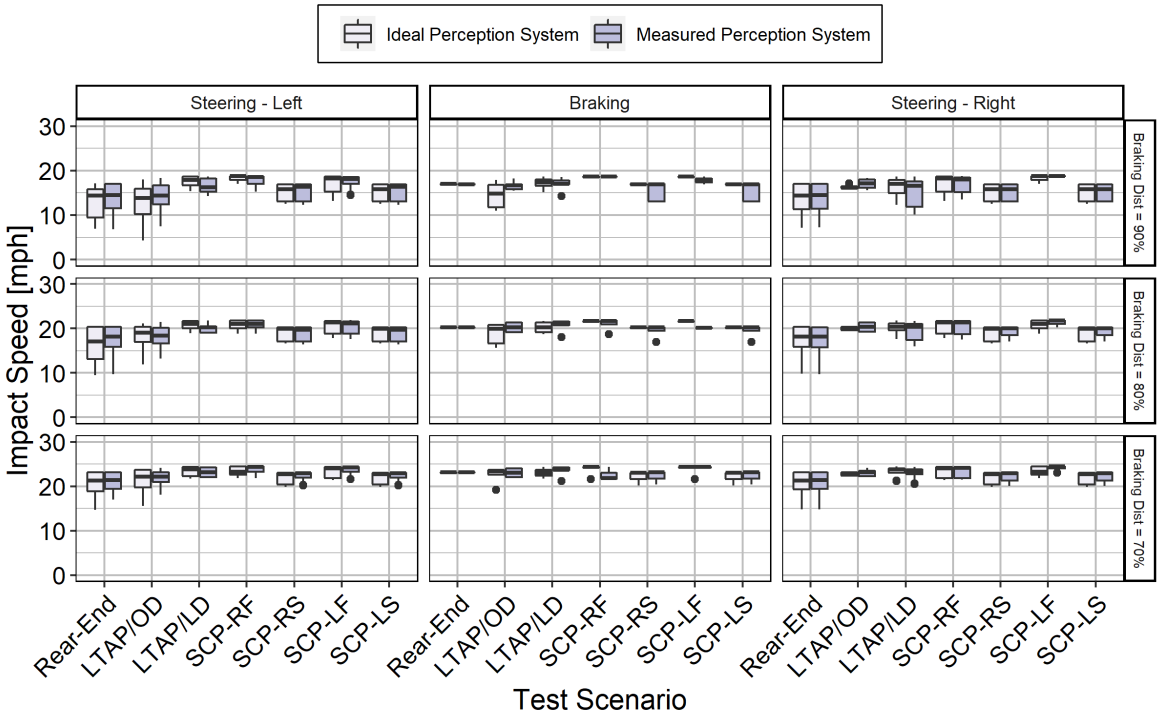

Figure 39. AV impact speed for each evasive maneuver category, broken out by crash scenario, activation point, and perception system performance

Figure 40 shows the delta-v for the AV in each evasive maneuver category. Figure 41 shows the same values for the turning vehicle. Evident within the AV, delta-v was found to change with perception system performance largely in the SCP collision scenarios. This difference also became more apparent in some scenarios as activation point decreased. This difference, however, was not as apparent in the turning vehicle, with the expectation being the SCP-LF scenario when steering right. Delta-v was comparable between the vehicles with slightly higher values being seen in the AV. Differences due to perception system performance were also found to be dependent on evasive maneuver. For example, for the LTAP/OD scenario, differences were seen within the AV under braking and right steering, but not during left steering.

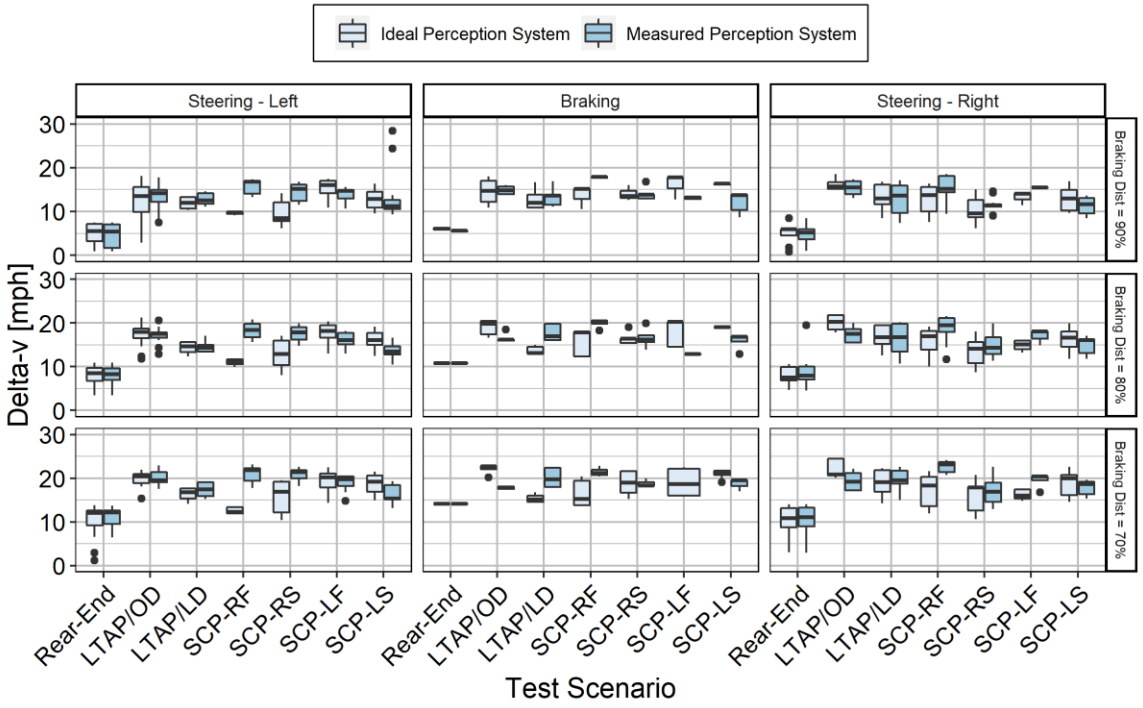

Figure 40. AV delta-v for each evasive maneuver category, broken out by crash scenario, activation point, and perception system performance

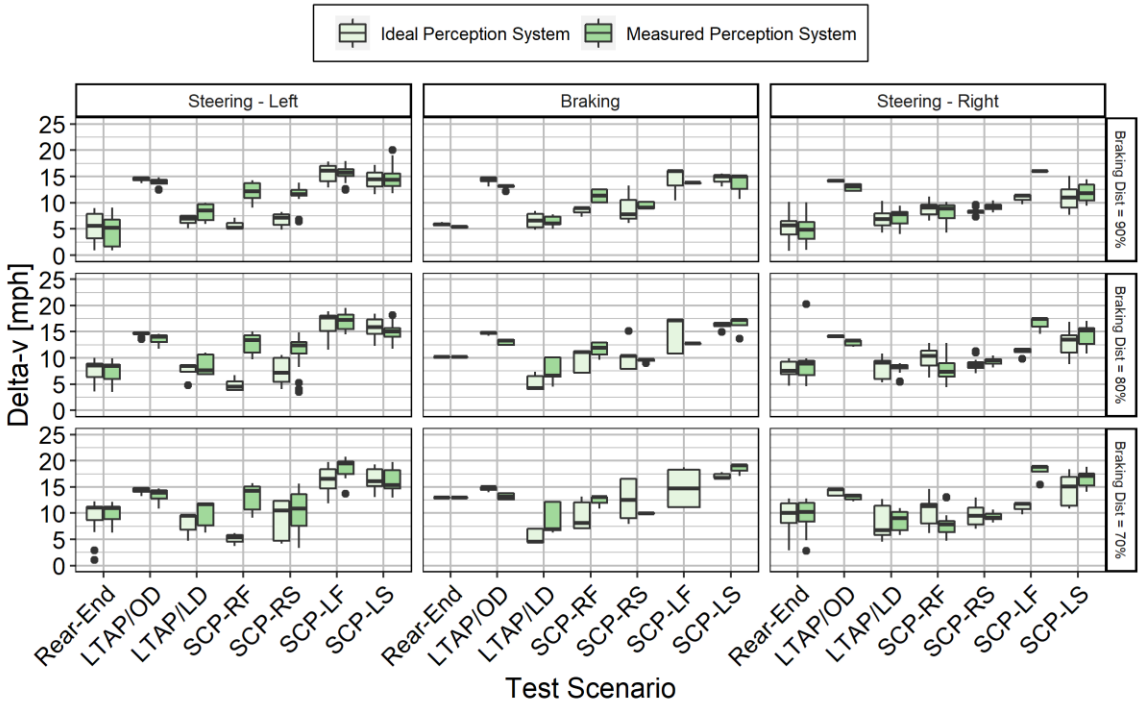

Figure 41. Turning vehicle delta-v for each evasive maneuver category, broken out by crash scenario, activation point, and perception system performance

Figure 42 shows the PDOF in the AV and for each evasive maneuver. Figure 43 shows this for the turning vehicle as well. Of the crash scenarios that were found to vary due to perception system performance, differences were found to decrease as the evasive maneuver is initiated closer. This showed that as the AV began evading at a closer point, the PDOF of the collisions that happened became less variable for most of the crash scenarios. For the AV, the variation in PDOF was also small for all scenarios expect the rear-end crash scenario. While the mean was comparable, large variations were seen for simulations with either left or right steering. This large variability was also seen in the turning vehicle primarily in the SCP and LTAP/LD crash scenarios in which the turning vehicle is being struck on the side.

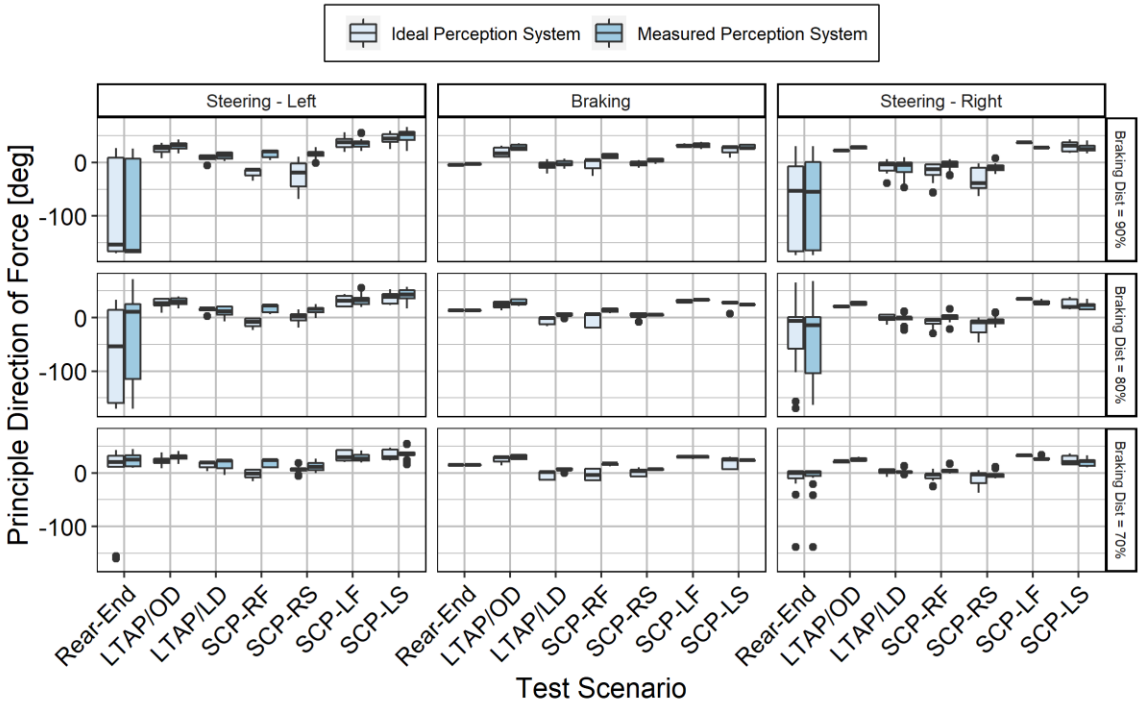

Figure 42. AV PDOF for each evasive maneuver category, broken out by crash scenario, activation point, and perception system performance

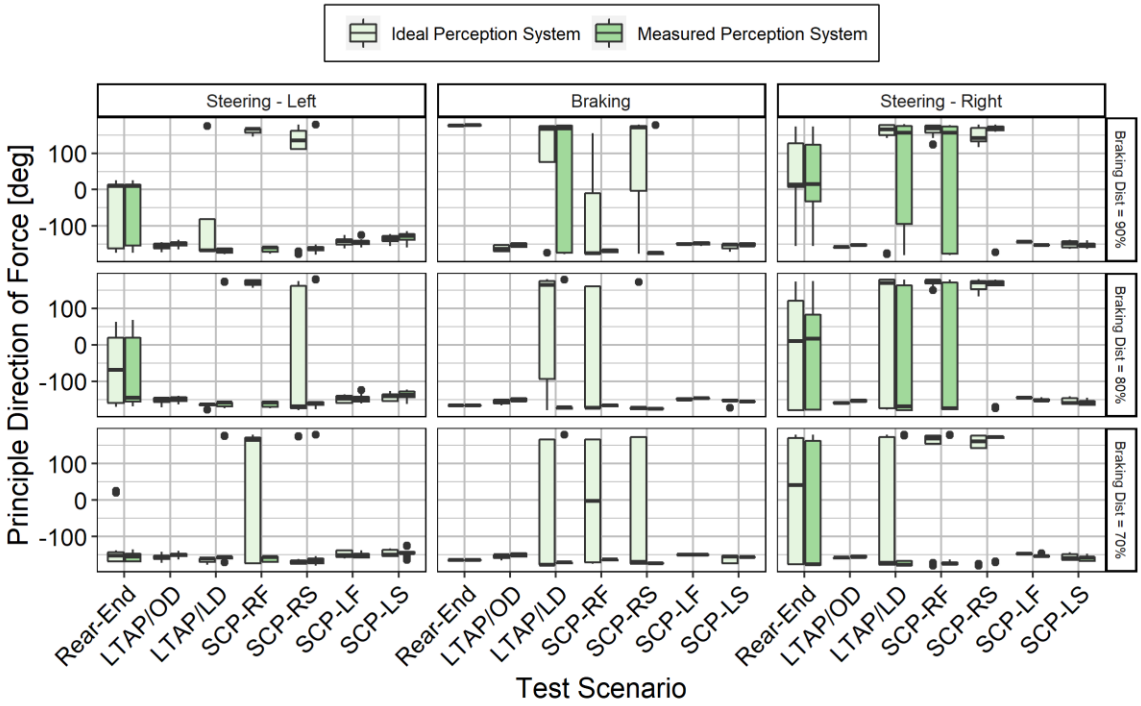

Figure 43. Turning vehicle PDOF for each evasive maneuver category, broken out by crash scenario, activation point, and perception system performance

Figure 44 shows the probability of MAIS3+F injury in the AV and for each evasive maneuver. Figure 45 shows this for the turning vehicle as well. Mean injury risk was generally higher in the AV than the turning vehicle. Varied differences due to perception system perception was also seen across multiple scenarios for the AV. This difference was also seen to become more prevalent as activation point decreased. Injury risk also varied for evasive maneuver. For example, differences due to perception system performance in the LTAP/OD crash scenario were apparent during braking and right steering, but not as much during left steering evasive maneuvers. Injury risk in the Av was lowest during the rear-end scenario, and highest among the SCP and LTAP/OD scenarios. This was likely the case as in the case of the LTAP/OD (steering left) and the SCP scenarios where the AV turns into the turning vehicle, the effect of the "head-on" nature of these impacts is seen as higher injury risk.

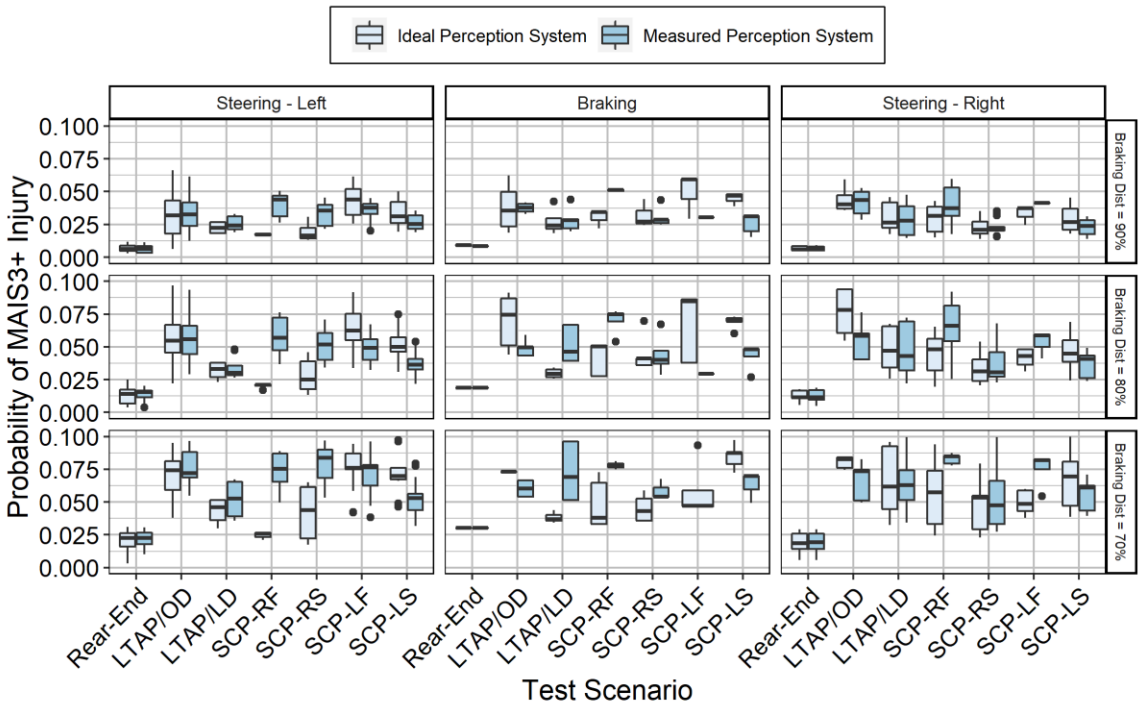

Figure 44. AV probability of MAIS3+F injury for each evasive maneuver category, broken out by crash scenario, activation point, and perception system performance

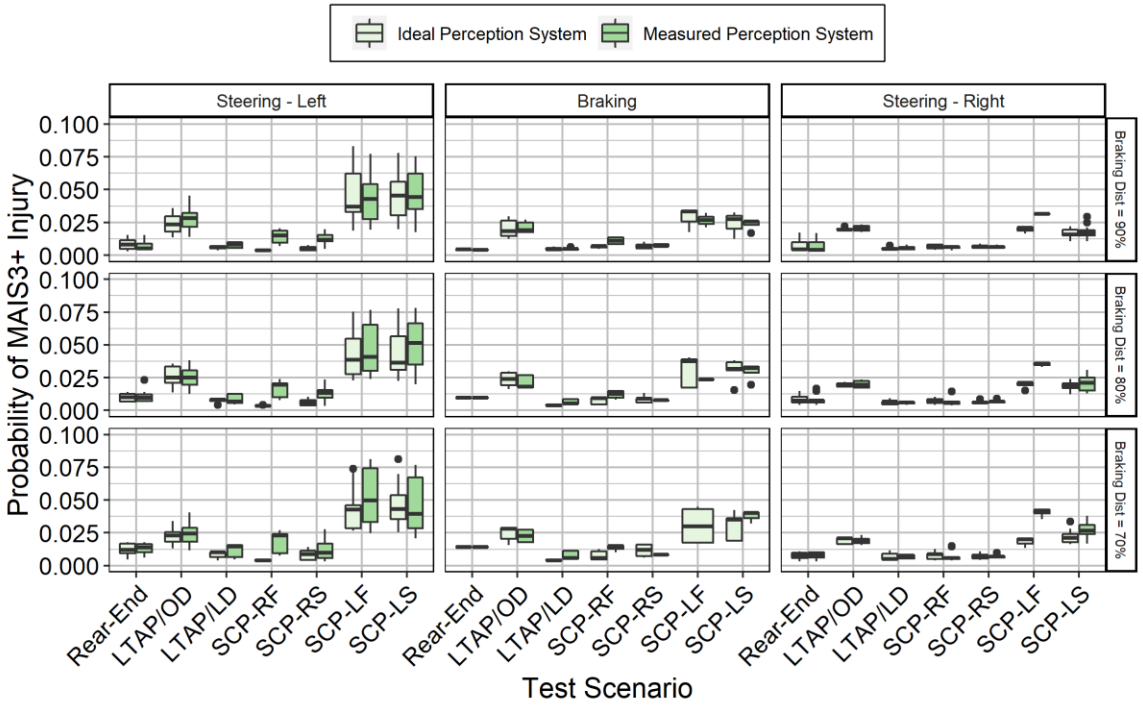

Figure 45. Turning vehicle probability of MAIS3+F injury for each evasive maneuver category, broken out by crash scenario, activation point, and perception system performance

4.4 Discussion and Limitations

Results from the crash simulations showed that injury risk mainly varied within the AV and less so in the turning vehicle. These simulations also showed that changes in injury risk varied based on the crash scenario and the evasive actions that were taken. Variations due to perception system performance were also seen to become more or less prevalent when the AV was simulated to brake/steer closer.

Figure XX shows the difference in mean injury risk within the AV (probability shown as a percentage) between the ideal perception system and the measured perception system, shown for each combination of crash scenario, evasive maneuver, and activation point. A positive value indicates that injury risk was higher with the measured system, and a negative value indicates that the ideal system had higher injury risk. The difference in injury risk was found to be between 0 and 6.2. Generally, injury risk was higher in the measured perception system, however there were multiple instances where injury risk was higher with the ideal system. Although differences between predicted outcomes should be minimized, instances where the measured system under-predicts injury risk (i.e., ideal system has higher injury risk then the measured system) represent higher safety concerns as the system is predicting that the crash will be less sever then it actually might be.

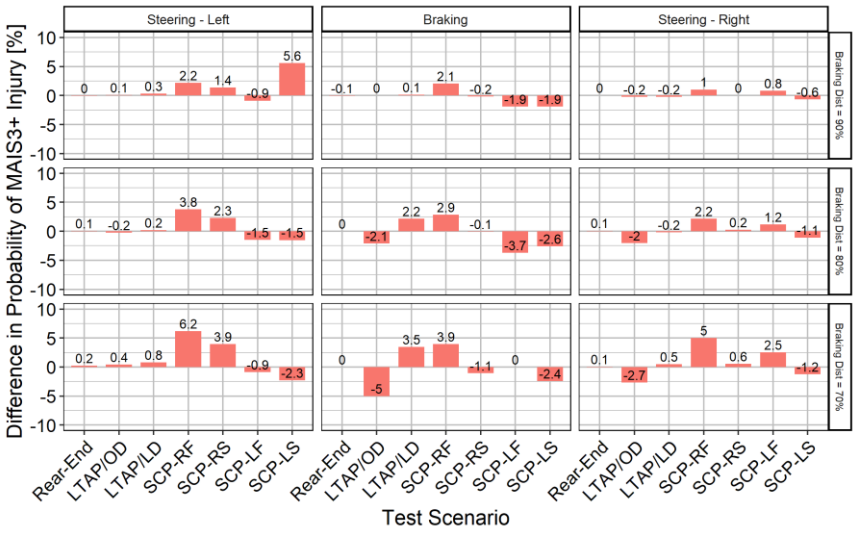

Figure 46. Summary of difference in injury risk prediction for the ideal system and the measured system

Differences were primarily seen to be caused by the interaction of changes in both delta-v and the PDOF for each crash simulation. The changes in PDOF were affected by changes in the impact orientation between simulations. Figure 47 highlights an example of this. The figure shows the simulation outputs for the LTAP/OD crash scenario, in which the AV is performing mainly evasive braking at an activation point of 70%. In this scenario, the simulation with ideal perception system performance showed a 3% higher probability of injury compared to the measured perception system. The difference between impact orientation is evident as the impact scenario for the ideal perception system is close to a full-frontal impact, whereas with the measured perception system, the impact is shifted towards the 1 O'clock position and creates a less severe collision with lower injury risk. A note for this situation is that this sensitivity was only apparent for the 70% activation point and not for the 90% activation. This also highlights that sensitivity likely changes with impact speed and therefore also delta-v. This is highlighted in Figure 37 as lower crash delta-v results in the probability of injury decreasing to lower values regardless of PDOF. And so, if the AV has more time to slow down, then the injury differences caused by changes to impact orientation decrease. This example also shows that the "ideal" system can potentially have worse injury outcomes than the incorrect system depending on the situation. The safety implications of this may be that an AV may predict a crash outcome to be less severe than it actually would be.

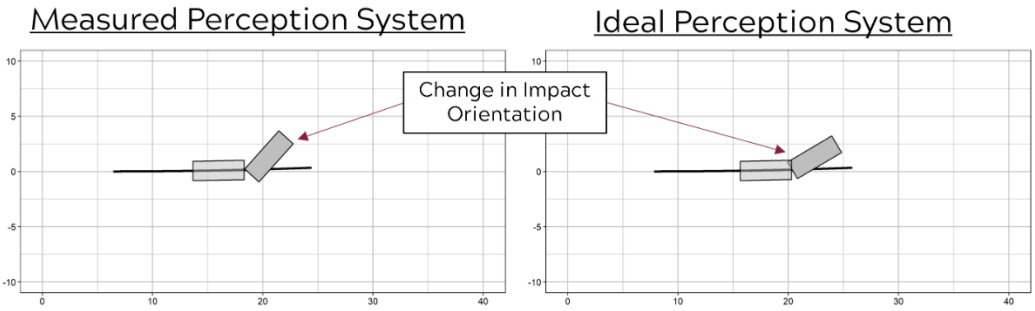

Figure 47. Example simulation outputs showing the change in impact orientation between the ideal perception system (right) and the measured perception system (left) for the LTAP/OD crash scenario and 70% activation point under primarily braking.

Injury outcome sensitivity to perception system performance is further illustrated in Figure 48. Within each crash simulation and for a given delta-v in either vehicle, the PDOF is very dependent on the exact

crash orientation of the two vehicles. For an ideal system, where a crash falls on the injury risk curve is dependent on the specific crash scenario which dictates the range of possible crash orientations that are generally assumed to be possible. However, due to the sinusoidal shape of the injury risk curves used in this study, a change in PDOF from an ideal system to the measured system can have large variations in injury outcomes depending on where these points fall on the curve. As such, when and where injury risk differences occur is related to a complex interaction of crash scenario and perception system performance for a specific system, as well as the values of delta-v and PDOF.

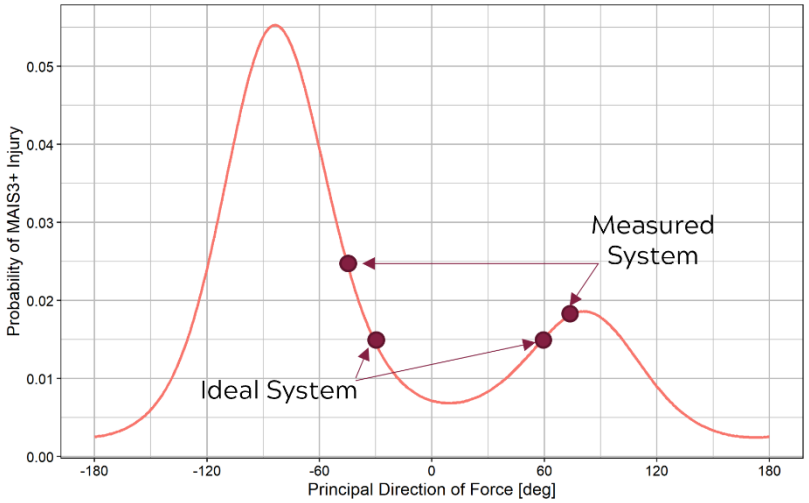

Figure 48. Highlight of injury risk sensitivities. The difference in injury outcomes between an ideal and a measured system differ greatly depending on where on the curve they fall.

The addition of the distance scaling factors makes the assumption that the AV in these scenarios cannot completely avoid the crash from just evasive braking alone. If the crash population from chapter 2 is taken as the crash event exposure, then this represents a conservative basis for calculating injury risk and would generally be inaccurate when computing collision avoidance benefits. This is because past studies have shown that many intersection crashes are potentially avoidable with just evasive breaking. Scanlon (2017) showed that crash prevention benefits could be as high as 59% in certain conditions involving SCP crashes and in a similar manner, Bareiss (2019) showed that crash prevention benefits could be as high as 84% under certain conditions in LTAP/OD crashes. The main conditions that effected crash prevention in each study was the Time-to-collision (TTC) that the system was simulated to activate at which is akin to the

activation distance used in this study and may be influenced by factors such as system latency and sightline obstructions.

This study also simulated the AV to activated evasive steering/braking at the same point for both initial conditions (actual and measured position/heading of the other vehicle). This was done as the goal was to assess the differences between each condition and so the activation point was kept constant. In an actual crash, however, the activation point would change, assuming the AV is reacting to the perceived position of the other vehicle. In instances where the AV thinks the other vehicle will be closer than it actually will be, the AV might begin braking at an earlier time and lessen the collision. The opposite is true when the AV thinks the other vehicle will be father away then it will be and so the collision can be worsened if the AV brakes later because of this. This highlights that although error should be minimized, in an actual crash scenario, the direction of error can have very different safety implications.

One limitation to these simulations was that only the trajectory of the AV was simulated. An assumption was made that the path of the turning vehicle was negligible however this may not be the case in crash scenarios with higher travel speeds such as during highway driving. One effect this may have is when the AV performs evasive steering, there may be situations where the turning vehicle then becomes the striking vehicle.

An additional limitation was that evasive steering was evaluated without any knowledge of the intersection geometry. This is important as although a crash may be able to be prevented with heavy evasive steering, there also exists the possibility that the AV could steering into another vehicle and/or a roadside object or feature. Detailed information of both the crash location and other road users at the time of the crash would be needed to address these concerns. This is a constraint that was included in the study by Scanlon et al. (2022), however, it was out of scope for this study.

4.5 Conclusions

The objective of this chapter was to simulate possible crash outcomes in order to assess the sensitivity of occupant injury risk due to perception system performance. A hybrid approach was developed in which the real-world ADS perception system performance was incorporated for a set of probable crash scenarios. Results showed that injury risk was mainly dependent on a complex interaction between changes in delta-v and PDOF, and this interaction was dependent on scenario and evasive maneuver. Results from this chapter are specific to the reference AV, however the development of this method was defined in a way that this analysis could be performed for any future AV.

5. Conclusions

The main objective of this study was to create a hybrid method for assessing changes in occupant injury risk within crash scenarios based on ADS perception system performance. This study first defined a set of high level crash scenarios with high probability of exposure for a hypothetical AV operating as an urban taxi. The real-world performance of an ADS platform was then characterized within these crash scenarios. Based on this performance, crash outcomes were simulated for different AV evasive maneuvers in these crash scenarios in order to identify where and when safety concerns may arise due to object detection performance.

This study first characterized a target population of intersection vehicle crashes that were consistent with the operating conditions for an urban taxi AV use case. Crashes from the years 2016-2019 from CRSS were characterized based on factors used for crash scenario creation. This chapter identified five main crash scenarios: Rear-End with the lead vehicle stopper, Left-Turn Across Path from the Opposite Direction (LTAP/OD), Left-Turn Across Path from the right lateral direction (LTAP/LD), and Straight Crossing Paths from the right and left directions (SCP). Environmental and target level factors were defined for all these crash modes and a total probability of exposure to each crash scenario was calculated. Within all the target population crashes, the probability of exposure to a crash scenario was between 0.012 and 0.062 and within crashes involving each crash mode, probability of exposure ranged between 0.128 and 0.282.

In the third chapter, the performance of a real-world ADS perception system was characterized. The object detection performance of object position, object heading, and object speed was measured using ground truth in each crash scenario defined previously. Median performance was seen to be similar across all metrics and all scenarios, however variability was seen to vary significantly. The measured performance then served as the basis for the next chapter.

In the fourth chapter, the measured perception system performance served as the basis for a series of vehicle simulations that were used to predict possible crash outcomes. These simulations first assumed an

initial crash configuration based on the impact locations of the vehicles within the target population. The AV was then assumed to perform some variation of steering and braking as an evasive maneuver. Evasive maneuvers were determined based on an adapted driver model. For simulations in which the vehicles contacted, collision and injury modeling was applied. Across all the simulations, the differences in impact speed, delta-v, principal direction of force, and probability of MAIS3+F injury to evasive action, evasive action activation point, and perception system performance was assessed. Results showed that injury risk was greatly dependent on specific scenario, and the evasive action performed in that scenario for the reference AV.

Overall, this study represents a hybrid methodology in which a risk sensitivity analysis can take place for an actual ADS platform. Specifically, this study addresses the unique contributions of perception system performance on imposed occupant injury risk during scenarios of crash avoidance. Future use of this method may be useful in understanding what evasive actions an AV should take in certain situations. For example, an AV that is "self-aware" of its perception system performance within a certain situation, may be able to more accurately predict which evasive action (ex. steering left or right) may lead to a lower overall injury risk. Similarly, the AV may be able to better recognize which actions may increase injury risk. The method defined in this study may also be useful in define system performance guidelines for AV perception systems. Following a notion of "how safe is safe enough" the results from applying this method could help in indicate how much perception error is tolerable for safe operation.

Possible future work as it relates to this study would be to address the contributions of the decision and motion control systems on injury risk. A similar method could be defined that assesses the effects of variations in path actuation due to errors in the motion control system. Future work may also better address the complexity of traffic scenarios during these crash events. This will be especially important in addressing the impact of decision making algorithms on crash outcomes.

Appendix A: List of CRSS Data Elements and Definitions

The following table lists all of the CRSS data elements used during any part of this thesis (either described or during analysis). CRSS variable name, SAS variable name, and a variable description is provided.

CRSS Variable	SAS Variable Name	Description
Number of Motor Vehicles in Transport	VE_FORMS	This data element is a count of the number of motor vehicles in transport involved in the crash. Legally parked vehicles are not included.
First Harmful Event	HARM_EV	This data element describes the first injury or damage producing event of the crash.
Manner of Collision – First Event	MAN_COLL	This data element describes the orientation of two motor vehicles in transport when they are involved in the "First Harmful Event" of a collision crash.
Relation to Junction	RELJCT2	This data element identifies the crash's location with respect to presence in or proximity to components typically in junction or interchange areas.
Type of Intersection	TYP_INT	This data element identifies and allows separation of various intersection types.
Relation to Trafficway	REL_ROAD	This data element identifies the location of the crash as it relates to its position within or outside the trafficway based on the "First Harmful Event."
Work Zone	WRK_ZONE	This data element identifies a motor vehicle traffic crash in which the first harmful event occurs within the boundaries of a work zone or on an approach to or exit from a work zone, resulting from an activity, behavior, or control related to the movement of the traffic units through the work zone.
Lighting Condition	LGT_COND	This data element records the type/level of light that existed at the time of the crash as indicated in the police crash report.
Weather Condition	WEATHER	This derived data element records the prevailing atmospheric conditions that existed at the time of the crash as indicated in the police crash report.
Maximum Injury Severity in Crash	MAX_SEV	This data element records the single most severe injury of all people involved in the crash and is derived from "Injury Severity" in the Person data file.
NCSA Body Type	BODY_TYPE	This data element identifies a classification of this vehicle based on its general body configuration, size, shape, doors, etc. as defined by NCSA.
Travel Speed	TRAV_SP	This data element records the speed the vehicle was traveling prior to the occurrence of the crash as reported by the investigating officer.
Initial Contact Point	IMPACT1	This data element identifies the area on this vehicle that produced the first instance of injury to non-motorists or occupants of this

		vehicle, or that resulted in the first instance of damage to other property or to this vehicle.
Trafficway Description	VTRAFWAY	This data element identifies the attribute that best describes the trafficway flow just prior to this vehicle's critical precrash event.
Number of Travel Lanes	VNUM_LAN	This data element identifies the attribute that best describes the number of travel lanes just prior to this vehicle's critical precrash event.
Speed Limit	VSPD_LIM	This data element records the posted speed limit in miles per hour.
Roadway Alignment	VALIGN	This data element identifies the attribute that best represents the roadway alignment prior to this vehicle's critical precrash event.
Roadway Grade	VPROFILE	This data element identifies the attribute that best represents the roadway grade prior to this vehicle's critical precrash event.
Traffic Control Device	VTRAFCON	This data element identifies the attribute that best describes the traffic controls in the vehicle's environment just prior to this vehicle's critical precrash event.
Generalized Crash Type	ACC_TYPE	This data element identifies the attribute that best describes the type of crash this vehicle was involved in based on the "First Harmful Event" and the precrash circumstances.
Driver's Vision Obscured By…	MVISOBSC	This data element records impediments to this driver's visual field that were noted in the police crash report.

References

A. Knauss, J. Schröder, C. Berger and H. Eriksson, "Paving the roadway for safety of automated vehicles: An empirical study on testing challenges," 2017 IEEE Intelligent Vehicles Symposium (IV), Los Angeles, CA, USA, 2017, pp. 1873-1880, doi: 10.1109/IVS.2017.7995978.

Association for the Advancement of Automotive Medicine. (2015). The Abbreviated Injury Scale: 2015 Revision. Chicago, IL: AAAM.

Bareiss, Max. (2019). Effectiveness of Intersection Advanced Driver Assistance Systems in Preventing Crashes and Injuries in Left Turn Across Path / Opposite Direction Crashes in the United States). (Master's thesis, Virginia Tech).

Burdett, Beau. (2014). Improving Accuracy of KABCO Injury Severity Assessment by Law Enforcement Officers. (Master's thesis, University of Wisconsin-Madison).

Berk, M., Schubert, O., Kroll, H., Buschardt, B. et al., "Assessing the Safety of Environment Perception in Automated Driving Vehicles," SAE Int. J. Trans. Safety 8(1):49–74, 2020, doi:10.4271/09-08-01-0004.

E. Marti, M. A. de Miguel, F. Garcia and J. Perez, "A Review of Sensor Technologies for Perception in Automated Driving," in IEEE Intelligent Transportation Systems Magazine, vol. 11, no. 4, pp. 94-108, winter 2019, doi: 10.1109/MITS.2019.2907630.

Favarò, F., Fraade-Blanar, L., Schnelle, S., Victor, T., Peña, M., Engstrom, J., Scanlon, J., Kusano, K., and Smith, D. (2023). Building a Credible Case for Safety: Waymo's Approach for the Determination of Absence of Unreasonable Risk. www.waymo.com/safety.

International Organization for Standardization (ISO). (2018). ISO 26262:2018 Road vehicles -- Functional safety. https://www.iso.org/standard/68383.html

International Organization for Standardization (ISO). (2019). ISO 21448:2019 Road vehicles -- Safety of the intended functionality. https://www.iso.org/standard/74579.html

J. Kocić, N. Jovičić and V. Drndarević, "Sensors and Sensor Fusion in Autonomous Vehicles," 2018 26th Telecommunications Forum (TELFOR), Belgrade, Serbia, 2018, pp. 420-425, doi: 10.1109/TELFOR.2018.8612054.

Jesper Sandin, An analysis of common patterns in aggregated causation charts from intersection crashes, Accident Analysis & Prevention, Volume 41, Issue 3, 2009, Pages 624-632, ISSN 0001-4575, https://doi.org/10.1016/j.aap.2009.02.015.

John M. Scanlon, Kristofer D. Kusano, Tom Daniel, Christopher Alderson, Alexander Ogle, Trent Victor, Waymo simulated driving behavior in reconstructed fatal crashes within an autonomous vehicle operating domain, Accident Analysis & Prevention, Volume 163,2021, 106454, ISSN 0001-4575, https://doi.org/10.1016/j.aap.2021.106454.

K. D. Kusano and H. C. Gabler, "Safety Benefits of Forward Collision Warning, Brake Assist, and Autonomous Braking Systems in Rear-End Collisions," in IEEE Transactions on Intelligent Transportation Systems, vol. 13, no. 4, pp. 1546-1555, Dec. 2012, doi: 10.1109/TITS.2012.2191542.

Kidambi, N., Wishart, J., Elli, M., and Como, S., “Sensitivity of Automated Vehicle Operational Safety Assessment (OSA) Metrics to Measurement and Parameter Uncertainty,” SAE Technical Paper 2022-01-0815, 2022, doi:10.4271/2022-01-0815.

Kristofer Kusano & Trent Victor (2022): Methodology for determining maximum injury potential for automated driving system evaluation, Traffic Injury Prevention, DOI:10.1080/15389588.2022.2125231

Kusano, K., Beatty, K., Schnelle, S., Favaro, F., Crary, C., and Victor, T.. (2019). Collision Avoidance Testing of the Waymo Automated Driving System. https://storage.googleapis.com/waymo uploads/CA_Testing_Paper.pdf

Lumley, T., 2019. survey: analysis of complex survey samples [WWW Document]. URL http://r-survey.r-forge.r-project.org/survey

M. M. Brady, R. R. McHenry, & R. W. Anderson. (2014). Vehicle Accident Analysis and Reconstruction Methods, Third Edition. CRC Press.

Max Bareiss, John Scanlon, Rini Sherony & Hampton C. Gabler (2019) Crash and injury prevention estimates for intersection driver assistance systems in left turn across path/opposite direction crashes in the United States, Traffic Injury Prevention, 20:sup1, S133-S138, DOI: 10.1080/15389588.2019.1610945

Menzel, Till & Bagschik, Gerrit & Maurer, Markus. (2018). Scenarios for Development, Test and Validation of Automated Vehicles. 10.1109/IVS.2018.8500406.

Najm, W., Ranganathan, R., Srinivasan, G., Smith, J., Toma, S., Swanson, E., and Burgett, A. (2014). Description of Light-Vehicle to-Vehicle Communications Pre-Crash Scenarios for Safety Applications Based on Vehicle-to-Vehicle Communications. https://www.nhtsa.gov/sites/nhtsa.dot.gov/files/v2v_communication_pre-crash_scenarios_report_0.pdf

National Center for Statistics and Analysis. (2021, August). Traffic safety facts 2019: A compilation of motor vehicle crash data (Report No. DOT HS 813 141). National Highway Traffic Safety Administration.

National Center for Statistics and Analysis. (2022, July (Revised)). Crash Report Sampling System analytical user's manual, 2016-2020 (Report No. DOT HS 813 236). National Highway Traffic Safety Administration.

National Highway Traffic Safety Administration (NHTSA). (2016). National Automotive Sampling System (NASS) General Estimates System (GES) Analytical User's Manual 1988–2015. https://crashstats.nhtsa.dot.gov/Api/Public/ViewPublication/812384

National Highway Traffic Safety Administration (NHTSA). (n.d.). National Motor Vehicle Crash Causation Survey (NMVCCS) [dataset]. https://www.nhtsa.gov/research-data/national-motor-vehicle-crash-causation-survey-nmvccs

National Highway Traffic Safety Administration. (2022, March). 2020 FARS/CRSS coding and validation manual (Report No. DOT HS 813 251).

Ploeg, Jeroen, Erwin de Gelder, Martin Slavík, Erich Querner, Thomas Webster and Niels de Boer. "Scenario-Based Safety Assessment Framework for Automated Vehicles." ArXiv abs/2112.09366 (2021).

R. Johansson and J. Nilsson, "The need for an environment perception block to address all ASIL levels simultaneously," 2016 IEEE Intelligent Vehicles Symposium (IV), Gothenburg, Sweden, 2016, pp. 1-4, doi: 10.1109/IVS.2016.7535354.

S. Behere and M. Torngren, "A functional architecture for autonomous driving," 2015 First International Workshop on Automotive Software Architecture (WASA), Montreal, QC, Canada, 2015, pp. 3-10, doi: 10.1145/2752489.2752491.

SAE International. (2018). Taxonomy and Definitions for Terms Related to On-Road Motor Vehicle Automated Driving Systems (SAE J3016) [Standard]. https://doi.org/10.4271/J3016_201806

Scanlon, J., Kusano, K., Engstrom, J., and Victor, T. (2022). Collision Avoidance Effectiveness of an Automated Driving System Using a Human Driver Behavior Reference Model in Reconstructed Fatal Collisions (White Paper).

Scanlon, John & Sherony, Rini & Gabler, Hampton. (2017). Injury Mitigation Estimates for an Intersection Driver Assistance System in Straight Crossing Path Crashes in the U.S. Traffic Injury Prevention. 18. 10.1080/15389588.2017.1300257.

Scanlon, John. (2017). Evaluating the Potential of an Intersection Driver Assistance System to Prevent U.S. Intersection Crashes. (Doctoral dissertation, Virginia Tech).

Timothy L. McMurry, Joseph M. Cormier, Tom Daniel, John M. Scanlon & Jeff R. Crandall (2021) An omni-directional model of injury risk in planar crashes with application for autonomous vehicles, Traffic Injury Prevention, 22:sup1, S122-S127, DOI:10.1080/15389588.2021.1955108

United States Congress. (n.d.). 49 U.S. Code Chapter 301 - Motor Vehicle Safety standard. Legal Information Institute, Cornell Law School. https://www.law.cornell.edu/uscode/text/49/subtitle-VI/part-A/chapter-301

Webb, N., Smith, D., Ludwick, C., Victor, T.W., Hommes, Q., Favarò F., Ivanov, G., and Daniel, T. (2020). Waymo's Safety Methodologies and Safety Readiness Determinations (White Paper). https://waymo.com/safety/waymo-safety-report-2020.pdf

Willke, D., Summers, S., Wang, J., Lee, J., Partyka, S., &Duffy, S. (1999, August). Ejection Mitigation Using Advanced Glazing: Status Report II. East Liberty, OH: Transportation Research Center.

Zhang, F., Noh, E. Y., Subramanian, R., & Chen, C.-L. (2019, May). Crash Report Sampling System: Sample design and weighting (Report No. DOT HS 812 706). Washington, DC: National Highway Traffic Safety Administration.